Since January 2020 Elsevier has created a COVID-19 resource centre with free information in English and Mandarin on the novel coronavirus COVID-19. The COVID-19 resource centre is hosted on Elsevier Connect, the company's public news and information website.

THE MOLECULAR BIOLOGY OF CORONAVIRUSES

Lawrence S. Sturman

Center for Laboratories and Research, New York State Department of Health
Albany, New York

Kathryn V. Holmes

Department of Pathology, Uniformed Services University of the Health Sciences
Bethesda, Maryland

ISBN 0-12-039828-1

> The image of progress in science as a kind of conquest of an unknown domain with a definite "frontier" and successive 'breakthroughs' seems to me more and more to be only a romantic illusion. . . . There are many frontiers and it comes down to the fact that in science one can only sometimes talk of progress. Whenever there is an advance, there is a frontier, not the other way around.
>
> George E. Uhlenbeck (1971, p. 449–450)[1]

> Facts are never completely independent of each other . . . every fact reacts upon many others. Every change and every discovery has an effect on a terrain that is virtually limitless. It is characteristic of advanced knowledge, matured into a coherent system, that each new fact harmoniously—though ever so slightly—changes all earlier facts. Here every discovery is actually a recreation of the whole world as construed by a thought collective.
>
> Ludwik Fleck (1979, p. 102)[2]

I. Introduction

A. Dedication

This contribution is dedicated to the memory of our colleague and friend, Frederik Bang, who uncovered some of the most intriguing questions about the biology of coronaviruses. Beginning with the discovery that mouse hepatitis virus (MHV) could grow in and destroy macrophages in culture (Bang and Warwick, 1959) and that macrophage susceptibility *in vitro* reflected a genetic determinant for susceptibility in the mouse, Bang and Warwick, (1960; Kantoch *et al.*, 1963) constructed a simple model to explain genetic resistance and susceptibility to this virus. For more than two decades, Bang (1978, 1981) and his colleagues explored genetic and environmental aspects of host resistance and susceptibility to MHV, and the effects of MHV on macrophages. At the Wurzburg Symposium on the Biochemistry and Biology of Coronaviruses in 1980, Dr. Bang (1981) recounted the changes in his thinking about mechanisms of host resistance, as many of the conclusions drawn from earlier experiments were reinterpreted in the light of subsequent findings. As always, he spoke with humility and humor, and displayed his distinctive interest in host–parasite interrelations. Unfortunately, that was his last opportunity to address his colleagues in this rapidly expanding field. We shall miss him.

[1]Reprinted by permission from *Nature* **232,** 449–450. Copyright © 1971 Macmillan Journals Limited.

[2]Reprinted from "Genesis and Development of a Scientific Fact" by Ludwig Fleck by permission of The University of Chicago Press. Copyright © 1979 by The University of Chicago Press.

B. Emergence of Coronaviruses

Coronaviruses have been known, although not by that name, for almost five decades. This previously unrecognized group emerged during the 1960s in the aftermath of the discovery of several new human respiratory pathogens. Avian infectious bronchitis virus (IBV), mouse hepatitis virus, and some newly described human respiratory viruses were noted to have a similar appearance (Almeida and Tyrrell, 1967; McIntosh *et al.*, 1967b; Becker *et al.*, 1967). In contrast to myxoviruses, with which they had been previously compared (Berry *et al.*, 1964; Mallucci, 1965), these viruses displayed a characteristic fringe of large, distinctive, petal-shaped peplomers or spikes which resembled a crown, like the *corona spinarum* in religious art; hence the name coronaviruses (Fig. 1A; Tyrrell *et al.*, 1968). In addition to their morphological similarities, some of the human coronaviruses (HCV) were noted to be antigenically related to MHV (Tyrrell *et al.*, 1968; McIntosh *et al.*, 1969; Bradburne, 1970). Between 1968 and 1974, research on coronaviruses emphasized morphologic and immunologic relationships and comparative biology. Several new viruses were added to the coronavirus group: porcine transmissible gastroenteritis virus (TGEV), porcine hemagglutinating encephalomyelitis virus (HEV), rat coronavirus (RCV), sialodacryoadenitis virus of rats (SDAV), turkey bluecomb disease virus (TCV), and neonatal bovine diarrhea coronavirus (BCV). A comprehensive review by McIntosh (1974) provides an excellent overview of early coronavirus research.

In 1975, the International Committee on the Taxonomy of Viruses approved the creation of a new family, Coronaviridae, with one genus, Coronavirus (Tyrrell *et al.*, 1975). Additional species were added later including canine coronavirus (CCV), feline infectious peritonitis virus (FIPV), and human enteric coronaviruses (HECV) (Tyrrell *et al.*, 1978), rabbit coronaviruses (Small *et al.*, 1979; LaPierre *et al.*, 1980), and several others (reviewed by Wege *et al.*, 1982). Table I shows the coronaviruses with their natural hosts and the major diseases which they induce. Clearly the coronaviruses are important pathogens of man and domestic animals. Timely reviews of several aspects of the biology and pathogenesis of coronaviruses have been published by Virelizier (1981), Macnaughton and Davies (1981), and Wege *et al.* (1982).

During the past several years, substantial progress has been made in understanding the structure and replication of coronaviruses. The Symposium on the Biochemistry and Biology of Coronaviruses held in Wurzburg in October, 1980 dramatized the emergence of exciting frontiers in coronavirus research (ter Meulen *et al.*, 1981). Siddell *et al.* (1982) have written an excellent review of the structure and replica-

TABLE I

MEMBERS OF THE CORONAVIRUS GROUP

Common name of virus	Designation	Natural host	Diseases
Avian infectious bronchitis virus	IBV	Chicken	Tracheobronchitis, nephritis, oviduct hypoplasia
Bluecomb disease virus	TCV	Turkey	Enteritis
Mouse hepatitis virus	MHV	Mouse	Hepatitis, encephalomyelitis, enteritis, interstitial pneumonia
Rat coronavirus	RCV	Rat	Pneumonia, rhinotracheitis
Sialodacryoadenitis	SDAV	Rat	Sialodacryoadenitis, keratoconjunctivitis, rhinotracheitis
Transmissible gastroenteritis virus	TGEV	Pig	Gastroenteritis
Hemagglutinating encephalomyelitis virus	HEV	Pig	Encephalomyelitis, gastroenteritis ("vomiting and wasting disease")
Porcine virus CV777	PCV	Pig	Enteritis
Neonatal calf diarrhea coronavirus	BCV	Bovine	Gastroenteritis
Human coronavirus	HCV	Human	Common cold
Human enteric coronavirus	HECV	Human	Gastroenteritis (?)
Canine coronavirus	CCV	Dog	Gastroenteritis
Feline infectious peritonitis virus	FIPV	Cat	Meningoencephalitis, panophthalmitis, peritonitis, pleuritis, pneumonia, wasting disease, vasculitis ("immune complex disease"), disseminated granulomatous disease
Feline enteric coronavirus	FECV	Cat	Enteritis
Pleural effusion disease virus	RbCV	Rabbit (?)	Pleuritis, myocarditis
Rabbit enteric coronavirus	RbECV	Rabbit	Enteritis

tion of coronaviruses, summarizing the state of knowledge shortly after the Wurzburg Symposium.

The purpose of this article is to describe the development of our present understanding of the molecular biology of coronaviruses. We have taken an historical approach to the subject, using figures from some of the key papers to illustrate the development of our present concepts. We are grateful to our colleagues for making these figures and their unpublished data available to us. We hope that this contribution will convey the sense of excitement and cooperation which has characterized this period in coronavirus research.

II. Structure and Organization of Virions

A. Viral Structure

Negative stains of coronaviruses from eggs, clinical specimens or media over tissue, or organ cultures infected with coronaviruses revealed the characteristic viral structure shown in Fig. 1A (Berry *et al.*, 1964; Tyrrell and Almeida, 1967; McIntosh *et al.*, 1967a; Almeida and Tyrrell, 1967; Apostolov *et al.*, 1970; Oshiro *et al.*, 1971; Kennedy and Johnson-Lussenberg, 1975–1976). The virions were spherical, enveloped particles ranging from 80 nm to 160 nm in diameter. They showed some pleiomorphism, and frequently had a shallow central hollow containing some negative stain. Indeed, on the basis of negatively stained images of IBV, Bingham and Almeida (1977) suggested that the morphology of coronavirus virions might resemble a punched-in sphere. Whether this represents the true morphology of the virions or is a deformation resulting from drying and negative staining remains to be determined. Coronavirus morphology has been reviewed by McIntosh (1974), Oshiro (1973), Pensaert and Callebaut (1978), and Robb and Bond (1979a).

Most coronaviruses appear to have only one morphologic type of surface projection or peplomer. The peplomers of coronaviruses are large and roughly club shaped. For MHV, each peplomer is about 20 nm long by 7 nm wide at the tip (Sturman *et al.*, 1980). There are approximately 200 peplomers per virion. It is not known how many glycoprotein molecules form each peplomer. The peplomers of different coronaviruses have somewhat different appearances in negatively stained preparations (Caul and Egglestone, 1977; Davies and Macnaughton, 1979).

For BCV, Bridger *et al.* (1978) have suggested that there may be two morphologically distinct types of peplomers. Analysis of the structural proteins of BCV (Section IIC) also suggested that there might be an additional species of glycoprotein in the virion (King and Brian, 1982). Possibly this additional glycoprotein forms the second type of peplomer. Two types of peplomers have been observed rarely on HEV and MHV virions (Greig *et al.*, 1971; Sugiyama and Amano, 1981). It is not clear to what extent the morphological differences between peplomers of coronaviruses reflect differences in amino acid sequence, glycosylation, proteolytic cleavage, or reduction of disulfide bonds (see Sections II,C and IV,A).

Many preparations of cornaviruses contain some virus particles which partially or completely lack peplomers. Storage of virions may lead to detachment of peplomers, and under some conditions virions lacking peplomers can be formed in infected cells (Holmes *et al.*,

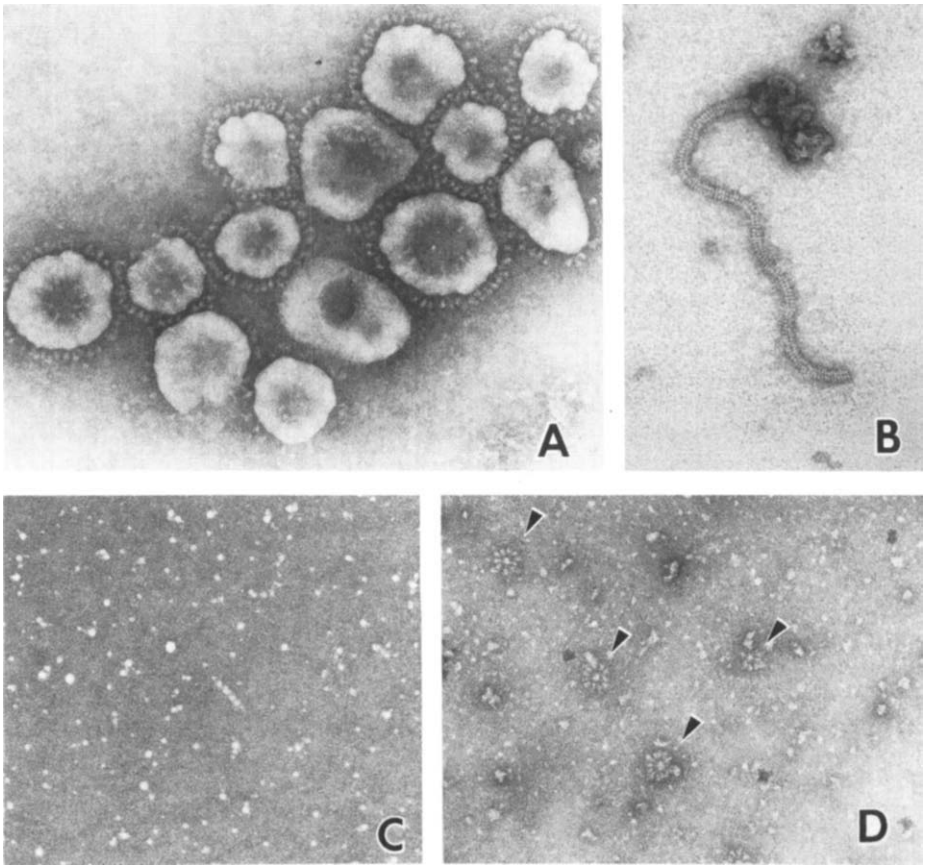

FIG. 1. Ultrastructure of coronavirus virions and viral components. (A) Virions of the avian coronavirus IBV in negatively stained preparation. Characteristic petal-shaped peplomers project from the viral envelope and a central hollow contains a shallow pool of negative stain. ×120,000. (Courtesy of J. Almeida.) (B) Nucleocapsid released from 229E virions and isolated by sucrose density gradient ultracentrifugation after the method in Caul *et al.*, (1979). The helical structure and the hollow central core of the necleocapsid are evident. ×150,000. (Courtesy of E. O. Caul.) (C) The membrane glycoprotein E1 of mouse hepatitis virus (MHV) purified by density gradient ultracentrifugation following detergent disruption of purified virions after the method in Sturman *et al.* (1980). The E1 glycoprotein forms aggregates of irregular sizes ×100,000. (D) The peplomeric glycoprotein E2 of MHV purified by the same technique forms rosettes or single peplomers. Arrows indicate rosettes. ×100,000. (C and D from K. V. Holmes.)

1981a,b; see Section III,D). Macnaughton and Davies (1980) isolated noninfectious, empty IBV particles. Such particles have not yet been identified for other coronaviruses.

The virions of coronaviruses are rather fragile and tend to disrupt upon storage and/or during the negative-staining procedure (Apos-

tolov *et al.*, 1970). This can be prevented by fixation of virions with glutaraldehyde prior to negative staining. In spontaneously disrupted preparations of coronaviruses, fragments of viral envelopes are frequently seen. However, the internal component of coronaviruses has been more difficult to visualize in negatively stained preparations. Thin sections of infected cells or virions demonstrated a flexible, cylindrical nucleocapsid which was probably helical (see Section III,F). Kennedy and Johnson-Lussenberg (1975–1976) showed that thread-like nucleocapsids, 8–9 nm in diameter, were released from disrupted HCV-229E virions. These were very pleiomorphic and may represent strands which had uncoiled from helical nucleocapsids. The most tightly coiled helical nucleocapsids were obtained from virions which were spontaneously disrupted by storage at 25°C overnight. Macnaughton *et al.* (1978) found hollow, helical nucleocapsids, 14–16 nm in diameter and up to 0.32 μm long, released from purified preparations of HCV-229E and MHV-3 virions. The unit length of coronavirus nucleocapsids has not yet been determined, although nucleocapsids up to 6 μm long have been observed (Davies *et al.*, 1981). Caul *et al.* (1979) purified helical nucleocapsids from HCV-229E (Fig. 1B). The nucleocapsid was about 9–11 nm in diameter. Coronavirus nucleocapsids appeared to be more flexible and easier to uncoil than paramyxovirus nucleocapsids. Recent studies of helical nucleocapsids of negative-stranded RNA viruses (Heggeness *et al.*, 1980, 1982) showed that these properties depended upon the ionic strength and cation composition of the buffers. It appears likely that the appropriate conditions for further characterization of the structure of coronavirus nucleocapsids will be identified in the near future.

In addition to permitting analysis of the viral nucleocapsid, disruption of coronaviruses with nonionic detergents such as NP-40 or Triton X-100 has permitted the isolation of the envelope glycoproteins of coronaviruses (Section II,G). The morphology of the two envelope glycoproteins of MHV isolated from detergent-disrupted virions on sucrose density gradients is shown in Fig. 1C and 1D (Sturman *et al.*, 1980).

B. Virus Growth and Purification

Early studies of coronaviruses were hampered by limited virus growth and difficulties with virus purification. Coronaviruses exhibited restricted host ranges in cell culture, low virus yields were usually obtained, and the viruses were highly labile. These difficulties have now been overcome for many coronaviruses (Siddell *et al.*, 1982). Suitable permissive cell types and virus strains have been identified and conditions have been described which result in greater virus stability.

Many human coronaviruses were first identified by their growth and

cytopathogenicity in human embryonic tracheal and nasal organ cultures (Tyrrell and Bynoe, 1965; Almeida and Tyrrell, 1967; McIntosh *et al.*, 1967a). Some of these viruses have not yet been grown in continuous cell lines, and great difficulties are still encountered with primary isolation of HCVs. Although permissive cell hosts have been described for HCV-229E (Hamre and Procknow, 1966; Hamre *et al.*, 1967) as well as for tissue culture-"adapted" HCV-OC43 (Bradburne and Tyrrell, 1969; Kapikian *et al.*, 1969; Bruckova *et al.*, 1970; Gerna *et al.*, 1979; Macnaughton *et al.*, 1980), virus yields of $<10^8$ PFU per milliliter are usually obtained. However, O. W. Schmidt *et al.* (1979) obtained high yields (up to 10^9 PFU per milliliter) of tissue culture-adapted strains of HCV-OC43 and -229E in a human rhabdomyosarcoma cell line. Good growth of some human enteric coronaviruses has also been reported in a human rectal carcinoma cell line (Laporte and Bobulesco, 1981).

Early studies of MHV revealed that productive infection could be obtained in NCTC1469 and L929 mouse cell lines (Manaker *et al.*, 1961; Tanaka *et al.*, 1962; Hartley and Rowe, 1963; Mosley, 1961). However, both of these cell lines contained endogenous retroviruses (David-Ferreira and Manaker, 1965; Dales and Howatson, 1961), thus limiting their usefulness for propagation and biochemical studies of MHV. In 1972, Sturman and Takemoto reported that the growth of MHV was enhanced in AL/N and BALB/c 3T3 mouse cells which were transformed by papovaviruses or retroviruses. A "spontaneously" transformed BALB/c 3T3 cell line, designated 17 Cl 1, was also shown to be a highly permissive host for MHV, yielding $>10^8$ PFU per milliliter. Two additional transformed cell lines have also been found to produce high yields of MHV: DBT, a Schmidt-Ruppin Rous sarcoma virus-induced mouse tumor cell line (Hirano *et al.*, 1974, 1976, 1978), and Sac (−), a Maloney sarcoma virus-transformed mouse cell line which is defective in retrovirus production (Spaan *et al.*, 1981). In contrast to HCV and MHV, no continuous cell line is available which produces large amounts of IBV. Limited growth of a few strains of IBV has been obtained in VERO and BHK-21 cells (Cunningham *et al.*, 1972; Coria and Ritchie, 1973; Otsuki *et al.*, 1979). However, high yields of some strains of IBV have been obtained in primary chick embryo kidney cells (Otsuki *et al.*, 1979; Stern and Kennedy, 1980a).

Another development which facilitated progress in this field was the recognition that coronaviruses are most stable between pH 6.0 and 6.5 (Pocock and Garwes, 1975; Alexander and Collins, 1975; Sturman, 1981) (Fig. 2). At pH 6.0, the half-life of MHV infectivity at 37°C in the presence of 10% fetal bovine serum was 24 hours, whereas at pH 8.0, a 50% loss in virus infectivity occurred in less than 1 hour. The rapid loss

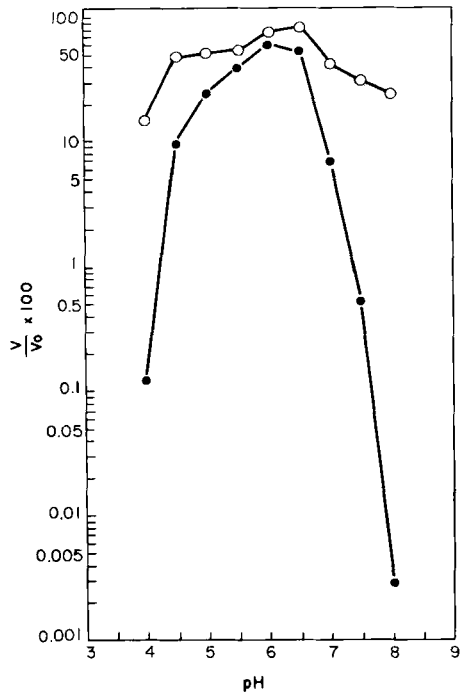

FIG. 2. pH dependennce of thermal inactivation of MHV. Purified virions of MHV were diluted in buffer at different pHs and incubated for 24 hours at 4° (○) or 37°C (●). Stability of viral infectivity is shown as the ratio of viral titer at 24 hours/titer at 0 time, ×100. At 4°C the virus is quite stable from pH 4 to 10. However, at 37°C the virus exhibits marked thermolability at pHs <4.5 and >6.5. (Reproduced from Sturman, 1981, with permission.)

of infectivity at pH 8.0 was associated with aggregation of the peplomeric glycoprotein (Sturman, 1981).

C. Structural Proteins

Several unique features of the coronavirus glycoproteins, as well as the lack of suitable permissive cell types for some coronaviruses and residual host-cell contamination of other coronaviruses, delayed recognition that coronaviruses all possess a similar pattern of structural proteins. Recently, the general organization of coronavirus structural proteins has become apparent. Figure 3 illustrates a model of the structure of MHV-A59. We will use this model and the nomenclature developed during our studies of the structural proteins of MHV for the following discussion of coronavirus structural proteins and their organization.

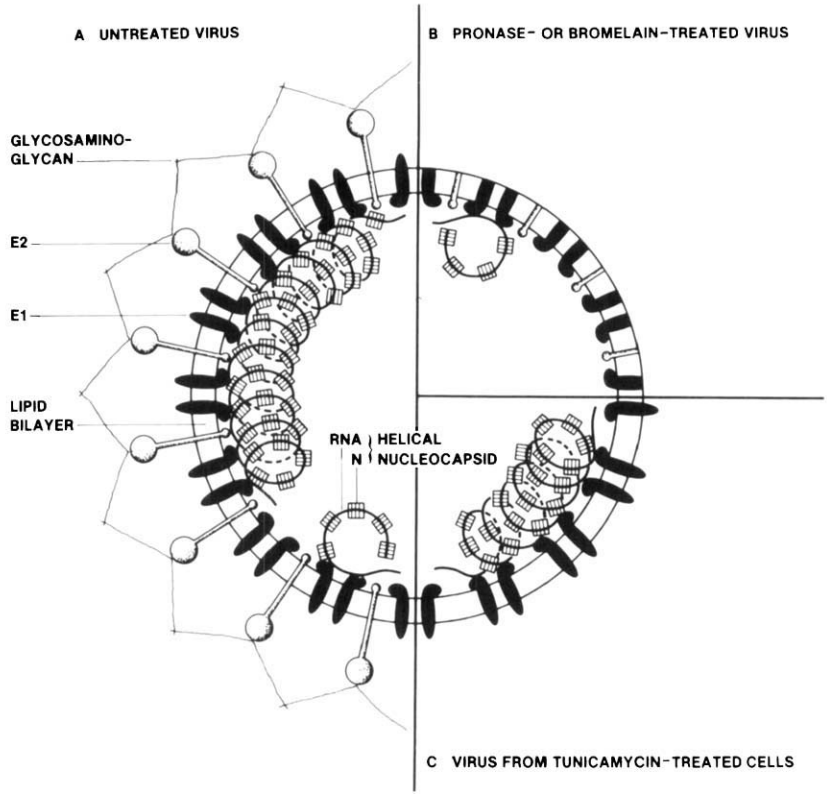

FIG. 3. Model for the structure of the coronavirus MHV. This model is based on studies of the proteins and nucleic acid of MHV virions. (A) The envelope of the intact virions contains two envelope glycoproteins, E1 and E2, in a lipid bilayer. The helical nucleocapsid is composed of a single long strand of message sense, genomic RNA with the nucleocapsid protein, N. Glycosaminoglycan is associated with the viral envelope. (B) Treatment of the virions with Pronase or bromelain removed the bulk of E2, a 5K glycosylated portion of E1, and the glycosaminoglycan, but leaves the nucleocapsid intact. (C) Virions released from cells treated with tunicamycin lack E2 but contain normal amounts of glycosylated E1 and nucleocapsid.

1. Mammalian Coronaviruses

In 1975, Garwes and Pocock characterized the structural polypeptides of TGEV, a porcine coronavirus. Although analysis of coronavirus polypeptides had been attempted earlier, those studies were less definitive since they utilized virus produced in animals or eggs which may have been contaminated with some host-cell components (Hierholzer *et al.*, 1972; Bingham, 1975). Working with radiolabeled TGEV produced in cell culture, Garwes and Pocock identified four major polypeptide peaks on sodium dodecyl sulfate (SDS)–polyacryl-

amide gels. Treatment of virions with bromelain removed the peplomers and the largest glycoprotein (200K), which is analogous to the one which we have called E2 in Fig. 3 (Garwes and Pocock, 1975). A single, nonglycosylated, arginine-rich, 50K species similar to N, and two smaller (28 and 30K) glycoproteins, analogous to E1 in Fig. 3, were also identified and partially characterized (Garwes *et al.*, 1976).

Using double-labeled virus grown in tissue culture, the structural polypeptides of the A59 strain of MHV were described next (Sturman, 1977; Sturman and Holmes, 1977). This virus was shown to contain a nonglycosylated basic polypeptide, N (50K) and five glycoprotein peaks which were separated into two families based on the ratios of incorporation of different radiolabeled precursors. The E2 glycopro-

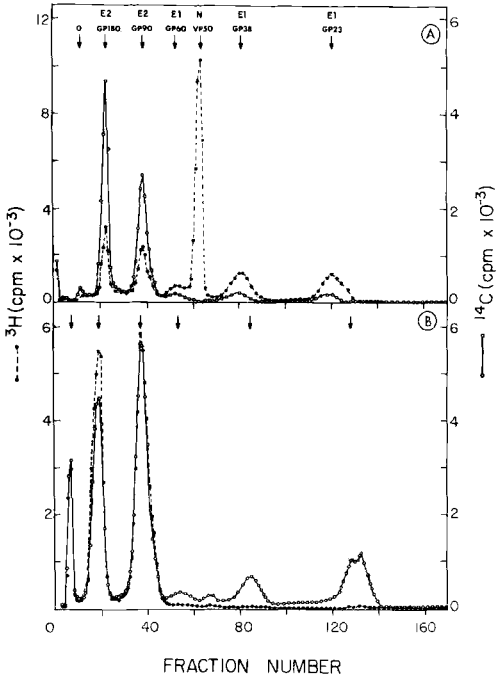

FIG. 4. Polypeptide composition of the virions of MHV. (A) Virions labeled with ^{3}H glucosamine (○——○) and ^{14}C-amino acids (●---●) were solubilized in SDS and analyzed by PAGE. Two classes of glycoproteins, E1 and E2, are identified by the ratios of labels, and a nonglycosylated nucleocapsid protein, N, is seen at 50K. Designation and molecular weights of the viral structural proteins are indicated above the arrows. (B) Virions labeled with ^{14}C glucosamine (○——○) and ^{3}H fucose (●---●) showed two classes of glycoproteins. The E1 glycoproteins were labeled with glucosamine but not with fucose, whereas the E2 glycoproteins were labeled with both. (Adapted from Sturman and Holmes, 1977, with permission.)

teins (gp180 and gp90) were labeled with both fucose and glucosamine, whereas the E1 glycoproteins (gp23, gp38, and gp60) were labeled with glucosamine but not fucose (Fig. 4B). A surprising finding was the demonstration that E1 (gp23) aggregated when heated to 100°C in the presence of SDS and mercaptoethanol, generating several forms of higher apparent molecular weights (Sturman, 1977; Fig. 4B). When virions were solublized in SDS at 37°C, only a single broad peak at 23K was observed (Fig. 5A). The 180K form of E2 could be converted quantitatively to 90K by treatment of intact virions with trypsin, which did not remove the peplomers (Fig. 6; Sturman and Holmes, 1977). When the 180 and 90K E2 glycoproteins were extracted from polyacrylamide gels and further digested with trypsin, virtually identical tryptic peptide patterns resulted. These results suggested either that proteolytic

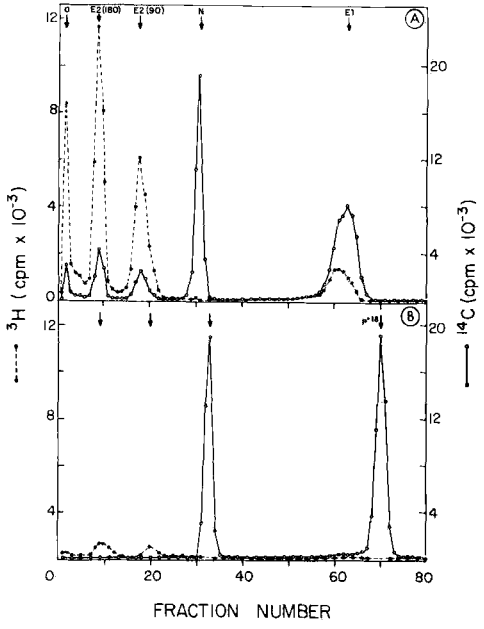

FIG. 5. Effect of boiling on viral polypeptides and effect of protease treatment of virions. (A) Virions labeled with ^{3}H glucosamine (●---●) and ^{14}C-amino acids (○——○) were prepared for PAGE by incubating at 37°C for 30 minutes instead of boiling. The E1 glycoprotein did not aggregate into dimers and trimers as shown in Fig. 4, but migrated as a broad peak of 23K. Designations and molecular weights of the viral structural proteins are indicated above the arrows. (B) When virions similarly labeled were incubated with the proteolytic enzyme bromelain, the E2 glycoprotein and the 5K glycosylated portion of E1 were removed, leaving an 18K portion protected within the viral envelope with the nucleocapsid protein N (VP 50K). (Adapted from Sturman and Holmes, 1977, with permission.)

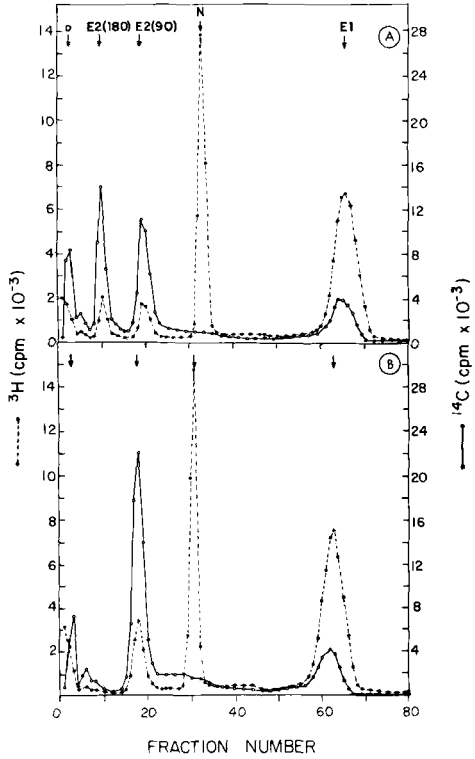

FIG. 6. Cleavage of the E2 glycoprotein by trypsin treatment of MHV virions. (A) Virions labeled with ^{14}C glucosamine (○——○) and ^{3}H valine (●---●) showed E1, N, and two peaks of the E2 glycoprotein at 90K and 180K. (B) Following treatment of intact virions with 10 μg/ml trypsin, the 180K form of E2 was quantiatively converted into the 90K form(s), while the other two structural proteins were unchanged. (Adapted from Sturman and Holmes, 1977, with permission.)

cleavage of the 180K form of E2 yielded two different 90K forms which comigrated, or that the 180K E2 might be a covalently linked dimer of a single 90K species. Thus, although the MHV virion was composed of only three major structural proteins, multiple forms of E1 and E2 were generated by aggregation and proteolysis. Similar observations have been made with some other coronaviruses (see below). The structures and functions of these two glycoproteins will be considered in detail in Section IV.

The study of MHV-A59 also provided information about the relative ratios of the structural proteins and their orientation in the virion. On the basis of incorporation of radioisotopic labels, we estimated that the proteins occur in virions in a ratio of 8 *N*: 16 *E1*:1 *E2* (Sturman *et al.*, 1980). As with TGEV, treatment of virions with bromelain or Pronase

resulted in the loss of E2 (Fig. 5B) and removal of the peplomers or spikes on the virion (Sturman and Holmes, 1977). Pronase also removed a 5K glycosylated portion of E1, which suggested that a terminal glycosylated region of E1 was exposed on the outer surface of the viral envelope, while a larger (18K) nonglycosylated region was protected within the envelope. Since Pronase treatment of intact virions did not affect N (50K), N was thought to be an internal protein. The structural relationships of these three viral polypeptides are summarized in the model in Fig. 3.

Wege *et al.* (1979), investigating the structural proteins of the JHM strain of MHV, detected two species of E1 on SDS–polyacrylamide gel electrophoresis (SDS–PAGE) which appeared to correspond to nonglycosylated and glycosylated forms of E1. In addition, they showed that the E2 (90K) of MHV-JHM could be resolved into two distinct bands. In contrast to E2 from MHV-A59, the E2 of JHM became aggregated with E1 when heated to 100°C and remained near the origin of the resolving gel (Wege *et al.*, 1979; Siddell *et al.*, 1981b). Comparison of a variety of strains of MHV revealed that some of the homologous polypeptides from different strains were distinguishable by PAGE (Stohlman and Lai, 1979; Anderson *et al.*, 1979; Bond *et al.*, 1979; Cheley *et al.*, 1981b). This may be useful in genetic and complementation studies.

Stohlman and Lai (1979) demonstrated that the N polypeptide of MHV was phosphorylated on serine residues (Fig. 7). Subsequently,

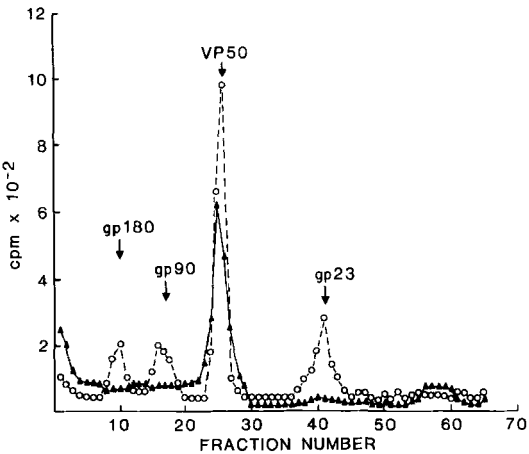

FIG. 7. Phosphorylation of the nucleocapsid protein of MHV. Polypeptides of MHV-A59 virions labeled with [^{32}P]orthophosphate (▲) and ^{3}H-amino acids (○) showing that only the N polypeptide is phosphorylated. (Reproduced from Stohlman and Lai, 1979, with permission.)

Siddell *et al.* (1981a) identified a cyclic AMP-independent protein kinase activity which copurified with the virion (Fig. 8). The functional significance of phosphorylation for transcription, translation, or maturation of the viral nucleocapsid is not yet known.

The nucleotide sequence of the RNA encoding the nucleocapsid protein of MHV-A59 was recently determined by Armstrong *et al.* (1983). This sequence contained a single long open reading frame encoding a protein of molecular weight 49,660 which was enriched in basic residues. There was also a second short, open reading frame in this sequence predicting a polypeptide of 90 amino acids. However, no such product has yet been identified.

The pattern of three major structural proteins and their organization in the virion as shown for MHV-A59 in Fig. 3 is generally applicable to most other species of coronaviruses (reviewed in detail by Siddell *et al.,* 1982). Although the proteins of different coronaviruses have different molecular weights, similar polypeptide patterns have been obtained with the porcine coronaviruses, transmissible gastroenteritis virus, and hemagglutination encephalomyelitis virus (Garwes and Pocock, 1975; Pocock and Garwes, 1977; Callebaut and Pensaert, 1980; K. Moreau and D. A. Brian, personal communication), and with canine coronavirus I71 (Garwes and Reynolds, 1981; Carmichael and Binn, 1981; see the review by Garwes, 1980). The structural polypeptides of several of the mammalian coronaviruses, including those from rats, cats, and rabbits, have not yet been investigated. Macnaughton (1980) and Schmidt and Kenny (1982) reexamined the polypeptide composition of the human coronaviruses 229E and OC43 and obtained results similar to MHV. Schmidt and Kenny demonstrated that the E1 of OC43 aggregated upon heating in SDS under reducing conditions, whereas E1 from 229E did not.

Several coronaviruses may have an additional envelope glycoprotein. In some bovine and porcine coronaviruses, three or four large glycoprotein peaks associated with the virus peplomers have been identified by SDS–PAGE (King and Brian, 1982; Callebaut and Pensaert, 1980), and more than one morphologically distinguishable spike has been detected by electron microscopy (Bridger *et al.,* 1978). It has been suggested that these viruses possess several different types of peplomers. However, the relationship between the components detected on SDS gels and the morphologic subunits of these viruses has not yet been elucidated.

2. *Avian Coronaviruses*

For some time it appeared that the structural polypeptides of an avian coronavirus, IBV, were more complex than those of mammalian

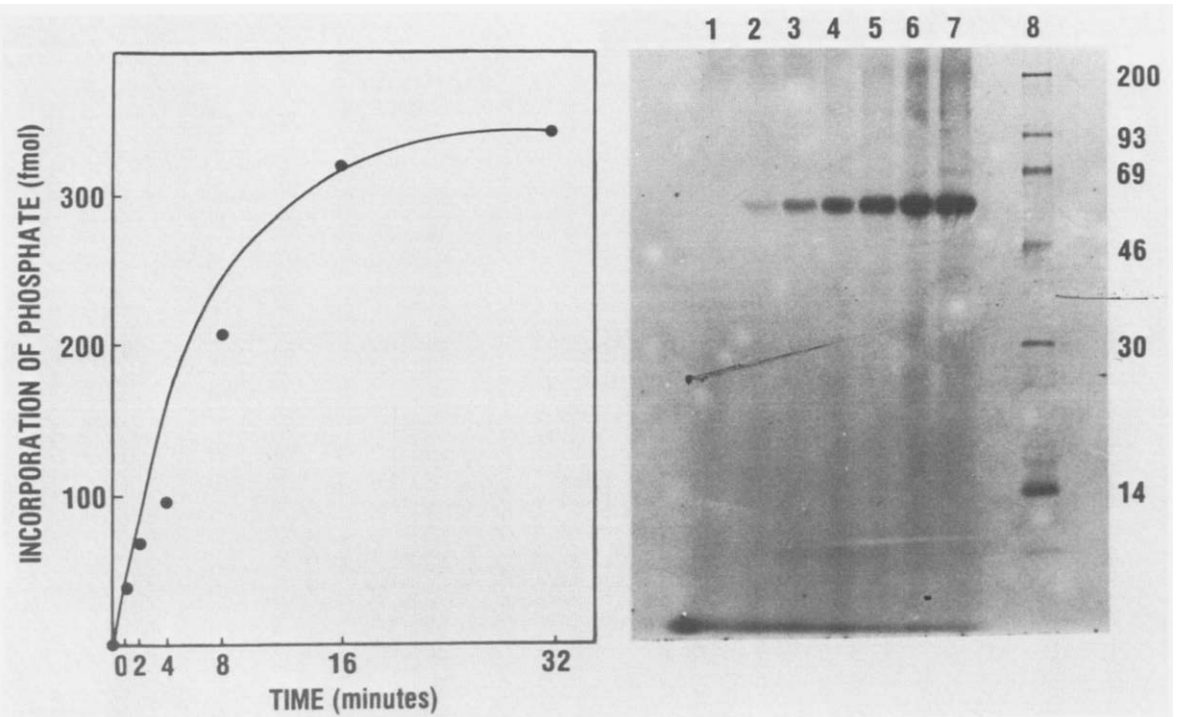

FIG. 8. Demonstration of virion-associated protein kinase activity. Virion-associated protein kinase activity is demonstrated in detergent-disrupted MHV virions by the incorporation of ^{32}P from orthophosphate into protein. The PAGE pattern on the right indicates that the only viral structural protein phosphorylated during this reaction is N. Lanes indicate times after initiation of the reaction; molecular weight standards are shown on the right. (Reproduced from Siddell *et al.*, 1981a, with permission.)

coronaviruses (Bingham, 1975; Collins *et al.*, 1976; Alexander and Collins, 1977). However, Macnaughton and Madge (1977a) demonstrated that harsh conditions of sample treatment generated spurious additional bands on SDS gels. These studies were extended by Collins and Alexander (1980a,b) and Lancer and Howard (1980). By 1981, it was apparent from the work of several investigators (Cavanagh, 1981; Wadey and Westaway, 1981; Lomniczi and Morser, 1981; Macnaughton, 1981; Stern *et al.*, 1982) that there were three major classes of IBV structural polypeptides. Contamination by host polypeptides seems to have caused many of the problems associated with studies using virus grown in embryonated egge (Wadey and Westaway, 1981; Cavanagh, 1981).

Lomniczi and Morser (1981) showed that the N polypeptide of IBV was phosphorylated like that of MHV (Stohlman and Lai, 1979). They found that actin was bound to the surface of purified IBV virions. In contrast, actin has not been detected in purified mammalian coronaviruses. The polypeptide composition of another avian coronavirus, turkey bluecomb disease virus, has not yet been reported.

3. *Oligosaccharides of Coronavirus Glycoproteins*

Differences in the carbohydrate compositions of E1 and E2 for MHV were first indicated by results obtained from metabolic labeling of virions with radioisotopic precursors. E2 was labeled with both fucose and glucosamine, whereas E1 was labeled with glucosamine but not with fucose (Sturman and Holmes, 1977). The carbohydrate compositions of E1 and E2 were analyzed by Niemann and Klenk (1981a,b). Their results are shown in Table II. As coronaviruses were often grouped with myxoviruses in early classification schemes, it is interesting to note that both E1 and E2 contained sialic acid, unlike the myxovirus glycoproteins. E2 also contained substantial amounts of mannose and galactose plus fucose, glucose, and *N*-acetylglucosamine. These sugars are all found in high mannose and complex oligosaccharides which are derived from a mannose–trisaccharide core N-glycosidically linked to asparagine residues in the protein. The oligosaccharide side chains of E1 were strikingly different from those of E2, in that they lacked fucose and contained a high proportion of *N*-acetylgalactosamine, which was absent from E2. Recent evidence indicates that in MHV-infected cells labeled with glucosamine, the glucosamine is converted to *N*-acetylgalactosamine prior to incorporation into the E1 glycoprotein (H. Niemann, personal communication). The carbohydrate composition of the E1 glycoprotein suggested that E1 oligosaccharides might possess O-glycosidic linkages to serine or threonine residues in the protein. The same conclusion was reached by

others (Holmes *et al.*, 1981a,b; Siddell *et al.*, 1981c; Rottier *et al.*, 1981b) based on the resistance of the glycosylation of E1 to tunicamycin, an inhibitor specific for N-glycosylation. Such O-linked glycoproteins had not been found previously in viruses. The glycopeptides of E1 and E2 were readily distinguishable by electrophoresis on borate–polyacrylamide gels at high pH (Sturman, 1981; Holmes *et al.*, 1981a) and by column chromatography on Biogel P6 (Niemann and Klenk, 1981a). Niemann and Klenk (1981b) demonstrated conclusively that the oligosaccharide moieties on E1 were attachd by O-glycosidic linkages since they could be released by β-elimination with sodium borohydride. Recently, H. Niemann *et al.* (personal communication) have used high-performance liquid chromatography (HPLC) to characterize two species of oligosaccharide chains released from E1 by β-elimination. These are shown in Fig. 9. It is highly probable that the virus makes use of host-cell enzymes for O-linked glycosylation as other viruses do for N-linked glycosylation. Thus, the E1 glycoprotein of MHV is of considerable interest as a model for studying the synthesis and glycosylation of O-linked cellular glycoproteins (see Sections III,D and IV,B).

There appears to be considerable variation in the glycosylation of the E1 glycoproteins of different coronaviruses. The E1 of some MHV strains could not be labeled with glucosamine (Anderson *et al.*, 1979) and the E1 of TGEV was labeled with both fucose and glucosamine (Garwes and Pocock, 1975; also see review by Garwes, 1980). Recent

TABLE II

SUGAR COMPOSITION OF GLYCOPEPTIDES FROM E1 AND E2 OF CORONAVIRUS A59[a]

	E1					
	WGA[b] bound		WGA unbound		E2	
Sugar constituent	%	Ratio	%	Ratio	%	Ratio
Fucose	0	0	0	0	3.5	0.47
Mannose	2.54	0.09	3.05	0.18	22.2	3.00[c]
Galactose	28.87	1.00[c]	17.02	1.00[c]	21.3	2.87
Glucose	2.26	0.12	8.76	0.51	6.8	0.92
GlcNAc	28.73	1.00	15.73	0.92	46.3	6.27
GalNAc	59.50	2.16	68.87	4.04	0	0
Neuraminic acid[d]	+		+		+	

[a] From Niemann and Klenk (1981a,b).
[b] WGA, wheat germ agglutinin.
[c] Ratios based on this derivative.
[d] Determinated by high-voltage paper electrophoresis.

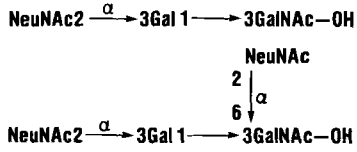

FIG. 9. Structures of the O-linked side chains of glycoprotein E1 of MHV. Two species of oligosaccharide chains were released from glycoprotein E1 of MHV-A59 by β-elimination and purified by high-performance liquid chromatography. The structures for oligosaccharides A and B are based on gas chromatographic–mass spectrometric analysis of partially methylated alditol acetates and sequential degradation by exoglycosidases. (Courtesy of H. Niemann, R. Geyr, and H.-D. Klenk after an article submitted to *J. Biol. Chem.*)

evidence from endoglycosidase H sensitivity and tunicamycin inhibition studies indicated that the E1 glycoprotein of IBV is N-linked, rather than O-linked (Stern and Sefton, 1982c). The biological signficance of N- versus O-linkage of the oligosaccharides is not known.

Other constituents of E1 and E2 have been identified. E1 and E2 could both be labeled with ^{35}S sulfate (Garwes *et al.*, 1976; L. S. Sturman, unpublished data). By analogy with glycoproteins of orthomyxo-paramyxo-, and rhabdoviruses (Nakamura and Compans, 1977; Prehm *et al.*, 1979; Hsu and Kingsbury, 1982), these sulfate moieties may be ester linked to glucosamine or galactosamine residues of oligosaccharide side chains and may contribute to the charge heterogeneity of the viral glycoproteins. Protein sulfation on tyrosine resides may also occur (Huttner, 1982), but this has not yet been reported for viral proteins. The significance of sulfate groups for antigenicity or other biological functions of viral glycoproteins is not known.

M. F. G. Schmidt and his co-workers (1979; Schmidt and Schlesinger, 1979, 1980; Schmidt, 1982a,b) demonstrated that palmitic acid was covalently attached to certain glycoproteins from a variety of enveloped viruses. Niemann and Klenk (1981a) showed that palmitic acid was present on the E2 glycoprotein of MHV, but not on E1 or N. Schmidt reported similar results with BCV (1982). Recently, we separated two E2 (90K) species from trypsin-treated MHV-A59 by SDS–hydroxyapatite chromatography (L. S. Sturman and K. V. Holmes, unpublished data). Only one of these 90K species contained palmitic acid. This palmitic acid may be useful as a marker to identify one 90K subunit of the E2 molecule.

Minor protein species associated with some coronaviruses have also been identified, such as gp65 in MHV-JHM (Wege *et al.*, 1979; Siddell *et al.*, 1981b). The relationship of such minor components to the other

structural proteins of the virion is not yet known. These may represent virus-specific polypeptides which are found in infected cells (see Section III,D).

D. Viral Genome

As with the structural proteins, the earliest data on the coronavirus genome were misleading. Initial observations suggested that coronaviruses contained segmented or multimeric genomes (Tannock, 1973; Garwes *et al.*, 1975). There were also indications of possible RNA polymerase activity associated with the virion (Tyrrell *et al.*, 1975). These findings were in accord with the belief then current that coronaviruses were probably similar to myxoviruses. Then Watkins *et al.* (1975) demonstrated that high-molecular-weight RNA could be extracted from IBV virions. The large, single-stranded, linear RNA molecules obtained from IBV were shown to be polyadenylated and infectious (Schochetman *et al.*, 1977; Lomniczi, 1977; Lomniczi and Kennedy, 1977; Macnaughton and Madge, 1977b). Lomniczi and Kennedy (1977) characterized the IBV genome by electrophoresis on methyl mercury gels and by T1 oligonucleotide fingerprinting. This approach also proved to be very useful in the comparative analysis of coronavirus genomes and subgenomic virus-specific mRNAs (see Section IID). Garwes *et al.* (1975) extracted high-molecular-weight (60–70 S) RNA from TGEV and HEV. However, they observed that the RNA was dissociable above 60°C into 35 and 4 S species. Tannock and Hierholzer (1977) also reported releasing 4 S RNA from HCV-OC43 RNA and fragmentation of the 70 S RNA after heating at 60°C. Lai and Stohlman (1978) found a variable amount of 4 S RNA in MHV preparations, in addition to 60 S RNA. Garwes *et al.* (1975), Pocock and Garwes (1975), Tannock and Hierholzer (1977), and Lai and Stohlman (1978) demonstrated that the size and heterogeneity of the virion RNA which was isolated was affected by the time of virus harvest, the pH of the culture medium, the method of virus purification and duration of virus storage, and the method of RNA extraction. Greater fragmentation of coronavirus RNA was observed if virions were harvested at 24 hours postinfection versus 16 hours, if cultures were kept at pH 7.2 or 8.0 and not at pH 6.5, if virus was purified on potassium tartrate equilibrium gradients instead of sucrose gradients, if virions were stored for 24 hours at 4°C before RNA extraction, and if the RNA was extracted in the presence of phenol. Fragmentation was readily detected after heating the RNA at 60°C or higher, and by centrifugation through dimethyl sulfoxide gradients. This behavior of coronavirus RNA, as well

as other aspects of the structure and physiocochemical properties of coronaviruses, is discussed in the excellent review by Garwes (1980).

It now appears that coronavirus genomes are 5.4–6.9 × 10^6 daltons in size, which corresponds to about 16,000–21,000 nucleotides. RNA genomes in this size range have been detected in virions of IBV (Schochetman *et al.*, 1977; Macnaughton and Madge, 1977b; Macnaughton, 1978; Stern and Kennedy, 1980a), MHV (Yógo *et al.*, 1977; Lai and Stohlman, 1978; Wege *et al.*, 1981b; Macnaughton, 1978; Spaan *et al.*, 1981; Leibowitz *et al.*, 1981; Weiss and Leibowitz, 1981), HCV (Tannock and Hierholzer, 1977; Macnaughton and Madge, 1978; Macnaughton, 1978), TGEV and HEV (Garwes *et al.*, 1975; Brian *et al.*, 1980), and BCV (Brian *et al.*, 1980). The genomic RNA is infectious (Lomniczi, 1977; Schochetman *et al.*, 1977; Wege *et al.*, 1978; Brian *et al.*, 1980), capped (Lai and Stohlman, 1981; Lai *et al.*, 1982a), and polyadenylated (Schochetman *et al.*, 1977; Lomniczi, 1977; Yogo *et al.*, 1977; Macnaughton and Madge, 1977b, 1978; Wege *et al.*, 1978; Lai and Stohlman, 1978; Guy and Brian, 1979; Lai *et al.*, 1981). For further details, see the reviews by Garwes (1980) and Siddell *et al.* (1982).

In 1980, Stern and Kennedy (1980b) mapped the location of the T1 oligonucleotides of the genome in a partial 3′ to 5′ order. Large fragments of RNA were produced by partial alkali fragmentation of the genome. These fragments were fractionated into different size classes by sedimentation on sucrose density gradients, and polyadenylated RNAs were selected for T1 oligonucleotide analysis. The same approach was applied to MHV by Lai *et al.* (1980). These studies disclosed that there was no significant reiteration of oligonucleotides within the genome. Analysis of the genetic complexity of the virion RNA indicated that it was all of the same sense. Since genomic RNA was infectious, the virion RNA must be of positive or message sense.

T1 oligonucleotide analysis of coronavirus genomes has been employed for comparisons of virus isolates and strains, for characterization of mutants, and for epidemiological investigations. The T1 oligonucleotide fingerprints of the two isolates of the Beaudette strain of IBV which were studied by Lomniczi and Kennedy (1977) and Stern and Kennedy (1980a) were found to be quite different. Subsequently, Clewley *et al.* (1981) distinguished 11 oligonucleotide fingerprint patterns from 13 isolates of IBV, revealing differences between IBV serotypes, and also between different preparations of a single serotype. This suggested that considerable variation in the genome may be characteristic of IBV, and possibly of other coronaviruses as well.

It is characteristic of RNA viruses that the frequency of spontaneous mutations is high (Holland *et al.*, 1982), and coronaviruses appear to be

no exception to this rule. Analyses of murine coronaviruses have also indicated that there is considerable diversity between different strains. Wege *et al.* (1981a) and Lai and Stohlman (1981) found that the oligonucleotide fingerprint pattern of the -JHM strain differed significantly from those of MHV-1, -2, -3, -S, and -A59, and that MHV-3 and -A59 were closest in oligonucleotide patterns. Lai *et al.* (1981) have attempted to correlate strain-specific oligonucleotide differences with hepatotropism and neurotropism of MHV-3 and -A59. Stohlman *et al.* (1982b) have characterized oligonucleotide patterns of plaque morphology variants of -JHM that differ in neuropathogenicity.

The genetic relatedness of coronaviruses has also been analyzed by nucleic acid hybridization. Using a cDNA probe representative of the entire genome of MHV-A59, Weiss and Leibowitz (1981) found that MHV-3 and -A59 were more closely related to one another than either was to -JHM. HCV-229E appeared to be quite unrelated to MHV by this technique. Cheley *et al.* (1981b), using a cDNA probe prepared against the mRNA of MHV-A59 which coded for the nucleocapsid protein, obtained evidence of 70–80% homology by analysis of hybridization kinetics of viral RNA from cells infected with MHV-1, -3, -S, and -JHM.

E. Viral Lipids

The lipid composition of coronavirus virions has not been analyzed in detail. It appears likely that the lipids of the viral envelope will reflect the lipid composition of the intracellular membranes from which virus budding occurs (see Section III,F). Indeed, Pike and Garwes (1977) observed that TGEV contained less cholesterol and fatty acid than was found in the plasma membrane of the cells in which the virus was grown. When the virus was grown in different cell types, the viral lipids reflected the overall lipid composition of the cells in which it was grown. These studies need to be extended using various cell-membrane fractions. The role of the lipid composition of cellular membranes in coronavirus maturation remains to be elucidated. It would be interesting to know whether E1 and the viral nucleocapsid preferentially associate with membranes of a certain lipid composition. Boundary lipids associated with the hydrophobic portions of E1 and E2 have not been identified, although palmitic acid has been shown to be covalently attached to E2 (Niemann and Klenk, 1981a,b; Schmidt, 1982a,b) (see Section II,C).

The derivation of coronavirus envelopes from intracellular membranes may render the viral envelope less susceptible to solubilization by bile salts and other detergents than enveloped viruses which bud

from the plasma membrane. Greater stability of the viral envelope to solubilization by bile salts would be consistent with the survival and replication of these viruses in the enteric tract. Comprehensive studies on the relative susceptibility to solubilization of coronavirus envelopes and other viral envelopes have not yet been carried out.

F. Other Host-Derived Components

Several components of normal host cells or tissues have been found to copurify with coronaviruses. The difficulty of obtaining IBV free from host-cell contamination and the association of actin with IBV have already been mentioned (Section II,B and C). In early studies of coronavirus antigens, host antigens were often detected in association with the purified virions. Some components of fetal bovine serum adsorb to and copurify with coronaviruses (Kraaijeveld *et al.*, 1980). It is not yet clear whether the protein kinase associated with coronavirus particles is a host contaminant or a product of the viral genome.

Another class of host molecules which copurified with several different coronaviruses was glycosaminoglycans (GAG) (Garwes *et al.*, 1976; Sturman, 1980). These are polyanionic, linear polysaccharides such as hyaluronic acid, chondroitin sulfate, keratin sulfate, heparan sulfate, and heparin, which are secreted by cells and which may remain associated with their external surfaces (Roden, 1980; Oldberg *et al.*, 1977; Prinz *et al.*, 1980). They tend to aggregate spontaneously with like molecules to form large complexes. Multiple chains of GAG molecules which are linked to core proteins are called proteoglycans. Garwes *et al.* (1976) showed that some sulfated GAG was associated with TGEV. Glycosaminoglycan associated with virions of MHV-A59 was partially characterized by enzymatic and chemical degradation (Sturman, 1980). The GAG associated with MHV-A59 resembled the heparan sulfate species produced by uninfected transformed mouse cells, which contained a reduced level of 6-O sulfated glucosamine residues (Sturman, 1980; Keller *et al.*, 1980; Winterbourne and Mora, 1981). The virion-associated GAG illustrated in Fig. 3 is known to be on the external surface of the viral envelope since it can be removed by protease treatment of intact virions. The number of GAG molecules associated with each virion is not yet known.

Cellular GAGs have been found in association with many types of enveloped viruses (Compans and Pinter, 1975; Pinter and Compans, 1975; Lindenmann, 1977; Kemp *et al.*, 1982), but the biological significance of this association is not known. In cells, heparan sulfate may play an important role in cell–cell and cell–substrate adhesion, growth control, and masking of cell surface receptors (Vannucchi and

Chiarugi, 1977; Rollins and Culp, 1979; Oldberg *et al.*, 1979; Kraemer and Smith, 1974). One could speculate that virion-associated GAGs or proteoglycans could alter viral functions by modifying viral structure, antigenicity, or susceptibility to proteolytic enzymes.

G. Subunits of Virions

Coronavirus particles may spontaneously disrupt to yield membrane fragments and threadlike or helical nucleocapsids (see Section II,A). Viral subunits have also been generated for structural and immunologic analysis by solubilization of the envelope with nonionic detergents such as NP-40 or Triton X-100 in low salt concentrations. After detergent disruption of the viral envelope, solubilized glycoproteins could be separated from the nucleocapsid by sedimentation in sucrose density gradients. Garwes *et al.* (1976) were the first to report isolation of the surface projections and nucleocapsid of a coronavirus, TGEV, by this technique. Immunization with NP-40-solubilized, gradient-purified TGEV suface projections (E2) induced neutralizing antibodies (see Section IV,A). Kennedy and Johnson-Lussenberg (1975–1976) isolated a nucleoprotein from 229E by a similar method. Similar studies were carried out with HEV and MHV-JHM (Pocock and Garwes, 1977; Wege *et al.*, 1979). In these studies, the nucleocapsid sedimented at a density of 1.24–1.29 gm/ml and was found to consist of RNA in association with both N and E1 structural proteins. Electron microscopy revealed spherical "cores" 60 to 70 nm in diameter, sometimes with a strand approximately 9 nm in diameter inside. Helical nucleocapsids (Fig. 1B) were not observed in these studies. In similar studies on NP-40-disrupted MHV-A59 (Sturman *et al.*, 1980), we found that the temperature of solubilization determined whether E1 would be isolated separately or in association with the nucleocapsid. Solubilization at 4°C yielded separate peaks of E1, E2, and nucleocapsid (ρ = 1.28 gm/ml; Fig. 10A), whereas incubation of the viral extract at 37°C for 30 minutes resulted in quantitative binding of E1 to the nucleocapsid forming an E1–N–RNA complex (ρ = 1.22 gm/ml; Fig. 10B). In negatively stained preparations, purified E1 formed irregular aggregates of varied size, whereas purified E2 was in the form of single peplomers or rosette-like aggregates of about 12 peplomers (Fig. 1C and D). Purified E1 and E2 were used to raise monospecific antisera (Sturman *et al.*, 1980) for the analysis of the functions of the glycoproteins (Holmes *et al.*, 1981b; Section IV).

The reasons for the difficulty in isolating helical nucleocapsids from coronaviruses are not yet clear. E. O. Caul (personal communication) has suggested that the helical nucleocapsid in the virion may be in the

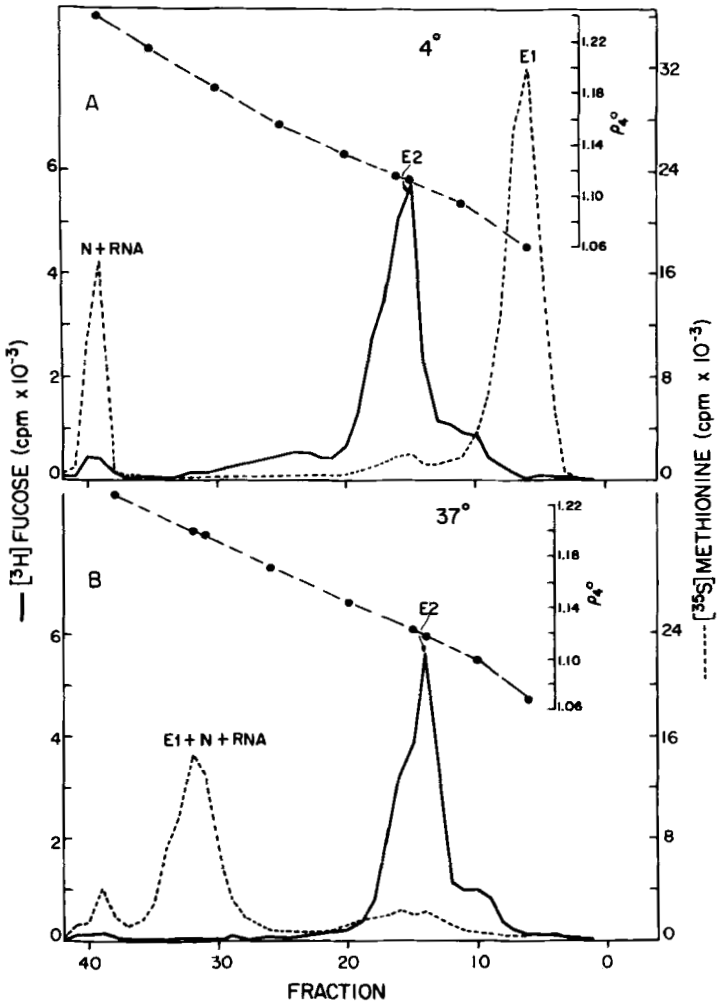

FIG. 10. Separation of components of MHV virions and aggregation of E1 with the nucleocapsid at elevated temperature. (A) The two glycoproteins, E1 and E2, and the nucleocapsid were separated by sucrose density gradient ultracentrifugation following detergent disruption of virions at 4°C. (B) When the solubilized virus was headed to 37°C for 30 minutes prior to centrifugation, the E1 quantitatively bound to the nucleocapsid, forming a new complex. (——) [3H] fucose; (---) [35S] methionine. (Reproduced from Sturman *et al.*, 1980, with permission.)

form of a labile supercoiled structure which may be identical to the 60- to 70-nm spherical forms described above. Alternatively, the 60- to 70-nm particles could represent incompletely solubilized nucleocapsids within a membrane-like structure containing E1. In some intracellular inclusions of nucleocapsids, such a structure has been visualized by

transmission electron microscopy (Dubois-Dalcq *et al.*, 1982; Section III,F). Holmes and Behnke (1981) observed that MHV-A59 virions changed from spherical to flattened, disk-shaped particles during migration from the rough endoplasmic reticulum to the Golgi (Section III,F). Such a change may be correlated with supercoiling of the nucleocapsid strands.

Several investigators have studied the susceptiblity of isolated coronavirus nucleocapsids to digestion with proteases or RNase. Using an electron microscopic assay, Davies *et al.* (1981) showed that the nucleocapsid of IBV was destroyed by trypsin or Pronase and was partially susceptible to degradation by pancreatic ribonuclease.

III. Viral Replication

A. Summary

During the past few years, a comprehensive understanding of coronavirus replication has begun to emerge. Our current concept of coronavirus replication is shown in Fig. 11. Although coronaviruses have structural similarities to the large, enveloped, negative-stranded orthomyxo- and paramyxoviruses, the coronaviruses demonstrate several unique features in their replicative cycle. A nested set of five or six subgenomic mRNAs are elaborated, each of which codes for a single protein. There is some evidence which suggests that RNA fusion may play a role in coronavirus replication. In some cases an O-linked envelope glycoprotein is formed which exhibits restricted intracellular transport. The cellular secretory apparatus may be used for release of virions. While much clearly remains to be learned about the replication of coronaviruses, it is already apparent that they utilize many novel ways of solving the problems of virus replication.

B. Adsorption, Penetration, and Uncoating

Relatively little is known about the earliest stages in coronavirus replication. Although the marked host and tissue tropisms of coronaviruses have frequently been ascribed to possible host-cell receptor specificities, studies on early virus–cell interactions have been limited.

In studies analogous to those done on myxoviruses, early studies of the interaction of coronaviruses with membranes used hemagglutination as a model for binding to the cell surface receptor. Several coronaviruses, including HEV (Greig *et al.*, 1962), IBV (Corbo and Cun-

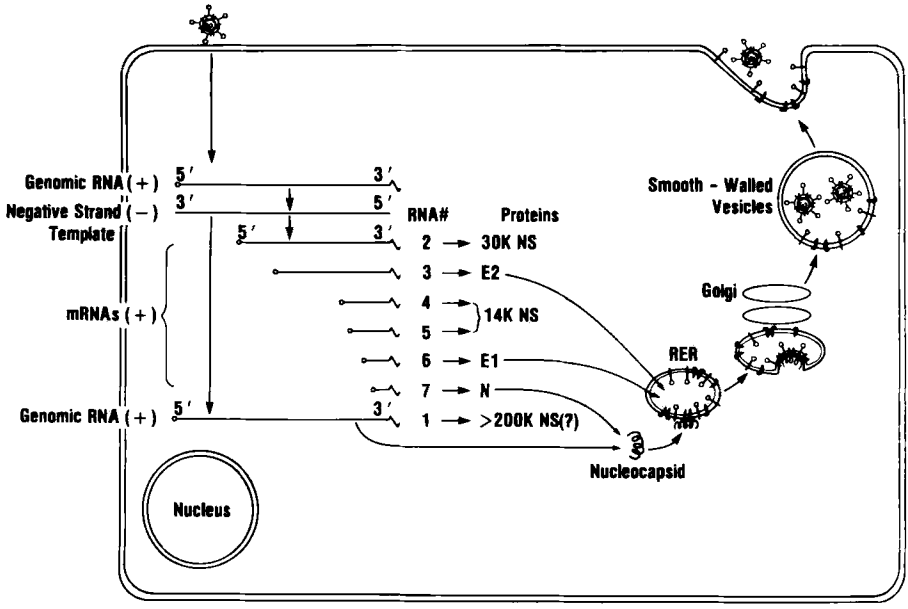

FIG. 11. Replication of coronaviruses. The major features of coronavirus replication are illustrated in this diagram. Virions bind to the cell membrane by means of the E2-containing peplomers. The viral envelope probably fuses with the plasma membrane or with a membrane of an endocytic vesicle releasing the nucleocapsid into the cytoplasm. The entire replicative cycle occurs in the cytoplasm. The genomic RNA acts as mRNA to direct the synthesis of viral RNA-dependent RNA polymerase. This enzyme copies the genomic RNA to form full-length, negative-stranded templates. From these templates, using the viral RNA polymerase, a series of subgenomic mRNAs are synthesized. These mRNAs form a nested set with common 3′ ends. All are capped and polyadenylated. Each of the mRNAs apparently codes for a single gene product. The functions of the nonstructural gene products NS 14K and NS 35K are not known. RNA7 codes for the synthesis of N protein on free ribosomes. The N protein associates with newly formed genomic RNA to form the viral nucleocapsid. RNA3 and -6 are translated on membrane-bound ribosomes to yield E2 and E1, respectively. The peplomeric glycoprotein E2 is cotranslationally glycosylated at asparagine residues and the core oligosaccharides are trimmed as the glycoprotein migrates through the Golgi apparatus. The membrane glycoprotein, E1, migrates to the Golgi apparatus where oligosaccharides are added to the serine residues posttranslationally. Virions are formed by budding in the rough endoplasmic reticulum and Golgi apparatus, but not at the plasma membrane. E2 migrates readily to the plasma membrane, but intracellular transport of E1 is limited to the Golgi apparatus. Virions are released from intact cells by fusion of post-Golgi vesicles with the plasma membrane, possibly using the cellular secretory apparatus. Numerous virions adsorb to the plasma membrane of infected cells. Coronavirus-induced cytopathic effects include cell fusion and rounding of infected cells.

ningham, 1959; Bingham *et al.*, 1975), BCV (Sharpee *et al.*, 1976), rabbit enteric coronavirus (LaPierre *et al.*, 1980), HCV-OC38/43 (Kaye and Dowdle, 1969), and MHV (Sugiyama and Amano, 1980; Walker and Clantor, 1980), can cause hemagglutination (see Section IV,A). Mengeling *et al.* (1972) showed that HEV bound to avian erythrocytes by the tips of the viral peplomers. Binding of IBV to erythrocytes was studied by Bingham *et al.* (1975), who found that the binding was inhibited by protease and neuraminidase treatment, and enhanced by phospholipase C treatment of erythrocytes.

Shif and Bang (1970) suggested that MHV-2 bound equally well to macrophages from mice genetically susceptible or resistant to MHV-2. They demonstrated equivalent amounts of infectious virus remaining in the supernatant medium over macrophage cultures after virus adsorption. Binding of MHV-A59 to L2 cells in spinner culture was studied by Richter (1976), who found that the cell surface receptor activity was removed by protease treatment of the cells. This suggested that the receptor was a protein. Attachment occurred at 4°C and more rapidly at 37°C. Saturation of virus receptor sites was achieved with only about 700 virus particles per cell. Additional studies (Haspel *et al.*, 1981) showed that at 4°C MHV-A59 bound to splenic lymphocytes from susceptible and resistant mice, but not to thymocytes. The interaction of MHV-3 with L cells and cells from susceptible and resistant strains of mice was studied by Krystyniak and Dupuy (1981). At 37°C, radioactive virions bound to macrophages, spleen cells, T lymphocytes, and thymocytes. The virus bound equally well to macrophages from genetically susceptible and resistant mice. This supports the conclusion of Shif and Bang (1970) that genetic susceptibility and resistance are not determined at the level of virus receptors.

The binding of coronaviruses to cells appeared to be via the peplomeric glycoprotein since antibody to the peplomeric glycoprotein E2 inhibited virus infectivity (Garwes *et al.*, 1978–1979), and isolated E2 competed with intact virions for the same cell surface receptor (K. V. Holmes, unpublished observation; see Section IV,B). Scanning electron microscopic analysis of the binding of HCV-229E to cultures of MRC human diploid cells showed that the virions bound randomly to the cell surface at 4°C (Patterson and Macnaughton, 1981). Warming the cultures to 37°C resulted in the loss of virions from the cell periphery, apparently by an energy-dependent capping mechanism.

The penetration and uncoating of enveloped RNA viruses has been studied extensively in recent years using biochemical and electron microscopic techniques. Semliki Forest virus, influenza virus, and vesicular stomatitis virus (VSV) virions bind to cell surface receptors and are internalized via coated pits (Helenius *et al.*, 1980a; Marsh and Hel-

enius, 1980; Matlin *et al.*, 1981, 1982). The vesicles containing virions, which may be similar to the receptosomes of Willingham and Pastan (1980), then appear to fuse with endosomes. At the low pH within the endosomes, the viral envelopes fuse with the endosomal membranes releasing nucleocapsids into the cytoplasmic sap. Proteolytic cleavage of the peplomeric HA glycoprotein is required for fusion of influenza virus envelopes (Huang *et al.*, 1981; White *et al.*, 1981).

Although detailed studies of coronavirus penetration and uncoating have not yet been performed, there are some indications that a similar pathway of virus uptake may occur. Electron microscopic studies of the uptake of MHV and IBV suggested that viral entry was by means of viropexis or endocytosis (Tanaka *et al.*, 1962; David-Ferreira and Manaker, 1965; Sabesin, 1971; Patterson and Bingham, 1976). However, other investigators suggested that coronaviruses entered the cell by fusion with the cell membrane (Doughri *et al.*, 1976). The possibility that MHV-3 may enter the cell by fusion with the plasma membrane was supported by the observation of Krystyniak and Dupuy (1981) that MHV-3 could infect cells treated with cytochalasin B to prevent phagocytosis. Adsorbed virions rapidly became associated with lysosomes (David-Ferreira and Manaker, 1965; Sebesin, 1971). Virus uptake via coated pits was also observed (Chasey and Alexander, 1976; Arnheiter *et al.*, 1982). Chloroquine, a lysosomotropic drug that elevates the pH in lysosomes and prevents penetration of Semliki Forest virus and influenza virus through the endosomal membrane (Helenius *et al.*, 1980b, 1982), was found to inhibit the replication of MHV by affecting a stage subsequent to virus adsorption (Mallucci, 1966).

C. Characterization of Viral mRNAs

In 1979, in the first report on virus-specific RNAs in coronavirus-infected cells, Robb and Bond (1979b) identified multiple size classes of virus-specific RNAs in MHV-JHM- and -A59-infected cells by fractionation of mRNAs on sucrose density gradients. Soon thereafter, Siddell *et al.* (1980) demonstrated that different size classes of poly(A)-containing intracellular MHV-JHM RNAs fractionated on sucrose–formamide gradients directed the synthesis of different structural proteins in cell-free translation systems. The N protein was translated from the smallest (17 S) fraction, whereas E1 was translated from a larger (19 S) class of RNA.

At almost the same time, Stern and Kennedy (1980a,b) showed, in a classic study of IBV RNA, that coronavirus infection resulted in the production of a nested set of subgenomic messenger RNAs with common 3′ ends. In IBV-infected cells, six virus-specific RNA species were

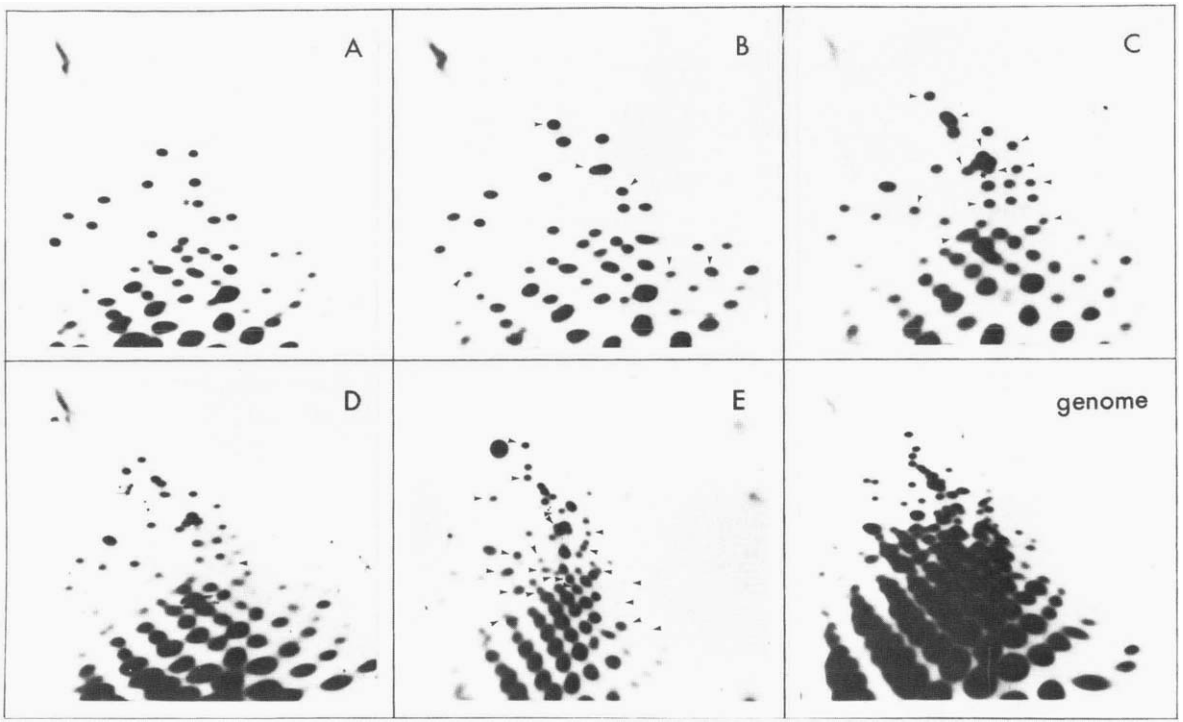

FIG. 12. Oligonucleotide fingerprints of the genomic and mRNAs of IBV. RNase T1 oligonucleotide fingerprints of the five subgenomic mRNAs of IBV are shown in (A) through (E). (A) represents the smallest mRNA, and (E), the largest. The oligonucleotide fingerprint of the genomic RNA is shown on the lower right. Arrowheads indicate the oligonucleotides which were not present in the fingerprints of any smaller mRNA species. Asterisks in (A) and (C) indicate anomalous spots which were not present in fingerprints of the next larger RNA species. Note that all other spots in (A) are present in (B), and those in (B) are present in (C), and so on. This shows that the mRNAs represent overlapping sequences with a common 3′ end. (Adapted from Stern and Kennedy, 1980a,b, with permission.)

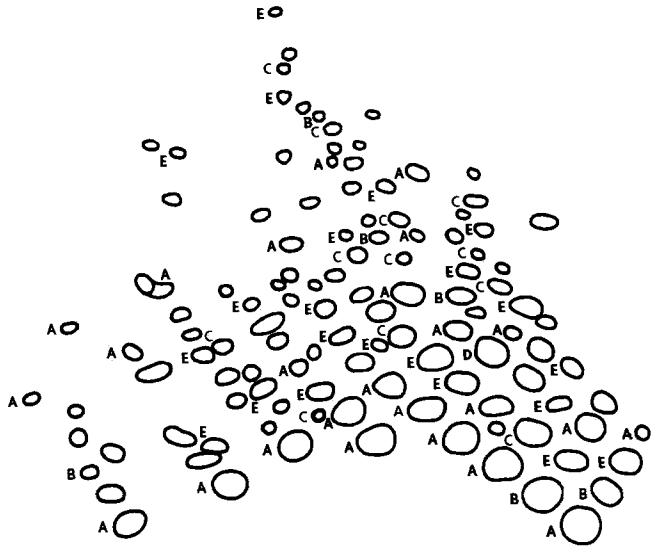

FIG. 13. Diagram of the oligonucleotide fingerprint of the IBV genome. In this diagram each oligonucleotide in the RNase T1 fingerprint is labeled according to the smallest subgenomic mRNA species in which it appears. The unlabeled nucleotides were not included in subgenomic RNA E and hence, presumably, represent sequences between the 5′ end of the genome and RNA E. (Adapted from Stern and Kennedy, 1980a,b, with permission.)

identified by electrophoresis on agarose–glyoxal gels. All of these RNAs were polyadenylated and therefore likely to be of message sense. Together, the five subgenomic species greatly exceeded the total size of the genomic RNA, suggesting that the subgenomic RNAs shared some sequences. Comparison of T1 oligonucleotide digests of these intracellular RNAs, as shown in Figs. 12 and 13, revealed that they formed a "nested" set of sequences. The oligonucleotides of the smallest mRNA were contained within the next larger mRNA, and so on. These data also showed that the genomic RNA was of the same sense as the mRNA since they shared the same oligonucleotides. The possible origin of several unique oligonucleotides found in RNAs A and C will be discussed later. By ordering the T1 oligonucleotides of the genomic RNA through analyses of poly(A)-containing fragments produced by limited alkaline hydrolysis (see Section II,D), Stern and Kennedy (1980b) showed that all of the subgenomic mRNAs shared common sequences extending from the 3′ terminus of the genome.

A similar structure for the intracellular RNAs of MHV was also demonstrated. Spaan *et al.* (1981) isolated six subgenomic, virus-specific RNAs from polysomes of MHV-A59 infected cells, and Wege *et al.*

(1981b) identified six intracellular RNA species in cells infected with MHV-JHM. Weiss and Leibowitz (1981) and Cheley *et al.* (1981a) showed, by hybridization with a cDNA probe against the 3′ end of the smallest message, that all of the subgenomic RNAs of MHV-A59 contained sequences common to the 3′ end. T1 oligonucleotide fingerprints of subgonomic RNAs of MHV were analyed by Leibowitz *et al.* (1981), Lai *et al.* (1981), and Spaan *et al.* (1982). The studies showed that, like avian coronaviruses, for the murine coronavirus MHV-A59, the oligonucleotides of each of the subgenomic RNAs were included within the next larger species, starting from the 3′ end of the genome. A tentative map of the MHV-A59 genome based on these data is shown in Fig. 14. Recently, a similar pattern of overlapping mRNAs has been demonstrated by Heilman *et al.* (1982, and personal communication) for the early and late regions of the DNA-containing bovine papilloma virus.

Using a cDNA probe for the 3′ end of MHV RNA, Cheley *et al.* (1981b) found differences in the elctrophoretic mobility of several subgenomic RNAs of MHV-S in comparison with homologous RNAs of MHV-1, -3, -A59, and -JHM. Leibowitz *et al.* (1981) found that the intracellular RNAs appeared to be present in different ratios in cells infected with different strains of MHV (Table III). The ratios of mRNAs to each other did not change significantly during the course of viral infection (Stern and Kennedy, 1980a; Wege *et al.*, 1981b; Spaan *et al.*, 1981; Leibowitz *et al.*, 1981).

Messenger RNA coding assignments for the structural proteins of MHV have been established by cell-free translation experiments by Siddell *et al.* (1980, 1981c), Leibowitz and Weiss (1981), and Leibowitz *et al.* (1982b), and from translation experiments in *Xenopus laevis* oocytes by Rottier *et al.* (1981a) (summarized in Fig. 11, and see Section III,D). The intracellular RNAs of MHV have been designated 1 through 7, beginning with genomic RNA1, and proceeding to the smallest mRNA, 7. Each virus-specific primary translation product has been shown to be associated primarily with one mRNA (Fig. 11).

FIG. 14. Tentative map of the genomic RNA of MHV. Based on the *in vitro* translation of isolated mRNAs for several MHV strains by Siddell *et al.* (1980,1981c), Leibowitz *et al.* (1982b), and Rottier *et al.* (1981a), and the oligonucleotide mapping of Lai *et al.* (1981), we have drawn a tentative map of the MHV genome. Although additional details will become available, it seems clear that the genes which have been identified to date are arranged in this order.

TABLE III

THE SIZE AND RELATIVE MOLAR AMOUNTS OF MHV-SPECIFIC RNA[a]

RNA species	Molecular weight	Relative molar amounts[b]	
		A59	JHM
Virion RNA	6.1×10^6	—	—
RNA1	6.1×10^6	3.33 (1.48–4.20)	1.50 (0.66–2.26)
RNA2	3.4×10^6	2.00 (1.31–2.81)	2.92 (2.63–3.24)
RNA3	2.6×10^6	3.24 (2.83–5.16)	5.23 (3.32–6.92)
RNA4	1.2×10^6	3.09 (1.00–4.52)	1.69 (1.14–2.21)
RNA5	1.08×10^6	11.0 (7.70–22.5)	0.86 (0.23–1.80)
RNA6	8.4×10^5	32.6 (26.5–38.1)	31.5 (24.7–46.3)
RNA7	6.3×10^5	100	100

[a] From Leibowitz *et al.* (1981).

[b] The data presented are the mean of five determinations of preparations labeled from 4 to 8 hours postinfection. The range of values observed is in parentheses.

Comparison of each RNA with the size of its translation products suggested that only the gene proximal to the 5′ end of each mRNA was translated. As shown in Fig. 15 from the study by Rottier *et al.* (1981a), the product of RNA7 was protein N (see Section III,C,1), that of RNA6 was E1, and of RNA3, E2. The coding assignments for several nonstructural proteins were deduced by Siddell *et al.* (1980, 1981c), Leibowitz and Weiss (1981), and Leibowitz *et al.* (1982b). RNA2 directed the synthesis of a 30–35K nonstructural (NS) protein; RNA4 or -5, a 14K NS protein; and RNA1, several related NS proteins which were >200K. These data have been incorporated into the tentative map for the genomic RNA of MHV-A59 shown in Fig. 14.

Thus, the current dogma of coronavirus replication is that each mRNA directs the synthesis of a single protein using only the gene at the 5′ end of the RNA. However, some caution must be exercised in accepting this as proven. In all of the *in vitro* translation studies, RNA6 has been shown to direct the synthesis of E1, plus a fairly large amount of N (Siddell, 1980, 1981c; Rottier *et al.*, 1981a; Leibowitz and Weiss, 1981; Leibowitz *et al.*, 1981; Fig. 15). This has been ascribed to contamination of RNA6 with RNA7 and a higher efficiency of translation of RNA7. It is possible that RNA6 alone might direct the synthesis of several gene products, both E1 and N. In Semliki Forest virus, an enveloped, positive-stranded RNA containing alphavirus, a large polycistronic mRNA is translated to yield both glycosylated envelope glycoprotein and nonglycosylated capsid protein (Schlesinger and Kaariainen, 1980).

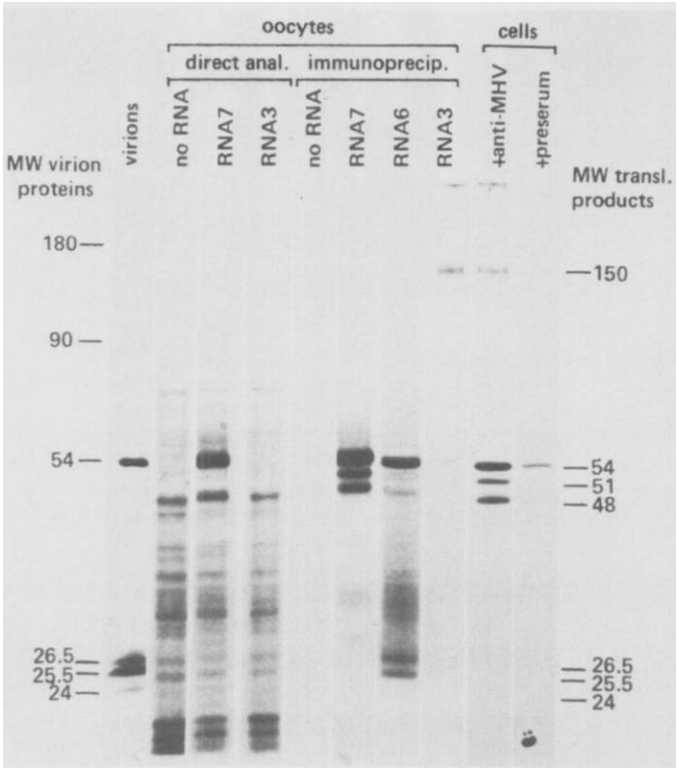

FIG. 15. *In vitro* translation of subgenomic mRNAs of MHV-A59. Isolated subgenomic mRNA 3, -6, and -7 from cells infected with MHV-A59 were translated in the frog oocyte system. Translation products were analyzed by PAGE directly or following radioimmunoprecipitation. Virion polypeptides are shown on the left, and immunoprecipitates of viral structural proteins from extracts of infected cells are shown on the right. (Reproduced from Rottier *et al.*, 1981a, with permission.)

The translation of RNA4 and -5 of MHV has been difficult to study because these RNA species are present in such small amounts. So far only the 14K NS protein has been identified as a product for these two mRNAs. *In vitro* translation studies using microsomal membrane fractions have not yet been done with coronavirus mRNAs. Such studies would permit the analysis of glycosylation, acylation, and processing of the glycoproteins.

D. Kinetics of Intracellular Synthesis, Processing, and Transport of Viral Proteins

Initial studies of intracellular virus-specific proteins (Bond *et al.*, 1979; Anderson *et al.*, 1979) identified the three major structural proteins, E1, E2, and N, and several nonstructural proteins. No high-

molecular-weight polyproteins were detected in infected cell . Concurrent studies of the structural proteins of the virion and analyses of the mRNAs and their translation products set limits on the probable number of virus-specific polypeptides, and established that the structural proteins were not derived from a large polyprotein precursor. The intracellular proteins of MHV and IBV were identified in many laboratories at almost the same time. Much of this information was presented at the 1980 Coronavirus Symposium (ter Meulen *et al.*, 1981) and was summarized in the review by Siddell *et al.* (1982). The intracellular proteins identified included N, E1, and E2, and three nonstructural species: 30–35K and 14K nonglycosylated polypeptides, and a 65K glycoprotein. The 30–35K species has not been detected in virions. However, minor proteins of approximately 14K and 65K have been found in some coronaviruses (Wege *et al.*, 1979; Siddell *et al.*, 1981a; Lai and Stohlman, 1981; Rottier *et al.*, 1981b, Stern *et al.*, 1982), though not in others (e.g., Sturman, 1977; Macnaughton, 1981; Rottier *et al.*, 1981b; Lomniczi and Morser, 1981; Niemann and Klenk, 1981a; Bond *et al.*, 1981; see Siddell *et al.*, 1982, for further references). The significance of these findings is not known. The 65K species has not yet been associated with a virus-specific mRNA.

Much of our understanding about the synthesis and processing of coronavirus proteins *in vivo* has been obtained from pulse-labeling and pulse-chase experiments with MHV. Several different virus–cell systems have been studied ranging from highly lytic ones involving L, DBT, and Sac(−) cells, in which virus infection induced syncytia formation and destroyed the cells within 10–12 hours (Anderson *et al.*, 1979; Cheley *et al.*, 1981b; Siddell *et al.*, 1980; Spaan *et al.*, 1981), to a more moderate infection in 17 Cl 1 cells, in which the infected cells could survive for more than 24 hours without significant cytopathic effects (CPE) (Robb and Bond, 1979b; Sturman *et al.*, 1980; Holmes *et al.*, 1981b). Not surprisingly, differences were detected in the rates of shutdown of cellular protein synthesis in these different systems. Other differences between lytic and moderate coronavirus-cell interactions were also noted. Synthesis of MHV proteins in lytic infections appeared to be coordinated throughout the replication cycle (Siddell *et al.*, 1981b; Rottier *et al.*, 1981b), whereas in cells showing minimal CPE, the synthesis of N was detected much earlier than that of E1 and E2 (J. Behnke, personal communication). Pulse-labeling experiments at different times after infection and at different temperatures revealed that the synthesis of E1 and E2 in these cells was coordinated, but different from the synthesis of N.

The transit time for the synthesis of the viral glycoproteins, their incorporation into virions, and release of the virions from the infected cells also differed in moderate and lytic infections. In moderate infec-

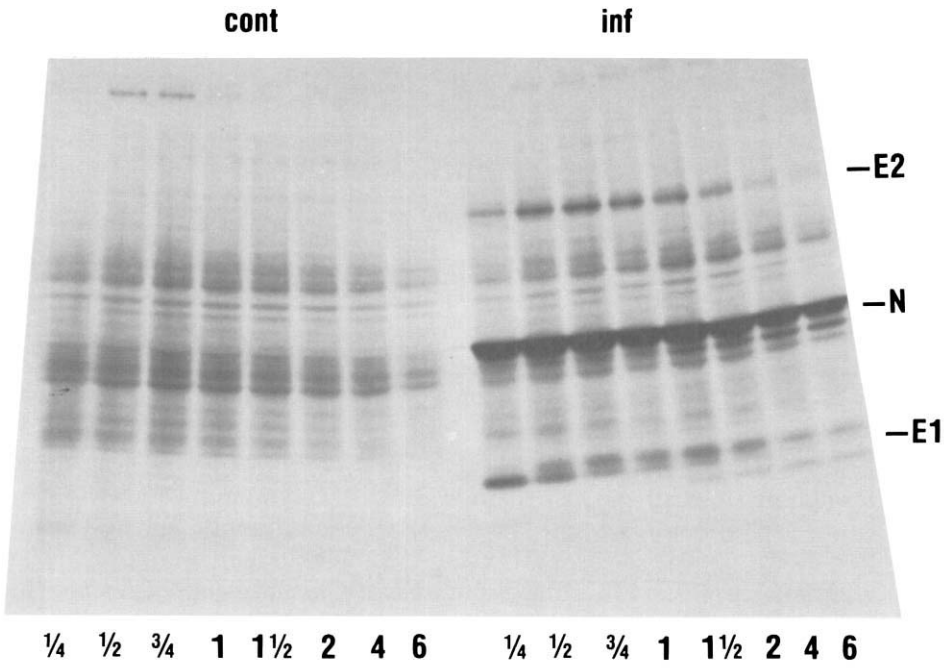

FIG. 16. Synthesis and processing of MHV structural polypeptides (cont, control; inf, infected). At 6 hours after infection with MHV-A59, cells were pulse labeled for 15 minutes with [^{3}H]-leucine and then incubated with excess cold leucine. There were no polyproteins observed. E2 is synthesized as the high-molecular-weight form, and no 90K E2 was observed in these cells. The N protein was synthesized in large amounts and appeared to be processed into two faster migrating species. The E1 was synthesized as a nonglycosylated species which was posttranslationally glycosylated. Both the glycoproteins were chased out of the cell into mature virions within 2–3 hours after labeling. Only a small fraction of the N protein was chased into mature virions. (Adapted from Holmes *et al.*, 1981b, with permission.)

tion, E1 and E2 were quantitatively chased out of cells and into virions within about 2 hours (Holmes *et al.*, 1981b; Fig. 16). However, in lytic infection of Sac(−) cells, E1 chased into virions within 2–2.5 hours after labeling, while much of the E2 remained cell associated for up to 3 hours (Siddell *et al.*, 1981b). Another difference between lytic and moderate infections related to the appearance of E1 and E2 on the surface of infected cells. Both E1 and E2 antigens of MHV-JHM were detected on the surface of lytically infected L cells prior to the release of progeny virions (Collins *et al.*, 1982). In contrast, E2 was the predominant viral glycoprotein on the surface of 17 Cl 1 cells during the

early stages of a moderate infection with MHV-A59 (Doller and Holmes, 1980; Section III,D,2). To date, cleavage of the E2 glycoprotein has been detected only in lytically infected cells. Indeed, cleavage of E2 may be responsible for the extensive cell fusion seen in lytically infected cultures (L. S. Sturman and K. V. Holmes, unpublished observation). These host-dependent differences may reflect differences in host-dependent processes required for maturation of coronaviruses. The features of the synthesis, processing, and transport of coronavirus structural proteins which are consistent in all cell systems are described in the following paragraphs.

1. N

Although the time of appearance of labeled N paralleled the time of appearance of the labeled glycoproteins in virions, no significant decrease in the amount of N in the infected cell was detected during a 90- to 120-minute chase period (Anderson *et al.*, 1979; Bond *et al.*, 1981; Holmes *et al.*, 1981b; Rottier *et al.*, 1981b; Siddell *et al.*, 1981b). This suggested that there was a large intracellular pool of N, most of which did not chase into virions, but was incorporated into nucleocapsids or replicative intermediates which never left the cell. Recently, it was shown that N was synthesized on free ribosomes (Niemann *et al.*, 1982). Intracellular N was phosphorylated at serine residues, as was N in the virion (Siddell *et al.*, 1981a,b). During a 2-hour chase, an intracellular form of N with slightly greater electrophoretic mobility was detected within infected L cells (Anderson *et al.*, 1979). This process was believed to be due to proteolytic processing of N (Cheley and Anderson, 1981). The proportion of the smaller species increased following immunoprecipitation (Siddell *et al.*, 1980; Rottier *et al.*, 1981a), which led to the suggestion that these additional species represented molecules of N partially degraded by serum or cellular proteases. In pulse-labeling studies, these forms of N have been detected in cells without immunoprecipitation late in the infectious cycle of MHV-A59 (J. N. Behnke and K. V. Holmes, unpublished observations). Analysis of peptide maps of these different forms of N will be required to determine their relationships.

2. E1

E1 appeared to be synthesized as a nonglycosylated 20K apoprotein which was posttranslationally glycosylated (Holmes *et al.*, 1981b; Niemann and Klenk, 1981a; Rottier *et al.*, 1981b; Siddell *et al.*, 1981c). The addition of sugars to this O-linked glycoprotein began 15 to 30 minutes after completion of the apoprotein, and continued for 1–2 hours (Holmes *et al.*, 1981b; Rottier *et al.*, 1981b) with production of

two or three discrete glycosylated species. However, not all of the E1 which entered the virion was glycosylated (Rottier *et al.*, 1981b). The oligosaccharide side chains of the E1 glycoprotein are shown in Fig. 9. Niemann *et al.* (submitted for publication) have estimated that there are three oligosaccharide chains per E1 molecule. Glycosylation of E1 is resistant to tunicamycin (Holmes *et al.*, 1981a,b; Niemann and Klenk, 1981a; Rottier *et al.*, 1981b; Siddell *et al.*, 1981c). Recent cell fractionation studies (Niemann *et al.*, 1982; M. Frana, unpublished observation) showed that E1 was translated on membrane-bound polysomes. Monensin inhibited glycosylation of E1 (Niemann *et al.*, 1982).

The intracellular transport of the E1 glycoprotein is markedly different from that of other viral glycoproteins. Immunofluorescent staining with monospecific anti-E1 antibody showed that early in the infectious cycle E1 was restricted to the perinuclear area of infected cells and accumulated in the Golgi apparatus (Doller *et al.*, 1982; Fig. 17). In contrast, E2 rapidly dispersed throughout the cell membranes and appeared on the plasma membrane. The mechanisms and signals for intracellular transport of E1 are not yet understood. Possibly E1 is transported by cellular mechanisms which transport cellular glycoproteins destined for the Golgi apparatus. Since E1 is a transmembrane protein and has been shown to interact with viral nucleocapsid *in vitro,* it appears likely that the localization of E1 on the rough endoplasmic reticulum and Golgi membranes determines the site of virus budding.

3. E2

E2, the peplomeric glycoprotein, was recently shown to be synthesized on membrane-bound ribosomes (Niemann *et al.*, 1982). Pulse-labeling studies showed that a large, 150–180K glycoprotein was the first form detected in infected cells (Holmes *et al.*, 1981a; Rottier *et al.*, 1981b; Siddell *et al.*, 1981c). As noted below, there is considerable controversy over the relationship between the 180 and 90K forms of E2. This controversy may relate to differences in processing of E2 in different cell types. A 110–120K apoprotein was detected in MHV-A59 infected Sac(−) and 17 Cl 1 cells treated with tunicamycin (Siddell *et al.*, 1981c; Rottier *et al.*, 1981b; Niemann and Klenk, 1981a). This is similar to the *in vitro* translation product of RNA3 in L-cell or reticulocyte lysates in which glycosylation does not occur (Rottier *et al.*, 1981a; Siddell *et al.*, 1980, 1981c), and probably represents the protein moiety of the E2 glycoprotein. Translation of mRNA3 in *Xenopus laevis* oocytes permitted glycosylation and yielded a 150K E2 glycoprotein (Rottier *et al.*, 1981a; Fig. 15). Pulse-labeling experiments with MHV-A59 and -JHM in Sac(−) cells showed that the first form of E2 detected

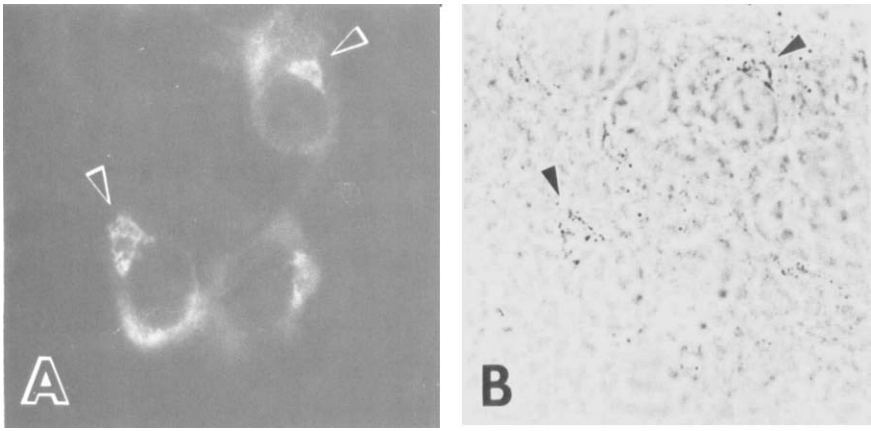

FIG. 17. Localization of E1 in the Golgi apparatus. (A) Monospecific anti-E1 antiserum was used to stain E1 antigens within the cytoplasm of infected cells. The E1 accumulated in a sharply demarcated region near the nucleus and did not migrate to the plasma membrane as readily as did E2. (B) The same cells were labeled by the thiamine pyrophosphatase histochemical reaction which labels the terminal saccules of the Golgi apparatus. This demonstrates that the E1 accumulates in the Golgi apparatus. ×960. (From E. W. Doller.)

in these cells was a 150K species (Siddell *et al.*, 1981b,c; Rottier *et al.*, 1981b). Similar experiments using MHV-3 and -A59 in L and 17 Cl 1 cells, respectively, demonstrated a 180K, rather than a 150K, product (Cheley and Anderson, 1981; Holmes *et al.*, 1981b). The difference between the 180 and 150K moieties has not been identified, but could relate to additional glycosylation, trimming, or sulfation of E2.

The appearance of the 90K species of E2 is different in different cell types. Although in moderate infection of MHV-A59 in 17 Cl 1 cells, little or no 90K E2 was detected at 8–10 hours after infection (Holmes *et al.*, 1981b; Fig. 16), in Sac (−) cells infected with MHV-JHM or -A59, a substantial amount of 90K E2 was detected after 60- to 90-minute chase (Siddell *et al.*, 1981c; Rottier *et al.*, 1981b). Siddell *et al.* (1981c) have suggested that the 150K precursor to E2 may be cleaved to a 90K protein which dimerizes to form the 180K E2. Based on our studies with MHV-A59, we believe that two different 90K forms of E2 result from proteolytic cleavage of the 180K E2 which occurs as a late step in the intracellular transport or processing of E2 and the maturation of the virions. Recently, Stern and Sefton (1982b) showed by tryptic peptide mapping that the two large virion glycoproteins of IBV, gp90, and gp84, were produced by cleavage of a 155K glycoprotein precursor (gp155). Although the cellular location at which the E2 glycoprotein

undergoes acylation has not been identified, acylation of the VSV glycoprotein has been shown to occur near the Golgi complex (Schmidt, 1982b).

The intracellular transport of E2 appears to be similar to that of N-linked glycoproteins of other viruses such as orthomyxo-, paramyxo-, rhabdo-, and alphaviruses. Immunofluorescent staining of E2 with monospecific antiserum stained the cytoplasm diffusely. E2 appeared on the plasma membrane at a time when intracellular transport of E1 was directed to the Golgi apparatus (Holmes *et al.*, 1981b; Doller *et al.*, 1983). Treatment of MHV-infected cells with tunicamycin resulted in a marked inhibition in the synthesis of E2 (Holmes *et al.*, 1981b), although late in infection some nonglycosylated E2 could be detected (Niemann and Klenk, 1981a). Virions isolated from tunicamycin-treated cells contained no E2 (Sturman, 1981) and no peplomers (Holmes *et al.*, 1981a,b). This suggested that E2 was not required for virus budding or for the release of virions from infected cells.

E. Transcription of Viral RNA

Dennis and Brian (1981, 1982) and B. W. J. Mahy *et al.* (1983) first detected RNA-dependent RNA polymerase activity in cells infected with TGEV and MHV. This activity was insensitive to antinomycin D and was associated with cytoplasmic membrane fractions like that of alphaviruses. Brayton *et al.* (1982) and Lai *et al.* (1982b) have characterized the viral RNA polymerase activity in MHV-A59-infected cells. By pretreatment of cells with actinomycin D for 1 hour before infection and synchronization of infection by adsorbing virus at 0–4°C, Brayton *et al.* (1982) detected virus-specific RNA synthesis in MHV-A59-infected cells as early as 1 hour after infection. Two peaks of virus-specific RNA synthesis were demonstrated, one early (2 hours) and the other late (6 hours) after infection (Fig. 18). Corresponding to these, two different virus-specific RNA polymerase activities were detected, early and late in infection. These two polymerases were distinguished by different responses to potassium and different pH optima. The RNA product of the early polymerase was of negative-strand polarity, complementary to the genomic RNA, whereas the products of the late polymerase activity were predominantly of positive polarity (P. R. Brayton, personal communication). Only a single virus-specific, negative-stranded RNA species was detected. This was the size of the complete viral genome. A double-stranded RNA form was isolated which contained RNA of genomic size. When this double-stranded RNA was isolated without RNase treatment and heated, subgenomic mRNAs were released. This suggested that the virus-specific mRNAs were

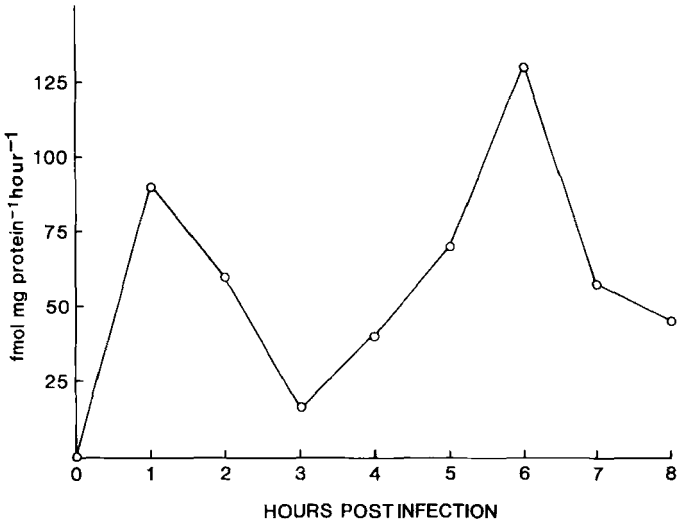

FIG. 18. RNA-dependent RNA polymerase activities in MHV-infected cells. Incorporation of radiolabel into virus-specific RNA in cells infected with MHV-A59 occurs in two peaks which show different ionic requirements. The early peak is believed to represent synthesis of full-length, negative-stranded RNA templates, and the later peak is believed to represent synthesis of mRNAs and genomic RNA. (Reproduced from Brayton *et al.*, 1982, with permission.)

transcribed from a negative-strand RNA template of genomic size (Lai *et al.*, 1982b).

The mechanism which regulates the frequency of transcription of each mRNA species from the negative-stranded RNA template remains to be elucidated. The relative rates of synthesis of the mRNAs appear to be constant throughout infection (Stern and Kennedy, 1980a; Wege *et al.*, 1981b; Spaan *et al.*, 1981; Leibowitz *et al.*, 1981). The smaller mRNAs (numbers 7 and 6), which represent the 3′ end of the genome, are far more abundant than the sum of all the others (Jacobs *et al.*, 1981; Lai *et al.*, 1981; Leibowitz *et al.*, 1981; Table III). In different virus strains, the relative abundance of the different viral mRNA species varies considerably. Leibowitz *et al.* (1981) have shown (Table III) that the relative molar amount of RNA5 synthesized in MHV-JHM-infected cells is about one tenth of that found in cells infected with MHV-A59.

A central question in the molecular biology of coronaviruses is how the subgenomic mRNAs and genomic RNA are transcribed from the negative-strand template. Ultraviolet transcription mapping was done to identify the size of the template(s) for the synthesis of the mRNAs. Jacobs *et al.*, (1981; Table IV) and Stern and Sefton (1982a) found that

TABLE IV

COMPARISON OF THE MOLECULAR WEIGHTS OF THE MHV-A59 INTRACELLULAR RNAS AND THE UV TARGET SIZES OF THEIR RESPECTIVE TEMPLATES[a]

Experiment	RNA	$K \times TS^{-1}$ [b]	Target size of template (MW, $\times 10^6$)[c]	RNA size (MW, $\times 10^6$)[d]
1	1	3.57×10^{-2}	5.6	5.6
	2	2.52×10^{-2}	3.9	4.0
	3	1.94×10^{-2}	3.0	3.0
	4 + 5	0.90×10^{-2}	1.4	1.2–1.4
2	4	1.44×10^{-2}	1.4	1.4
	5	1.28×10^{-2}	1.2	1.2
	6	1.00×10^{-2}	0.97	0.9
	7	0.77×10^{-2}	0.75	0.6

[a] From Jacobs *et al.* (1981).

[b] $K \times T$ was calculated from the relationship in $(N_t N_0) = K \times T \times t$, where N_t represents the incorporation of [^{3}H]uridine into RNA after t seconds of UV irradiation, N_0 is the RNA synthesis in the unirradiated culture, T is the target size, and K is a constant. The calculation was made from the data points by using linear regression analysis. The value of K was calculated as $6.38 \times 10^{-9} S^{-1}$ by substituting a value of 5.6×10^6 for the target size of RNA1 (experiment 1), or as 10.3×10^{-9} by inserting a value of 1.4×10^6 for RNA4 (experiment 2).

[c] By using the two values for K described in footnote *b*, the target sizes for the other RNAs were calculated.

[d] The molecular weights of the denatured, virus-specific RNAs were determined by agarose gel electrophoresis.

the UV target sizes of the templates for the mRNAs of MHV-A59 and IBV were the same as the sizes of the respective mRNAs. Since the UV mapping studies were done at 5.5 and 6.0 hours postinfection, when synthesis of the negatively stranded template may have been completed, it appears likely that only the synthesis of the mRNA species was being inactivated by UV.

Comparison of the oligonucleotide fingerprints of subgenomic mRNAs and virion RNA of MHV suggested that some RNA splicing mechanism or other modification of the RNA may take place during mRNA synthesis. Stern and Kennedy (1980a,b) found several T1 oligonucleotides in mRNA species which were not present in larger mRNAs. Lai *et al.* (1981), Leibowitz *et al.* (1981), and Spaan *et al.* (1982) also identified several T1 oligonucleotides in subgenomic mRNAs which were not present in the viral genome of MHV, or were not found in the same region in the genome. Preliminary evidence indicated that some of these oligonucleotides from several subgenomic

RNAs had similar sequences (Lai *et al.*, 1981). It has been suggested that these may represent junction sequences from the splicing of two unlinked stretches of RNA (Lai *et al.*, 1981). Since coronaviruses can replicate in enucleated cells (Wilhelmsen *et al.*, 1981; Brayton *et al.*, 1981), it appears unlikely that this splicing is done by cellular mechanisms located in the cell nucleus.

Lai *et al.* (1982a) found that the nucleotides adjacent to the cap structures of each of the subgenomic mRNAs contained the same sequence, 5′-CAP-N-UAAG. It is not known how many additional nucleotides are shared at the 5′ end of these mRNAs. It is not clear how the cap with its adjacent nucleotide sequences is added to each mRNA. One possibility would involve RNA splicing. A leader sequence which originates by splicing from large precursor molecules would appear to be contraindicated by the results of UV transcriptional mapping. However, a leader sequence with or without an attached cap may be derived from a small RNA of viral or cellular origin. Since viral RNA synthesis was not inhibited by antinomycin D, this leader RNA may be virus specific or perhaps derived from a stable, small, cellular RNA. The sequence -UAAG which was found adjacent to the cap structure at the 5′ end of viral subgenomic mRNAs and genomic RNA (Lai *et al.*, 1982a) is also present in some small host coded cytoplasmic RNAs, including 5s ribosomal RNA (Delihas and Andersen, 1982) and 7s RNA (Busch *et al.*, 1982), and U2 and U3 small nuclear RNAs (Busch *et al.*, 1982). Furthermore, the same order is contained in the consensus sequence at the 5′ exon–intron boundary of many splice junctions (Lerner *et al.*, 1980). The complementary sequence which is present in U1 SnRNA is thought to assist in the proper orientation of exons for splicing of RNA. Several models have been postulated for the utilization of a leader sequence in coronavirus transcription (Lai *et al.*, 1982a; Spaan *et al.*, 1982).

1. Such a leader could act as a primer for the initiation of RNA transcription along the full-length, negative-strand template.
2. Alternatively, a leader sequence could be fused onto the 5′ end of newly synthesized viral transcripts. This sequence could come from viral or cellular RNA.
3. An RNA polymerase jumping mechanism could explain the common nucleotide sequences at the 5′ end of each viral mRNA and genomic RNA. Thus, a short segment of the 5′ region would be transcribed from the 3′ end of the negative-strand template, and then the polymerase would translocate through intervening sequences on the negative-strand template and resume transcription at the beginning of a particular cistron.

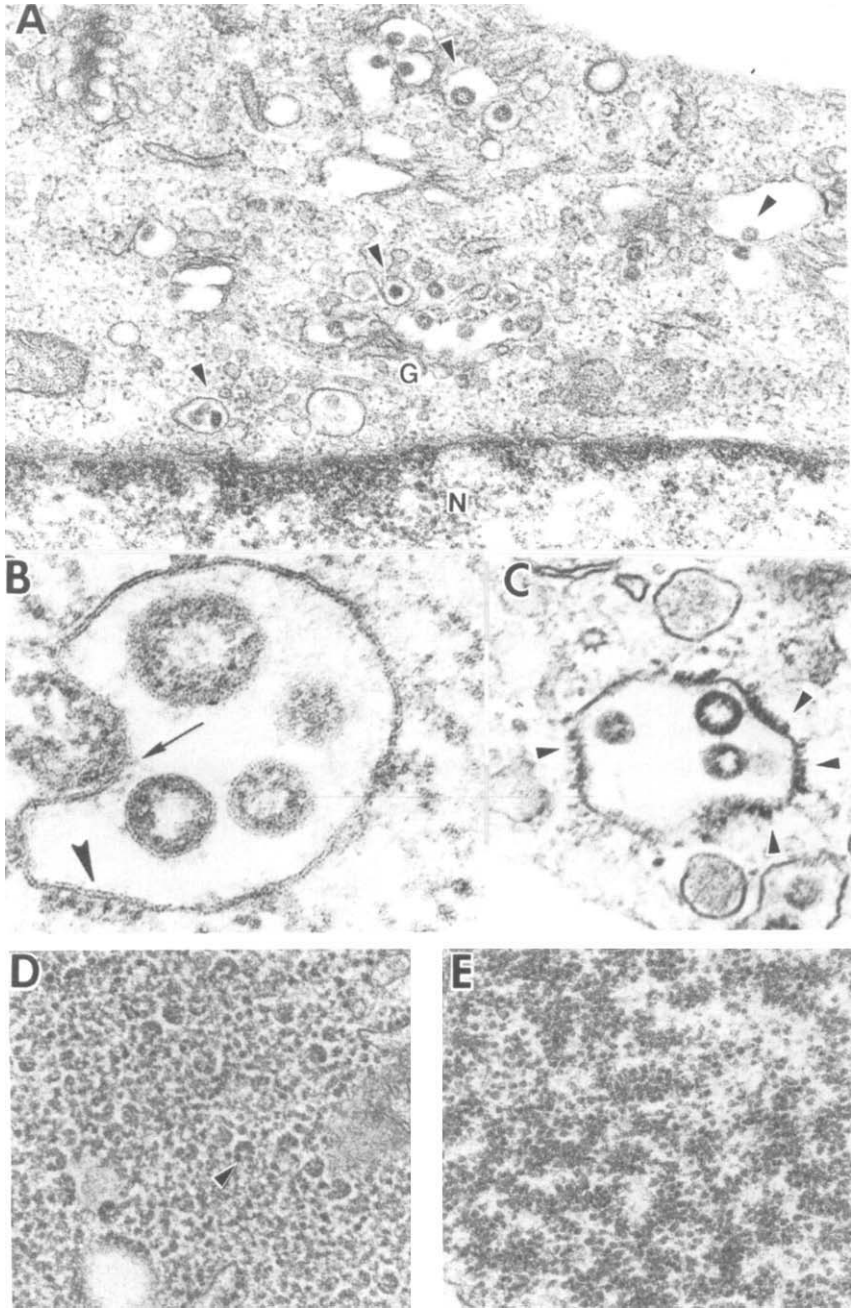

FIG. 19.

The UV transcription data do not contradict any of these models, since the leader sequence may be too small a target to have been detected.

F. Virion Assembly, Release, and Cytopathic Effects

Some of the early studies on coronavirus replication emphasized ultrastructural changes in infected cells (Svoboda *et al.*, 1962; Tanaka *et al.*, 1962; David-Ferreira and Manaker, 1965; Hamre *et al.*, 1967; Becker *et al.*, 1967). All of these studies showed that the entire replicative cycle of coronaviruses occurred in the cytoplasm. Indeed, MHV has been shown to replicate in enucleated cells (Brayton *et al.*, 1981; Wilhelmsen *et al.*, 1981), although replication of IBV in enucleated BHK-21 cells was significantly reduced (Evans and Simpson, 1980). Ultrastructural studies on the binding and penetration of coronaviruses have been described (Section III,B.). The early morphological events associated with coronavirus infection were rather nonspecific ones, such as increase in cytoplasmic membranes or in the size of polysomes (David-Ferreira and Manaker, 1965; Sebesin, 1971). Toward the end of the viral latent period, about 6–7 hours postinfection, spherical virions approximately 60–100 nm in diameter were observed in the lumens of the rough endoplasmic reticulum, Golgi apparatus, and smooth-walled vesicles (David-Ferreira and Manaker, 1965; Massalski *et al.*, 1981; Ducatelle *et al.*, 1981; Dubois-Dalcq *et al.*, 1982; Fig. 19a–c). In most instances these virions had electron-lucent centers with electron-dense granular or tubular nucleocapsids associated with the inner surface of the viral envelope. Tubular nucleocapsids were also observed under the membranes of the rough endoplasmic reticulum or Golgi apparatus (Oshiro, 1973; Holmes *et al.*, 1981a; Massalski *et al.*, 1981, 1982; Dubois-Dalcq *et al.*, 1982; Fig. 19B and C). Chasey and Alexander (1976) showed that the envelopes of budding virions were covered with peplomers. During the early stages of viral

FIG. 19. Formation of coronavirus virions and inclusions. (A) At 9 hours after infection with MHV-A59, numerous virions (arrowheads) are observed in vesicles associated with the Golgi apparatus. ×48,000. (From K. V. Holmes.) (B and C) Virions of MHV-JHM are observed budding into smooth-walled intracytoplasmic vesicles. The arrowheads indicate helical nucleocapsids within virions and aligned under regions of the vesicle membrane which contain viral peplomers (arrow). (B) ×180,500; (C) ×85,500. (D and E) Masses of helical nucleocapsids form large intracytoplasmic inclusions in cells infected for several days with MHV-JHM (D) and the *ts8* mutant of this virus(E). The strands of the MHV-JHM nucleocapsid appear to be forming supercoiled structures (arrowhead). (D) ×68,200; (E) ×51,000. (B–D are reproduced from Dubois Dalcq *et al.*, 1982, with permission.)

infection, virions appeared singly or in small clusters, whereas later in infection, scores of virions were found within large vesicles and occasionally within the lumen of the nuclear membrane (Fig. 20). Budding of virions from the plasma membrane was almost never visualized. An exception was a single particle visulaized several days after virus infection of a neural cell culture (Dubois-Dalcq *et al.*, 1982). Although Sugiyama and Amano (1981) reported that the virions were budding from the plasma membrane, the scanning electron microscopic (SEM) images were not of sufficient resolution to demonstrate budding. In some studies, although numerous intraluminal virions were observed, no budding virions were detected. Detection of budding images apparently depended on the viral strain, the host cell type, and the time after virus inoculation (Watanabe, 1969). Budding virions were most likely to be detected late in the infectious cycle. This suggests that these images represent arrested buds, and that during the early stages of infection coronavirus budding may be a very rapid process.

Several investigators have suggested that coronaviruses were released by lysis of the infected cells (Hamre *et al.*, 1967; Oshiro *et al.*, 1971; Takeuchi *et al.*, 1976; Chasey and Alexander, 1976). Release by fusion of virus-filled, smooth-walled vesicles with the plasma membrane has also been observed (Doughri *et al.*, 1976). When the kinetics of release of infectious virus was correlated with cell lysis by microcinematography, however, it was apparent that the infectious virions were released from intact cells (K. V. Holmes, unpublished observations). Indeed, it appears that release of virus depends upon the good condition of the host cells. The generally accepted mechanism of coronavirus release from infected cells is via fusion of virus-filled vesicles with the plasma membrane (Doughri *et al.*, 1976). Thus, the coronaviruses may be released from cells by utilizing a cellular transport mechanism developed for secretion or exocytosis of the contents of secretory vesicles. *In vivo*, the target cells for replication of many coronaviruses are epithelial cells with tight junctions in the respiratory or gastrointestinal tract. In polarized cells such as these, influenza virus and VSV have been shown to bud specifically from the apical or basilar plasma membranes (Rodriguez-Boulan and Sabatini, 1978). There is as yet little evidence to show whether the fusion with the plasma membrane of vesicles filled with coronaviruses exhibits specificity for basal or apical membranes. Secretory cells do demonstrate strong polarity in the direction of secretion of cellular secretory products such as enzymes from pancreatic acinar cells. It is possible that some polarity of coronavirus release may be identified. To date, in the only study which addresses this point, Doughri and Storz (1977) observed that porcine coronavirus could be seen on both apical and basal cell surfaces of intestinal epithelial cells.

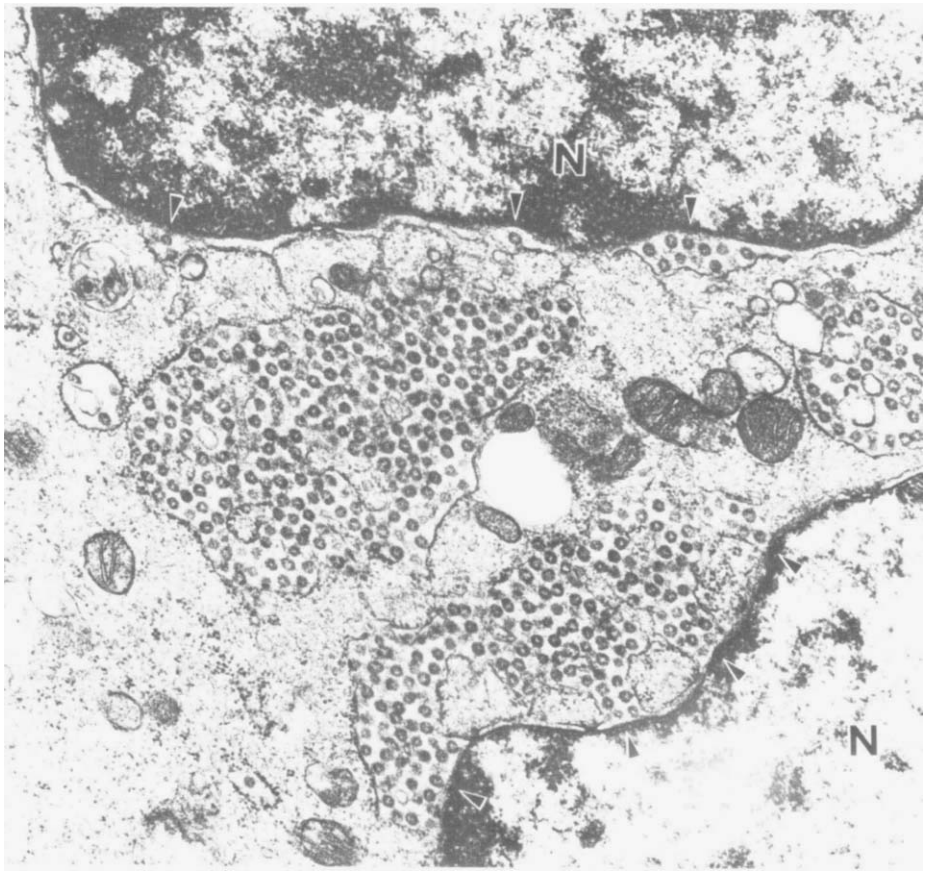

FIG. 20. Coronavirus virions in the rough endoplasmic reticulum and nuclear envelope. Late in the infectious cycle, numerous spherical virions accumulate within the rough endoplasmic reticulum and the nuclear envelope (N) (arrows). ×36,000. (From J. N. Behnke.)

Late in the infectious cycle, it was common to find very large numbers of virions adsorbed to the surface of infected cells (Oshiro *et al.*, 1971; Oshiro, 1973; Doughri and Storz, 1977). Scanning electron microscopy showed these most effectively (Sugiyama and Amano, 1981). It is not clear what function, if any, may be served by this adsorption to infected cells. Most of the virions appeared to remain on the surface without being internalized, although some were found in lysosomes (Sabesin, 1971).

Characteristic features of coronavirus infection were vacuolization of cells and virus-induced cell fusion (Oshiro, 1973; McIntosh, 1974). The time of appearance of these depended on the virus and the host cell type. It is noteworthy that large intracytoplasmic inclusions of nu-

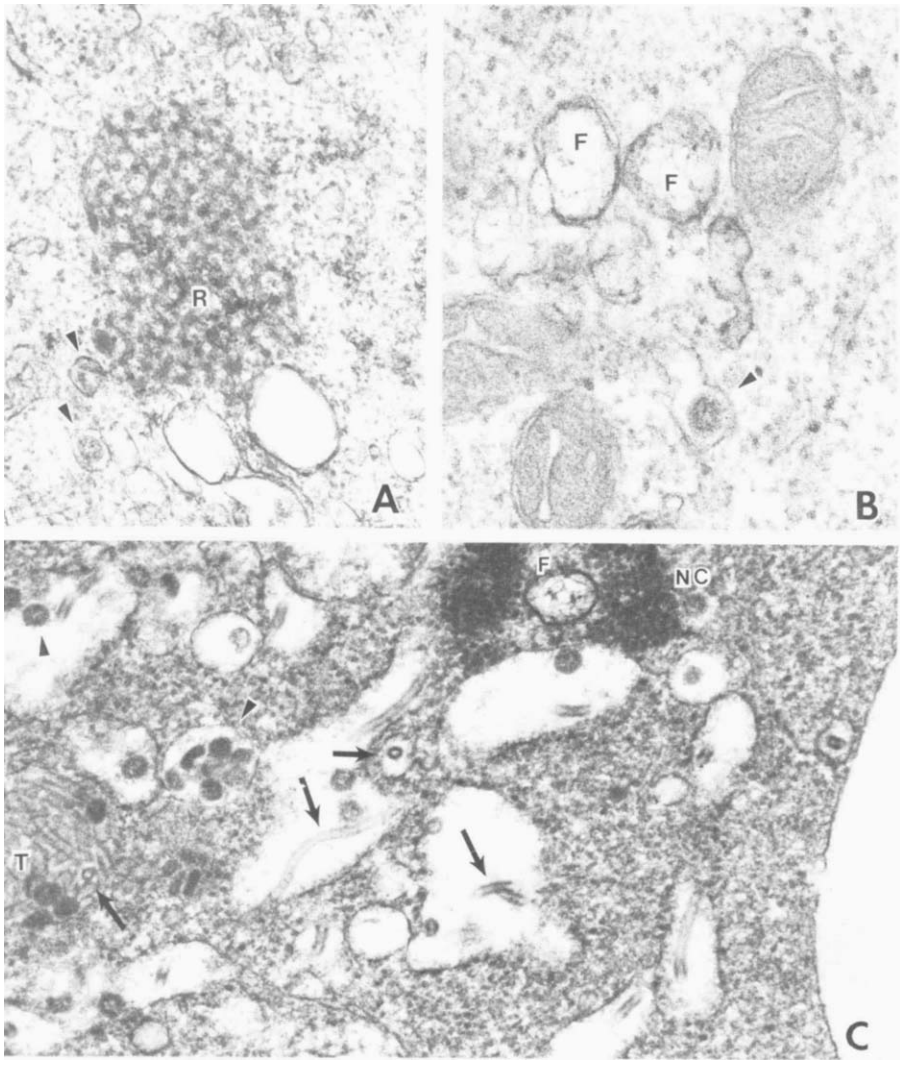

FIG. 21. Unusual features of the replication of MHV. (A) Occasionally in cells infected with MHV-A59, reticular (R) inclusions consisting of closely opposed lamellae of endoplasmic reticulum have been observed. ×57,000. (B) Late in infection with MHV-A59, vesicles containing fine filaments (F) are sometimes observed. ×100,000. (C) Late in infection with MHV-A59 and in infected cells treated with tunicamycin, long tubular structures (arrows) about 50 nm in diameter are occasionally observed in the lumen of the rough endoplasmic reticulum. Nucleocapsid inclusions (NC) and a vesicle containing filaments (F) ar also shown. Virions are indicated by arrowheads. ×46,000. (From K. V. Holmes.)

cleocapsids were not observed in most early studies of coronavirus-infected cells. Caul and Egglestone (1977) did observe such inclusions in cells infected with HECV, and others have seen them also (Watanabe, 1969). Massalski *et al.* (1982) suggested that nucleocapsid inclusions accumulate after the cessation of virus budding. Dubois-Dalcq *et al.* (1982) showed that several types of inclusions that could be produced by the intracytoplasmic nucleocapsids of different strains of MHV in differentiated cultures of central nervous system (CNS) cells (Fig. 19D and E). They also found an increase in "myelin figures" in the cytoplasm of MHV-infected cells.

Additional features of coronavirus CPE included several types of intracytoplasmic inclusions whose origins and functions remain unclear. David-Ferreira and Manaker (1965) found "reticular inclusions" in MHV-infected cells. These consisted of masses of interconnected tubules of smooth membranes in continuity with the rough endoplasmic reticulum (Fig. 21A). They have only occasionally been observed with other coronaviruses. A second type of inclusion was observed near the reticular inclusions. This consisted of vacuoles about 200 nm in diameter containing flexible coiled filaments about 30 nm in diameter. These filamentous structures were surrounded by a double membrane (Fig. 21B; David-Ferreira and Manaker, 1965; Takeuchi *et al.*, 1976). Third, "tubular inclusions" consisting of interconnected tubules 16 to 25 nm in diameter were observed near the reticular inclusions (David-Ferriera and Manaker, 1965; Watanabe, 1969). Inclusions consisting of interconnected virions within the lumen of smooth-walled vesicles have also been observed (Oshiro *et al.*, 1971). Within the lumen of the rough endoplasmic reticulum and smooth-walled vesicles, long, rigid, cylindrical structures about 50 nm in diameter have occasionally been detected (Fig. 21C; Dubois-Dalcq *et al.*, 1982). These may represent an excess of the E1 glycoprotein since they occur frequently in tunicamycin-treated infected cells, where synthesis of E2 is greatly reduced (Holmes *et al.*, 1981a). It is evident from the preceding descriptions that coronaviruses produce a wide variety of effects in different cell types. Further studies are needed to determine the composition of these different virus-associated structures.

G. Viral Mutants

In other virus systems, conditional lethal mutants have been important in elucidating many steps in virus replication. With coronaviruses, this effort is still at an early stage. Although many variants have been isolated from natural infections, there are few well-charac-

terized, chemically induced mutants of coronaviruses. Recently, several groups have obtained and partially characterized temperature-sensitive (ts) mutants of MHV. Almost all of the MHV mutants have been selected for failure to induce syncytium formation. Unfortunately, most of these mutants grow rather poorly, even under permissive conditions. There are few, if any, chemically induced mutants of other coronaviruses. Clearly, other phenotypes and additional mutants are needed.

The first collections of chemically induced mutants of MHV-JHM were made by Haspel *et al.* (1978) with 5-azacytidine or 5-fluorouracil, and by Robb *et al.* (1979) using *N*-methyl-*N'*-nitrosoguanidine and 5-fluorouracil. Temperature-sensitive mutants were selected for failure to induce fusion of susceptible cells at the nonpermissive temperature (39.5° or 38.5°C). The majority of the 34 mutants identified by Robb *et al.* were found to be RNA negative. Only three were RNA positive and exhibited synthesis of viral proteins. Some of these mutants produced altered neuropathogenesis in mice. Leibowitz *et al.* (1982a) performed complementation analysis of 37 ts mutants of MHV-JHM and identified seven complementation groups. Six of these affected virus-specific RNA synthesis. The gene product affected by each mutation has not yet been identified. Several of the mutants described by Haspel and his co-workers, including the *ts8* mutant, are of particular interest because they induce demyelination with a much higher frequency than the wild type (Haspel *et al.*, 1978; Knobler *et al.*, 1981c, 1982), and because they may form aberrant inclusions in CNS cells *in vitro* (Dubois-Dalcq *et al.*, 1982). Wege *et al.* (1981c, 1983) also isolated temperature-sensitive mutants of MHV-JHM with 5-fluorouracil and found that these mutants caused higher rates of subacute and chronic neurological diseases than did wild type virus in suckling and weanling rats.

Twenty chemically induced (with 5-fluorouracil), temperature-sensitive mutants of MHV-A59 have been partially characterized by Koolen *et al.* (1981, 1983). Most of these mutants, selected for their inability to induce syncytium formation at 40°C, were RNA negative also. Several of the mutants exhibited altered neuropathogenic properties. A variety of coronavirus mutants have been isolated from persistently infected cultures of MHV, and are described in Section III,H. Clearly, the potential contributions of these and other coronavirus mutants to the study of coronavirus replication are enormous. In combination with cloning of the viral mRNAs and genomic RNA, which is being done in several laboratories, mutants will be invaluable for the analysis of coronavirus genetics, pathogenesis, and replication.

H. Persistent Infection

Coronaviruses are capable of inducing persistent infection in animals (Robb and Bond, 1979a; Wege *et al.*, 1982) and in tissue cultures. Many persistent infections were summarized at the Wurzburg Symposium on Coronaviruses (ter Meulen *et al.*, 1981; Siddell *et al.*, 1982). The salient feature of these infections was that in most cases the majority of cells remained antigen negative, yet all of the cells were resistant to superinfection with wild-type virus. Stohlman *et al.* (1979) derived cold-sensitive mutants of JHM from persistently infected neuroblastoma cells. These were rescued from latently infected cells by polyethylene glycol-induced fusion to permissive cells. Hirano *et al.* (1981) obtained small plaque mutants of JHM, and Holmes and Behnke (1981) isolated small plaque and temperature-sensitive mutants of A59 from persistently infected cells. These mutants have not yet been fully characterized.

In order to understand the balance between virus and host which permits this persistent infection, it is necessary to identify the host functions which are utilized by the viruses during the replicative cycle and to characterize in detail the controls exerted upon coronavirus transcription and translation.

I. Host Regulation of Viral Replication

There are important host controls over coronavirus replication at several levels. Immune response genes may play an important role in resistance to coronavirus-induced disease (Dupuy *et al.*, 1975). However, genetic factors are also important at the single-cell level. These are the focus of our discussion.

Bang and Warwick (1960) demonstrated that while the PRI strain of MHV (MHV-2) caused fatal hepatitis in mice of the PRI strain, this virus did not kill C3H mice. This susceptibility of PRI mice to death induced by MHV-2 was found to be inherited as a dominant gene (Bang and Warwick, 1960; Kantoch *et al.*, 1963). By backcrossing, Weiser *et al.* (1976) created a strain of mice congenic to C3H mice, but bearing the dominant susceptibility to MHV-2 (C3H-ss strain). Extensive studies were done comparing the effects of MHV-2 on C3H and C3H-ss mice (Weiser and Bang, 1976; Taylor *et al.*, 1981; Bang, 1981). By various manipulations, Bang and his associates were able to modulate the effects of MHV on the susceptible and resistant mice. Treatment of resistant animals with cortisone (Gallily *et al.*, 1964) or a protein-deficient diet (Bang, 1981) rendered them susceptible so that they died

from a small dose of MHV-2, and treatment of susceptible animals with concanavalin A rendered them resistant so that they could survive a normally fatal dose of MHV-2 (Weiser and Bang, 1977).

The susceptibility or resistance of different mouse strains to MHV-2, as measured by survival of animals, was directly correlated with the response of peritoneal macrophages from each strain in culture to this virus (Bang and Warwick, 1960; Bang, 1981). However, the cell culture conditions greatly affected these results. When fetal bovine serum was substituted for horse serum in the medium, the difference in virus yields between macrophages from resistant and susceptible mice was significantly reduced (Lavelle and Bang, 1971; Bang, 1981). The mechanism for this cellular restriction of MHV-2 synthesis in cells from resistant animals under defined conditions has not yet been characterized. Shif and Bang (1970) demonstrated that the restriction was at a stage subsequent to virus adsorption, and suggested that degradation of virions within the resistant cell might be responsible. Later, Cody showed that the virus grew equally well in resistant and susceptible cells, but was one-twentieth as infective for resistant cells (Cody, 1980; Bang, 1981). In his last publications (Bang and Cody, 1980; Bang, 1981), Bang described recent experiments which suggested that macrophage resistance to MHV-2 was also dependent upon associated lymphocyte action. He also suggested that cell-bound interferon might play a role in protecting the genetically resistant cell.

The pioneering studies of Bang and his co-workers were extended by other investigators using different strains of MHV. These studies demonstrate that MHV-2, MHV-3, and MHV-JHM exhibit different patterns of host susceptibility and resistance. Although replication of MHV-2 was restricted in C3H mice, replication of MHV-3 was only partially reduced (LePrevost *et al.*, 1975; Virelizier and Allison, 1976; Yamada *et al.*, 1979; Taguchi *et al.*, 1981). Furthermore, A/J mice, which were resistant to MHV-3, were susceptible to MHV-JHM (Knobler *et al.*, 1981b). Resistance to MHV-3 and MHV-JHM correlated with failure of the virus to replicate and with delayed appearance of CPE after low-multiplicity infection of cultures of peritoneal macrophages (Virelizier and Allison, 1976; Macnaughton and Patterson, 1980; Krzystyniak and Dupuy, 1981; Knobler *et al.*, 1981a,b; Stohlman and Frelinger, 1981; Stohlman *et al.*, 1982a), neuronal cells (Knobler *et al.*, 1981a,b), and hepatocytes (Arnheiter and Haller, 1981; Arnheiter *et al.*, 1982). Resistance was partially overcome by infection at higher multiplicities, resulting in cell destruction, although virus yields remained low (Virelizier and Allison, 1976; Macnaughton and Patterson, 1980; Arnheiter *et al.*, 1982; Knobler *et al.*, 1981b). Arnheiter *et al.* (1982) showed by fluorescent antibody staining that in the first cycle of

virus replication, resistant cultures of hepatocytes had fewer cells expressing viral antigen. However, after infection at high multiplicty (multiplicity of infection of 100), all cells contained viral antigens, including E2 and E1, but virus production was delayed and virus yields remained low. The characterization of this cellular restriction to MHV replication remains incomplete.

IV. Structure and Biological Activities of Coronavirus Glycoproteins

A. The Peplomeric Glycoprotein, E2

Much of our present knowledge about the structure and functions of coronavirus glycoproteins comes from studies of MHV. A model for the structure of the E2 glycoprotein of MHV-A59 is shown in Fig. 22. Some of the important features of this model include (1) anchoring of one end of the protein in the viral envelope; (2) covalent attachment of palmitic acid; (3) a single trypsin-sensitive site accessible in the native glycoprotein on the virion; (4) the presence of SH groups and disulfide bonds; (5) noncovalent association between the subunits (90A and 90B) of E2; and (6) oligosaccharide side chains on both subunits.

E2 is probably anchored to the viral envelope through a short hydrophobic region, as Pronase or bromelain quantitatively removed both 180K and 90K species from the intact virions, while the peplomers were removed (Sturman and Holmes, 1977). Palmitic acid is covalently attached, probably at or near the hydrophobic domain which anchors the peplomer in the viral envelope, since this has been demonstrated for the influenza virus hemagglutinin (Schmidt, 1982a) and the G protein of VSV (Petri and Wagner, 1980. Although detergent-sol-

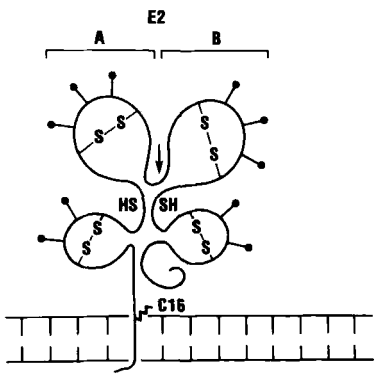

FIG. 22. Model of the peplomeric glycoprotein E2. This is a provisional model of E2 which shows some of the important structural features of the peplomeric glycoprotein such as the acylation, glycosylation, presence of both sulfhydryl groups and disulfide bonds, and the existence of a trypsin-sensitive cleavage site in the center of the molecule which results in the formation of two species, tentatively called E2A and E2B, which comigrate at 90K.

ubilized E2 could be digested by trypsin into many peptide fragments, there appears to be only a single trypsin-sensitive cleavage site accessible in the native 180K molecule on the MHV-A59 virion (Sturman and Holmes, 1977.

Disulfide linkages mask proteolytic cleavage in the hemagglutinin of HEV. Upon reduction, the 140K hemagglutinin (E2) of strain VW527 disappeared and a new polypeptide species (gp76) appeared, indicating that the 140K E2 was composed of two 76K subunits which were linked through disulfide bonds (Callebaut and Pensaert, 1980). The hemagglutinin of HEV strain FS255 was also sensitive to treatment with sulfhydryl reagents; exposure to dithiothreitol resulted in the loss of hemagglutinating activity and release of gp125 from the virion (Pocock, 1978).

Several investigators have reported that coronavirus infectivity was most stable below pH 7 (Pocock and Garwes, 1975; Alexander and Collins, 1975; Sturman, 1981). The pH-dependent thermolability of MHV infectivity shown in Fig. 2 appeared to be the result of a conformational change in E2 which led to aggregation of the peplomeric glycoprotein (Sturman, 1981). Intrachain disulfide and sulfhydryl groups appeared to be important in determining the conformation of E2, as pH and temperature-dependent aggregation of E2 on virions or of isolated, NP-40-solubilized E2 were enhanced by reducing agents and sulfhdryl blocking reagents (Sturman, 1981).

There is no evidence for interchain disulfide bridges between the 90A and 90B subunits of MHV-A59 E2; they remained associated noncovalently on the virion after trypsin cleavage of the peplomer (Sturman, 1977; Sturman and Holmes, 1977). During pH 8 inactivation, however, some 90K E2 was released, and incubation with reducing agents caused release of more 90K E2. This was probably associated with a change in the conformation of this molecule following reduction of intramolecular disulfide bonds. The same appears to be true for the liberation of gp125 from HEV strain FS255 (Pocock, 1978).

Present evidence indicates that E2 possesses six or more biological activities (Table V):

1. Binding of virions to receptors on the plasma membrane of susceptible cells (adsorption and hemagglutination) appears to be mediated by E2. Purified, radiolabeled E2 bound to susceptible cells but not to cells lacking in virus receptors, such as erythrocytes (K. V. Holmes, unpublished data). Binding of E2 was inhibited by preincubation of cells with excess MHV. Virions from which the peplomers had been removed, or particles without peplomers, exhibited markedly reduced capacities for cell attachment and infection (Holmes *et al.*, 1981a). In

TABLE V

FUNCTIONS OF CORONAVIRUS GLYCOPROTEINS[a]

E2, the peplomeric glycoprotein
1. Binding to receptors on the cell membrane (adsorption and/or hemagglutination)
2. Inducing neutralizing antibody
3. Eliciting cell-mediated cytotoxicity
4. Causing pH-dependent thermolability of coronaviruses
5. Inducing cell fusion; may be activated by proteolytic cleavage
6. Fusing viral envelope with cell membrane for infection; may be activated by proteolytic cleavage

E1, the matrix glycoprotein
1. Determining location of viral budding
2. Forming viral envelope
3. Interacting with viral nucleocapsid

[a] Adapted from Holmes *et al.* (1981b).

HCV-OC43, monospecific antibody to E2 inhibited hemagglutination (Schmidt and Kenney, 1982). Coronaviruses which hemagglutinate include some strains of IBV, HEV, HCV-OC38/43, MHV-3, a murine enteric coronavirus, rabbit enteric coronavirus, and BCV (see Section III,B).

Initially, trypsin treatment of virions appeared to be necessary for activation of IBV hemagglutinin (Corbo and Cunningham, 1959). Subsequently, however, the IBV hemagglutinin was shown to be inactivated by trypsin (Bingham *et al.*, 1975). Trypsin also destroyed the hemagglutinating activity of OC38/43 viruses (Kaye and Dowdle, 1969). There appeared to be significant strain differences in IBV hemagglutination (Bingham *et al.*, 1975), and the response of IBV to trypsin was also strain dependent.

2. E2 is responsible for the induction of neutralizing antibody. Garwes *et al.* (1976, 1978–1979) were the first to show that antibody against purified surface projections (of TGEV) possessed virus-neutralizing activity *in vivo*. In accordance with this, Macnaughton *et al.* (1981) found that most of the antibody induced during infection of human volunteers with HCV-229E was directed against the surface projections of the virus. Hasony and Macnaughton (1981) also showed that immunization of mice with E2 protected them against infection with MHV-3, whereas immunization with E1 or N failed to provide protection against virus challenge. Holmes *et al.* (1981b) demonstrated that monospecific antibody against MHV-A59 E2 neutralized infectivity in cell culture, and similarly Schmidt and Kenny (1981, 1982) showed that monospecific antibody to E2 of HCV-OC43 neutralized the

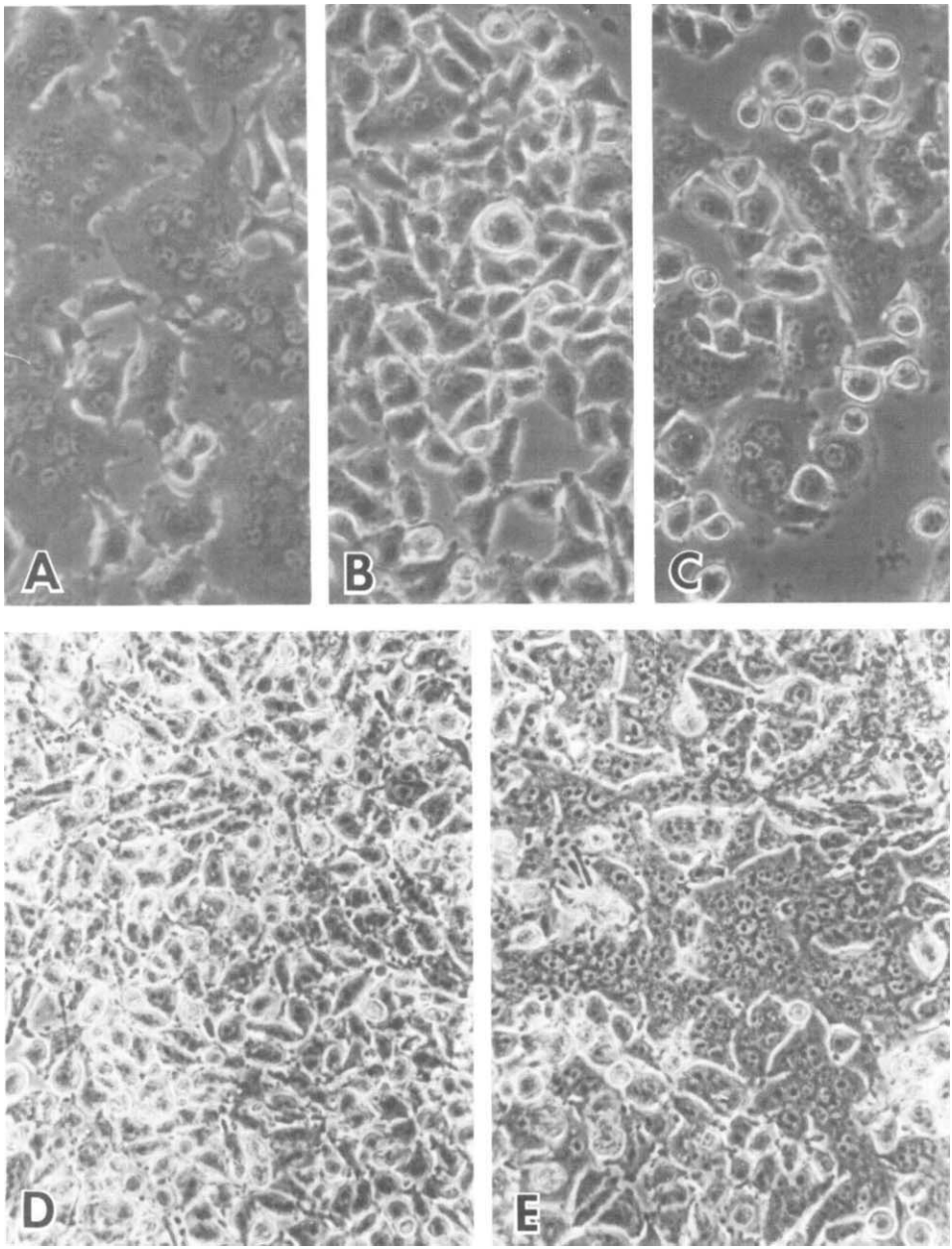

FIG. 23.

virus *in vitro*. Monoclonal antibodies against MHV-JHM E2 were shown by Collins *et al.* (1982) to neutralize MHV-JHM virus infectivity in the absence of complement, whereas monoclonal antibody to E1 exhibited neutralizing activity only in the presence of complement.

3. E2 on the surface of infected cells renders them susceptible to cytotoxic effects of spleen cells. The cell-mediated cytotoxicity of spleen cells from uninfected mice to MHV-A59-infected cells was also inhibited by antibody to E2 (Haspel *et al.*, 1981).

4. The pH-dependent thermolability of coronavirus virions is due to aggregation of E2. This conformational change in E2, which occurs above pH 6.5 at 37°C, is sensitive to sulfhydryl reagents (Sturman, 1981).

5. E2 is responsible for cell fusion. Cell fusion was frequently a prominent feature of coronavirus infection *in vivo* and *in vitro*. The extent of cell fusion depended upon the virus strain, host cell, and the conditions of infection. The role of E2 in the induction of cell fusion is indicated by the observation that coronavirus-induced fusion was inhibited by monospecific and monoclonal antibodies to E2 (Holmes, 1981b; Collins *et al.*, 1982; Fig. 23A and B), and by the finding that treatment of infected cells with tunicamycin inhibited both the synthesis of E2 and cell fusion (Holmes *et al.*, 1981a).

Trypsin in the overlay medium enhanced plaque formation of an enteropathogenic bovine coronavirus and several strains of IBV (Storz *et al.*, 1981a,b; Otsuki and Tsubokura, 1981). In the presence of trypsin, infection with coronaviruses was associated with cell fusion (Storz *et al.*, 1981a,b; Toth, 1982). Similar findings were obtained with a mutant of MHV-S which did not ordinarily induce cell fusion (Yoshikura and Tejima, 1981). Trypsin treatment of infected cells also enabled MHV-S to form fusion plaques on otherwise resistant cells, and allowed MHV-2 to form fusion-type plaques. This effect of trypsin on the ability of coronaviruses to induce cell fusion is similar to that

FIG. 23. The role of E2 in coronavirus-induced cell fusion. L2 cells infected with MHV-A59 at a multiplicity of 3 PFU/cell show significant cell fusion after 19 hours (A). However, if monospecific antibody against the E2 glycoprotein is added to the culture from 2 hours after infection, the virus-induced cell fusion is prevented (B). Monospecific antiserum against the E1 glycoprotein does not prevent coronavirus-induced cell fusion; this suggests that E2 is the fusion factor of MHV(C). ×100. (From K. V. Holmes.) (D and E) Fusion of uninfected L2 cells by direct action of concentrated MHV-A59 on the plasma membrane does not occur within 2 hours (D). However, if the virions had been previously treated with trypsin to cleave the E2 180K to E2 90K, then rapid fusion of uninfected cells was observed (E). This and other observations suggest that coronaviruses have a protease-activated cell fusion factor like those found in other enveloped RNA viruses. (From L. S. Sturman.)

observed with the F protein of paramyxoviruses and the HA protein of myxoviruses (Klenk and Rott, 1981). Sturman and Holmes (1977) showed that trypsin treatment of MHV-A59 resulted in cleavage of 180K E2 to 90K.

Recently, direct evidence has been obtained for the role of proteolytic cleavage of E2 in cell fusion. Regardless of the multiplicity of infection, efforts to obtain rapid cell fusion with a coronavirus had been unsuccessful until we employed virus which had been treated with trypsin which caused cleavage of E2 (180K) to E2 (90A + 90B). Cell fusion occurred rapidly after addition of this virus and in the absence of viral protein synthesis (Fig. 23C and D).

6. Proetolytic cleavage of E2 may be required for viral infectivity. However, this has not yet been proven. Many investigators have studied the effects of trypsin on coronavirus infectivity with mixed results. For example, trypsin treatment at low concentrations (10 μ/ml) enhanced MHV-A59 infectivity two- to threefold, whereas at high concentrations (1 mg/ml), infectivity was reduced by the same relative degree (Sturman and Holmes, 1977). Since a large proportion of MHV-associated E2 was already in the 90K form, it has not been possible to assess the role of proteolytic cleavage of E2 as was done with the F_0 glycoprotein of Sendai virus and the HA_0 glycoprotein of influenza virus (Klenk and Rott, 1981). When a source of coronavirus with uncleaved E2 is identified, the effect of specific cleavage of E2 on virus infectivity can be demonstrated conclusively.

B. The Matrix Glycoprotein, E1

E1 is in many ways a unique viral glycoprotein. It performs functions associated with matrix proteins of other viruses, yet it is glycosylated and protrudes from the viral envelope. E1 comprises approximately 40% of the protein of the virion and contains 70% of the methionine label. At first, E1 was difficult to study because of its unusual tendency to aggregate upon heating at 100°C in SDS (Figs. 4 and 5; Sturman, 1977). The generation of multimers of E1 produced a variety of polypeptide patterns on SDS–PAGE depending upon the conditions of sample treatment. Aggregation of E1 in SDS has been described for other strains of MHV (Wege *et al.*, 1979) and for other coronaviruses as well (Callebaut and Pensaert, 1980; Schmidt and Kenny, 1982). Multiple forms of E1 were also distinguished within the 20–25K apparent-molecular-weight range (Wege *et al.*, 1979; Siddell *et al.*, 1981b; Rottier *et al.*, 1981b; Holmes, *et al.*, 1981b). These may reflect differences in the number or heterogeneity of the oligosaccharide chains on E1.

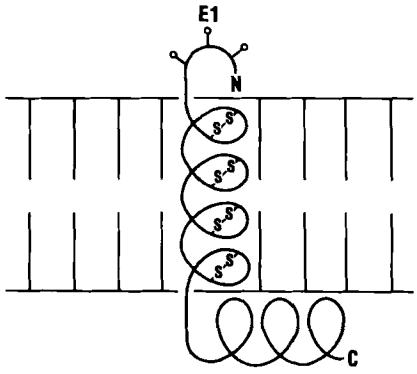

FIG. 24. Model of the membrane glycoprotein E1. This is a provisional model of the E1 glycoprotein which is associated with the coronavirus envelope, showing some of the characteristic features of the molecule. These include the amino-terminal end (N) of the protein which protrudes from the envelope and bears the O-linked carbohydrate side chains, and the extensive domains of the E1 within and beneath the membrane where they can interact with other E1 molecules, with the nucleocapsid, or with E2. Many of the characteristics of coronaviruses, such as their intracellular budding site, may be determined by the properties of the E1 glycoprotein.

A model for the E1 glycoprotein of MHV-A59 is shown in Fig. 24. E1 appears to possess three domains:

1. A small 5K hydrophilic region, containing all of the carbohydrate on the molecule, extends outside the viral envelope and can be removed by Pronase of bromelain (Sturman and Holmes, 1977). Stern *et al.* (1982) have shown that for the E1 of IBV, this external domain represents the amino-terminal portion of the molecule. We do not know anything about the functions of this glycosylated portion of E1 which may have important cooperative effects with E2.
2. A hydrophobic domain resides within the lipid bilayer. Disulfide bonds are illustrated in this region because aggregation of E1 in SDS at 100°C was markedly enhanced in the presence of reducing agents, which indicated that reduction of disulfide bonds exposed a highly hydrophobic domain (Sturman and Holmes, 1977).
3. The third domain of E1 resides on the inner surface of the envelope and may be associated with the nucleocapsid. As described earlier, after solubilization of the viral envelope with NP-40 at 4°C, the nucleocapsid could be separated from both E1 and E2, but at 37°C, E1 reassociated with the nucleocapsid (Sturman *et al.*, 1980; see Fig. 10B). E1 has been shown to bind to RNA in the nucleocapsid. However, this interaction was not specific for MHV RNA. Nucleocapsid structures of other coronaviruses also interacted with E1 (Garwes *et al.*, 1976; Pocock and Garwes, 1977).

E1 appears to be the only glycoprotein required for coronavirus budding, as shown by the fact that in MHV-infected, tunicamycin-treated cells, in which E2 was made in markedly reduced amounts and not

incorporated into virions, MHV virions were formed and released normally. Therefore, we infer that E1 is responsible for the formation of the viral envelope. E1 of IBV contained N-linked, rather than O-linked, oligosaccharides (Stern and Sefton, 1982c). Glycosylation of the E1 of IBV was inhibited by tunicamycin, but virions which lacked E2 and contained nonglycosylated E1 were produced. Thus, glycosylation of E1 was not essential for formation of IBV virions.

The intracellular localization of E1 on intracytoplasmic membranes (Fig. 17) may determine the characteristic budding sites of coronaviruses, which are limited to the endoplasmic reticulum and the Golgi apparatus (Holmes *et al.*, 1981b; Doller *et al.*, 1983). E1 may also contain sites for interaction with the viral peplomers. Some monoclonal antibodies to E1 have been shown to exhibit neutralizing activity, but only in the presence of complement (Collins *et al.*, 1982). The possibility has not been excluded that E1 may also have a role in other functions which are presently thought to involve E2, such as the interaction of virions with cell receptors, production of a cell-mediated immune response, and induction of cell fusion.

V. Antigenic Relationships among Coronaviruses

Antigenic relationships among IBV, HCV, and MHV strains were first studied in detail, by immunofluorescence, hemagglutination inhibition, and neutralization, by McIntosh *et al.* (1969) and Bradburne (1970). These investigators established that MHV and some human coronaviruses were antigenically related, while IBV did not cross-react with HCV or MHV. McIntosh's data indicated that there were at least two subgroups of human coronaviruses. HCV-OC38, and the very similar OC43, showed a close antigenic relationship to MHV, but none of these cross-reacted with HCV-229E. Bradburne also found an antigenic relationship between OC43 and MHV; however, he detected some cross-reactivity between HCV-229E and both OC43 and MHV. More recently, Schmidt and Kenny (1982), using rocket immunoelectrophoresis, found no evidence of cross-reactivity between any of the structural proteins of HCV-229E and OC43, whereas Gerdes *et al.* (1981a,b) and Hasony and Macnaughton (1982) detected some antigenic cross-reactivity between the N proteins of HCV-229E and MHV by immunoprecipitation and enzyme-linked immunoassay.

Using immunofluorescence, Pedersen *et al.* (1978) separated eight mammalian coronaviruses into two antigenically distinct groups. One group consisted of MHV, HEV, HCV-OC43, and BCV. The second group included TGEV, HCV-229E, FIPV, and CCV. Additional anti-

genic cross-reactions between other coronaviruses have been detected: the rat coronaviruses, RCV and SDAV, were antigenically related to MHV (Parker *et al.*, 1970; Bhatt *et al.*, 1972), and the rabbit coronavirus which produces pleural effusion disease (RbCV) cross-reacted with both HCV-229E and HCV-OC43 (Small *et al.*, 1979). Another mammalian coronavirus, the procine enteropathogenic coronavirus designated CV777, did not cross-react with any other coronavirus tested, including TGEV, HEV, FIPV, CCV, BCV, and IBV (Pensaert *et al.*, 1981). These antigenic relationships are summarized in Table VI.

Recent studies of antigenic relationships among coronaviruses have focused on antigens of individual structural proteins and have employed monospecific and monoclonal antibodies. Gerdes, Burks, and their co-workers showed that two coronaviruses (SD and SK) isolated from fresh autopsy brain tissue from two patients with multiple sclerosis (Burks *et al.*, 1980) were serologically related to MHV-A59 and HCV-OC43 (Gerdes *et al.*, 1981a,b). Antisera prepared against each of the four viruses, SD, SK, A59, and OC43, precipitated all three structural proteins (E1, E2 and N) of the other three viruses, demonstrating that the structural proteins of these viruses were antigenically related. Gerna *et al.* (1981) found a high degree of cross-reactivity between E2s of OC43 and BCV. Reynolds *et al.* (1980) showed cross-reactivity between E2s of TGEV and CCV, and Horzinek *et al.* (1982) have demonstrated cross-reactivity between analogous E1, E2, and N proteins of TGEV, FIPV, and CCV using radioimmune precipitation, electroblotting, and enzyme-linked immunosorbent assay. At the present time, coronaviruses can be classified into two major subgroups: avian coronaviruses and mammalian coronaviruses. Mammalian coronaviruses can be further subdivided into at least two subtypes. Within each subtype, individual virus species can be readily distinguished. There appears to be a great degree of antigenic diversity within some coronavirus species which have been studied extensively, including IBV and MHV. This suggests that there may be considerable antigenic drift in these coronaviruses (see Section III,G).

VI. Conclusions

Coronaviruses have recently emerged as an important group of animal and human pathogens which share a distinctive replicative cycle. Some of the unique characteristics in the replication of coronaviruses illustrated in Fig. 11 include generation of a 3′ coterminal-nested set of five or six subgenomic mRNAs, each of which appears to direct the synthesis of one protein. Two virus-specific RNA polymerase activities

TABLE VI

ANTIGENIC RELATIONSHIPS OF CORONAVIRUSES[a,b]

Antiserum against	Viral substrates														
	IBV	MHV	RCV	SDAV	HCV-OC43	HEV	BCV	RbCV	RbECV	TGEV	HCV-229E	FIPV	FECV	CCV	PCV
IBV	+	–	*	*	–	*	*	–	–	*	–	*	*	–	–
MHV	–	+++	+++	+++	+++	+++	++	*	*	–	–(+)	–	*	–	*
RCV	*	+++	+++	+++	*	*	*	*	*	*	*	*	*	–	*
SDAV	*	+++	+++	+++	*	*	*	*	*	*	*	*	*	*	*
HCV-OC43	–	+++	*	*	+++	+++	++	++	*	–	–(+)	–	*	–	*
HEV	*	±	*	*	++	+++	++	*	–	–	–	*	–	–	–
BCV	*	±	*	*	++	+++	+++	*	*	–	–	–	*	–	–
RbCV	–	–	–	*	–	*	*	*	*	*	+	*	*	*	*
RbECV	–	*	*	*	*	*	*	*	*	*	*	*	*	*	*
TGEV	*	–	*	*	–	–	–	*	*	+++	+	+++	*	+	–
HCV-229E	–	–(+)	*	*	–(+)	–	–	++	+	++	+++	+	*	–	*
FIPV	*	–	*	*	–	–	–	*	*	+++	±	+++	+++	+++	*
FECV	*	*	*	*	*	*	*	*	*	+++	*	+++	+++	+++	*
CCV	–	–	*	*	–	–	–	*	*	–	–	+	*	+++	–
PCV	–	*	*	*	*	*	–	*	*	–	*	–	*	–	+

[a] Adapted from Pedersen *et al.* (1978).

[b] *, not tested.

have been identified. Early RNA polymerase snythesizes a negative strand of genome size. A double-stranded form has been identified in the infected cell. The subgenomic mRNAs are synthesized from a full-length, negative-stranded template by a second (late) RNA polymerase. RNA fusion or some other type of RNA modification appears to be involved in mRNA synthesis.

Many of the distinctive features of coronavirus infection and coronavirus-induced diseases may result from the properties of the two coronavirus glycoproteins. The intracellular budding site, which may be important in the establishment and maintenance of persistent infections, appears to be due to the restricted intracytoplasmic migration of the E1 glycoprotein, which acts as a matrix-like transmembrane glycoprotein. E1 also exhibits distinctive behavior by self-aggregating on heating at 100°C in SDS and by its interaction with RNA in the viral nucleocapsid. The E1 of MHV is an O-linked glycoprotein, unlike most other viral glycoproteins. Thus, the coronavirus system may be a useful model for the study of synthesis, glycosylation, and transport of O-linked cellular glycoproteins.

E2 is a large, multifunctional, peplomeric glycoprotein which exhibits unusual pH-and temperature-dependent conformational changes. As for the myxo- and paramyxoviruses, it appears that specific proteolytic cleavage of E2 is necessary for coronavirus-induced cell fusion, and may also be an important determinant of coronavirus pathogenicity. Future research must address the difficult problems of determining the functional relationships and their roles in infection and disease.

Thus, in recent years a large collection of facts about the replication of coronaviruses has been compiled. The interaction of these facts has formed a coherent system such as that described by Fleck (1979), so that a comprehensive understanding of the replication of the coronaviruses has begun to emerge. As Uhlenbeck (1971) visualized, a new frontier has developed from the contributions of many investigators. From this frontier in coronavirus research, many new and exciting developments may now be anticipated.

ACKNOWLEDGMENTS

We wish to thank the many investigators who generously shared their knowledge, illustrations, and unpublished data with us for this article. Excellent secretarial assistance was provided by Kathleen Cavanagh, Mary Tribley, and Elinore Dunphy. This work was supported by grants numbered AI18997 and GM31698 from the National Institutes of Health, and R07043 from the Uniformed Services University of the Health Sciences. The opinions expressed are the private views of the authors and should not be

construed as official or necessarily reflecting the views of the Uniformed Services University School of Medicine or the Department of Defense.

REFERENCES

Alexander, D. J., and Collins, M. S. (1975). Effect of pH on the growth and cytopathogenicity of avian infectious bronchitis virus in chick kidney cells. *Arch. Virol.* **49,** 339–348.

Alexander, D. J., and Collins, M. S. (1977). The purification and polypeptide composition of avian infectious bronchitis virus. *Microbios* **18,** 87–98.

Almeida, J. D., and Tyrrell, D. A. J. (1967). The morphology of three previously uncharacterized human respiratory viruses that grow in organ culture. *J. Gen. Virol.* **1,** 175–178.

Anderson, R., Cheley, S., and Haworth-Hatherell, E. (1979). Comparison of polypeptides of two strains of murine hepatitis virus. *Virology* **97,** 492–494.

Apostolov, K., Flewett, T. H., and Kendal, A. P. (1970). Morphology of influenza ABC and infectious bronchitis virus (IBV) virions and their replication. *In* "The Biology of Large RNA Viruses" (R. D. Barry and B. W. J. Mahy, eds.), pp. 3–26. Academic Press, New York.

Armstrong, J., Smeekens, S., and Rottier, P. (1983). Sequence of the nucleocapsid gene from coronavirus MHV-A59. *Nucleic Acids Res.* **11,** 883–891.

Arnheiter, H., and Haller, O. (1981). Inborn resistance of mice to mouse hepatitis virus type 3 (MHV3). *In* "Biochemistry and Biology of Coronaviruses" (V. ter Meulen, S. Siddell, and H. Wege, eds.), pp. 409–417. Plenum, New York.

Arnheiter, H., Baechi, T., and Haller, O. (1982). Adult mouse hepatocytes in primary monolayer culture express genetic resistance to mouse hepatitis virus type 3. *J. Immunol.* **129,** 1275–1281.

Bang, F. B. (1978). Genetics of resistance of animals to viruses. I. Introduction and studies in mice. *Adv. Virus Res.* **23,** 269–348.

Bang, F. B. (1981). The use of a genetically incompatable combination of host and virus (MHV) for the study of mechanisms of host resistance. *In* "Biochemistry and Biology of Coronaviruses" (V. ter Meulen, S. Siddell, and H. Wege, eds.), pp. 359–373. Plenum, New York.

Bang, F. B., and Cody, T. S. (1980). Is genetic resistance to mouse hepatitis based on immunological reactions? *In* "Genetic Control of Natural Resistance to Infection and Malignancy" (E. Skamene, P. A. L. Kongshavn, and M. Landy, eds.), pp. 215–226. Academic Press, New York.

Bang, F. B., and Warwick, A. (1959). Macrophages and mouse hepatitis. *Virology* **9,** 715–717.

Bang, F. B., and Warwick, A. (1960). Mouse macrophages as host cells for the mouse hepatitis virus and the genetic basis of their susceptibility. *Proc. Natl. Acad. Sci. U.S.A.* **46,** 1065–1075.

Becker, W. B., McIntosh, K., Dees, J. H., and Chanock, R. M. (1967). Morphogenesis of avian infectious bronchitis virus and a related human virus (strain 229E). *J. Virol.* **1,** 1019–1027.

Berry, D. M., Cruickshank, J. G., Chu, H. P., and Wells, R. H. J. (1964). The structure of infectious bronchitis virus. *Virology* **23,** 403–407.

Bhatt, P. N., Percy, D. H., and Jonas, A. M. (1972). Characterization of the virus of sialodacryoadenitis of rats: A member of the coronavirus group. *J. Infect. Dis.* **126,** 123–130.

Bingham, R. W. (1975). The polypeptide composition of avian infectious bronchitis virus. *Arch. Virol.* **49,** 207–216.

Bingham, R. W., and Almedia, J. D. (1977). Studies on the structure of a coronavirus-Avian infectious bronchitis virus. *J. Gen. Virol.* **36,** 495–502.

Bingham, R. W., Madge, M. H., and Tyrrell, D. A. (1975). Haemagglutination by avian infectious bronchitis virus—a coronavirus. *J. Gen. Virol.* **28,** 381–390.

Bond, C. W., Leibowitz, H. L., and Robb, J. A. (1979). Pathogenic murine coronaviruses. II. Characterization of virus-specific proteins of murine coronavirus JHMV and A59V. *Virology* **94,** 371–384.

Bond, C. W., Anderson, K., Goss, S., and Sardinia, L. (1981). Relatedness of virion and intracellular proteins of the murine coronavirus JHM and A59. *In* "Biochemistry and Biology of Coronaviruses" (V. ter Meulen, S. Siddell, and H. Wege, eds.), pp. 103–110. Plenum, New York.

Bradburne, A. F. (1970). Antigenic relationships amongst coronaviruses. *Arch. Gesamte Virusforsch.* **31,** 352–364.

Bradburne, A. F., and Tyrrell, D. A. J. (1969). The propagation of "coronaviruses" in tissue-culture. *Arch. Gesamte Virusforsch.* **28,** 133–150.

Brayton, P. R., Ganges, R. G., and Stohlman, S. A. (1981). Host cell nuclear function and murine hepatitis virus replication. *J. Gen. Virol.* **56,** 457–460.

Brayton, P. R., Lai, M. M. C., Patton, C. D., and Stohlman, S. A. (1982). Characterization of two RNA polymerase activities induced by mouse hepatitis virus. *J. Virol.* **42,** 847–853.

Brian, D. A., Dennis, D. E., and Guy, J. S. (1980). Genome of porcine transmissible gastroenteritis virus. *J. Virol.* **34,** 410–415.

Bridger, J. C., Woode, G. N., and Meyling, A. (1978). Isolation of coronaviruses from neonatal calf diarrhoea in Great Britain and Denmark. *Vet. Microbiol.* **3,** 101–113.

Bruckova, M., McIntosh, K., Kapikian, A. Z., and Chanock, R. M. (1970). The adaptation of two human coronavirus strains (OC38 and OC43) to growth in cell monolayers (35068). *Proc. Soc. Exp. Biol. Med.* **135,** 431–435.

Burks, J. S., DeVald, B. D., Jankovsky, L. C., and Gerdes, C. (1980). Two coronaviruses isolated from central nervous system tissue of two multiple sclerosis patients. *Science* **209,** 933–934.

Busch, H., Reddy, R., Rothblum, L., and Choi, Y. C. (1982). SnRNAs, SnRNPs, and RNA processing. *Ann. Rev. Biochem.* **51,** 617–654.

Callebaut, P. E., and Pensaert, M. B. (1980). Characterization and isolation of structural polypeptides in haemagglutinating encephalomyelitis virus. *J. Gen. Virol.* **48,** 193–204.

Carmichael, L. E., and Binn, L. N. (1981). New enteric viruses in the dog. *Adv. Vet. Sci. Comp. Med.* **25,** 1–37.

Caul, E. O., and Egglestone, S. I. (1977). Further studies on human enteric coronaviruses. *Arch. Virol.* **54,** 107–117.

Caul, E. O., Ashley, C. R., Ferguson, M., and Egglestone, S. I. (1979). Preliminary studies on the isolation of coronavirus 229E nucleocapsids. *FEMS Microbiol. Lett.* **5,** 101–105.

Cavanagh, D. (1981). Structural polypeptides of coronavirus IBV. *J. Gen. Virol.* **53,** 93–103.

Chasey, D., and Alexander, D. J. (1976). Morphogenesis of Avian infectious bronchitis virus in primary chick kidney cells. *Arch. Virol.* **52,** 101–111.

Cheley, S., and Anderson, R. (1981). Cellular synthesis and modification of murine hepatitis virus polypeptides. *J. Gen. Virol.* **54,** 301–311.

Cheley, S., Anderson, R., Cupples, M. J., LeeChan, E. C. M., and Morris, V. L. (1981a).

Intracellular murine hepatitis virus-specific RNAs contain common sequences. *Virology* **112,** 596–604.

Cheley, S., Morris, V. L., Cupples, M., and Anderson, R. (1981b). RNA and polypeptide homology among murine coronaviruses. *Virology* **115,** 310–321.

Clewley, J. P., Morser, J., Avery, R. J., and Lomniczi, B. (1981). Oligonucleotide fingerprinting of the RNA of different strains of infectious bronchitis virus. *Infect. Immun.* **32,** 1227–1233.

Cody, T. S. (1980). Factors governing the responses of macrophages to MHV *in vitro*. Doctor of Science Thesis, Johns Hopkins University School of Hygiene and Public Health, Baltimore, Maryland.

Collins, A. R., Knobler, R. L., Powell, H., and Buchmeier, M. J. (1982). Monoclonal antibodies to murine hepatitis virus 4 (strain JHM) define the viral glycoprotein responsible for attachment and cell-cell fusion. *Virology* **119,** 358–371.

Collins, M. S., and Alexander, D. J. (1980a). Avian infectious bronchitis virus structural polypeptides. Effect of different conditions of disruption and comparison of different strains and isolates. *Arch. Virol.* **63,** 239–251.

Collins, M. S., and Alexander, D. J. (1980b). The polypeptide composition of isolated surface projections of avian infectious bronchitis virus. *J. Gen. Virol.* **48,** 213–217.

Collins, M. S., Alexander, D. J., and Harkness, J. W. (1976). Heterogeneity of infectious bronchitis virus grown in eggs. *Arch. Virol.* **50,** 55–72.

Compans, R. W., and Pinter, A. (1975). Incorporation of sulfate into influenza virus glycoproteins. *Virology* **66,** 151–160.

Corbo, L. J., and Cunningham, C. H. (1959). Hemagglutination by trypsin-modified infectious bronchitis virus. *Am. J. Vet. Res.* **20,** 876–883.

Coria, M. F., and Ritchie, A. E. (1973). Serial passage of three strains of avian infectious bronchitis virus in African green monkey kidney cells (Vero). *Avian Dis.* **17,** 697–704.

Cunningham, C. H., Spring, M. F., and Nazerian, K. (1972). Replication of avian infectious bronchitis virus in African green monkey kidney cell line Vero. *J. Gen. Virol.* **16,** 423–427.

Dales, S., and Howatson, A. F. (1961). Virus-like particles in association with L strain cells. *Cancer Res.* **21,** 193–197.

David-Ferreira, J. F., and Manaker, R. A. (1965). An electron microscope study of the development of a mouse hepatitis virus in tissue culture cells. *J. Cell Biol.* **24,** 57–78.

Davies, H. A., and Macnaughton, M. R. (1979). Comparison of the morphology of three coronaviruses. *Arch. Virol.* **59,** 25–33.

Davies, H. A., Dourmashkin, R. R., and Macnaughton, M. R. (1981). Ribonucleoprotein of Avian infectious bronchitis virus. *J. Gen. Virol.* **53,** 67–74.

Delihas, N., and Andersen, J. (1982). Generalized structures of 5S ribosomal RNAs. *Nucleic Acids Res.* **10,** 7323–7344.

Dennis, D. E., and Brian, D. A. (1981). Coronavirus cell-associated RNA-dependent RNA polymerase. *In* "Biochemistry and Biology of Coronaviruses" (V. ter Meulen, S. Siddell, and H. Wege, eds.), pp. 155–170. Plenum, New York.

Dennis, D. E., and Brian, D. A. (1982). RNA-dependent RNA polymerase activity in coronavirus-infected cells. *J. Virol.* **42,** 153–164.

Doller, E. W., and Holmes, K. V. (1980). Different intracellular transportation of the envelope glycoproteins E1 and E2 of the coronavirus MHV. *Am. Soc. Microbiol. Abstr. Annu. Meet.* Abstract No. T190.

Doller, E. W., Oliver, C., and Holmes, K. (1983). The two glycoproteins of a coronavirus show different patterns of intracellular migration. Submitted for publication.

Doughri, A. M., and Storz, J. (1977). Light and ultrastructural pathologic changes in intestinal coronavirus infection of newborn calves. *Zentralbl. Veterinaermed., Reihe B* **24,** 367–387.

Doughri, A. M., Storz, J., Hajer, I., and Fernando, H. S. (1976). Morphology and morphogenesis of a coronavirus infecting intestinal epithelial cells of newborn calves. *Exp. Mol. Pathol.* **25,** 355–370.

Dubois-Dalcq, M. E., Doller, E. W., Haspel, M. V., and Holmes, K. V. (1982). Cell tropism and expression of mouse hepatitis viruses (MHV) in mouse spinal cord cultures. *Virology* **119,** 317–331.

Ducatelle, R., Coussement, W., Pensaert, M. B., DeBouck, P., and Hoorens, J. (1981). *In vivo* morphogenesis of a new procine enteric coronavirus CV 777. *Arch. Virol.* **68,** 35–44.

Dupuy, J. M., Levy-Leblond, E., and Prevost, C. (1975). Immunopathology of mouse hepatitis virus type 3 infection. II. Effect of immunosuppression in resistant mice. *J. Immunol.* **114,** 116–120.

Evans, M. R., and Simpson, R. W. (1980). The coronavirus avian infectious bronchitis virus requires the cell nucleus and host transcriptional factors. *Virology* **105,** 582–591.

Fleck, L. (1979). "Genesis and Development of a Scientific Fact." Univ. of Chicago Press, Chicago, Illinois.

Gallily, R., Warwick, A., and Bang, F. B. (1964). Effect of cortisone on genetic resistance to mouse hepatitis virus *in vivo* and *in vitro*. *Proc. Natl. Acad. Sci. U.S.A.* **51,** 1158–1164.

Garwes, D. J. (1980). Structure and physiocochemical properties of coronaviruses *Colloq.—Inst. Nat. Sante Rech. Med.* **90,** 141–162.

Garwes, D. J., and Pocock, D. H. (1975). The polypeptide structure of transmissible gastroenteritis virus. *J. Gen. Virol.* **29,** 25–34.

Garwes, D. J., and Reynolds, D. J. (1981). The polypeptide structure of canine coronavirus and its relationship to porcine transmissible gastroenteritis virus. *J. Gen. Virol.* **52,** 153–157.

Garwes, D. J., Pocock, D. H., and Wijaskza, T. M. (1975). Identification of heat-dissociable RNA complexes in two porcine coronaviruses. *Nature (London)* **257,** 508–510.

Garwes, D. J., Pocock, D. H., and Pike, B. V. (1976). Isolation of subviral components from transmissible gastroenteritis virus. *J. Gen. Virol.* **32,** 283–294.

Garwes, D. J., Lucas, M. H., Higgins, D. A., Pike, B. V., and Cartwright, S. F. (1978–1979). Antigenicity of structural components from porcine transmissible gastroenteritis virus. *Vet. Microbiol.* **3,** 179–190.

Gerdes, J. C., Jankovsky, L. D., De Vald, B. L., Klein, I., and Burks, J. S. (1981a). Antigenic relationships of coronaviruses detectable by plaque neutralization, competitive enzyme-linked immunoabsorbent assay and immunoprecipitation. *In* "Biochemistry and Biology of Coronaviruses" (V. ter Meulen, S. Siddell, and H. Wege, eds.), pp. 29–42. Plenum, New York.

Gerdes, J. C., Klein, I., De Vald, B., and Burks, J. S. (1981b). Coronavirus isolates SK and SD from multiple sclerosis patients are serologically related to murine coronaviruses A59 and JHM and human coronavirus OC43, but not to human coronavirus 229E. *J. Virol.* **38,** 231–238.

Gerna, G., Cereda, P. M., Revello, M. G., Torsellini-Gerna, M., and Costa, J. (1979). A rapid microneutralization test for antibody determination and serogianosis of human coronavirus OC43 infections. *Microbiologica* **2,** 331–344.

Gerna, G., Cereda, P. M., Grazia-Revello, M., Cattaneo, E., Battaglia, M., and Torsellini-Gerna, M. (1981). Antigenic and biological relationships between human coronavirus OC43 and neonatal calf diarrhoea coronavirus. *J. Gen. Virol.* **54,** 91–102.

Greig, A. S., Mitchell, D., Corner, A. H., Bannister, G. L., Meads, E. B., and Julian, R. J. (1962). A hemagglutinating virus producing encephalomyelitis in baby pigs. *Can. J. Comp. Med.* **26,** 49–56.

Greig, A. S., Johnson, C. M., and Bouillant, A. M. P. (1971). Encephalitis of swine caused by a haemagglutinating virus. VI. Morphology of the virus. *Res. Vet. Sci.* **12,** 305–307.

Guy, J. S., and Brian, D. A. (1979). Bovine coronavirus genome. *J. Virol.* **29,** 293–300.

Hamre, D., and Procknow, J. J. (1966). A new virus isolated from the human respiratory tract. *Proc. Soc. Exp. Biol. Med.* **121,** 190–193.

Hamre, D., Kindig, D. A., and Mana, J. (1967). Growth and intracellular development of a new respiratory virus. *J. Virol.* **1,** 810–816.

Hartley, J. W., and Rowe, W. P. (1963). Tissue culture cytopathic and plaque assays for mouse hepatitis viruses. *Proc. Soc. Exp. Biol. Med.* **113,** 403–406.

Hasony, H. J., and Macnaughton, M. R. (1981). Antigenicity of mouse hepatitis virus strain 3 subcomponents in C57 strain mice. *Arch. Virol.* **69,** 33–41.

Hasony, H. J., and Macnaughton, M. R. (1982). Serological relationships of the subcomponents of human coronavirus strain 229E and mouse hepatitis virus strain 3. *J. Gen. Virol.* **58,** 449–452.

Haspel, M. V., Lambert, P. W., and Oldstone, M. B. (1978). Temperature-sensitive mutants of mouse hepatitis virus produce a high incidence of demyelination. *Proc. Natl. Acad. Sci. U.S.A.* **75,** 4033–4036.

Haspel, M. V., Holmes, K. V., and Welsh, R. M. (1981). Natural cell-mediated cytotoxicity against mouse hepatitis virus (MHV) infected cells. *Am. Soc. Microbiol. Abstr. Annu. Meet.* Abstract No. E9.

Heggeness, M. H., Scheid, A., and Choppin, P. W. (1980). Conformation of the helical nucleocapsids of paramyxoviruses and vesicular stomatitis virus: Reversible coiling and uncoiling induced by changes in salt concentration. *Proc. Natl. Acad. Sci. U.S.A.* **77,** 2631–2635.

Heggeness, M. H., Smith, P. R., Ulmanen, J., Krug, R. M., and Choppin, P. W. (1982). Studies on the helical nucleocopsid of influenza virus. *Virology* **118,** 466–470.

Heilman, C. A., Engel, L., Lowry, O. R., and Howley, P. M. (1982). Virus-specific transcription in bovine papillomavirus-transformed mouse cells. *Virology* **119,** 22–34.

Helenius, A., Kartenbeck, J., Simons, K., and Fries, E. (1980a). On the entry of Semliki Forest virus into BHK-21 cells. *J. Cell Biol.* **84,** 404–420.

Helenius, A., Marsh, M., and White, J. (1980b). The entry of viruses into animal cells. *Trends Biochem. Sci.* **5,** 104–106.

Helenius, A., Marsh, M., and White, J. (1982). Inhibition of Semliki Forest virus penetration by lysosomotropic weak bases *J. Gen Virol.* **58,** 47–61.

Hierholzer, J. C., Palmer, E. L., Whitfield, S. G., Kaye, H. S., and Dowdle, W. R. (1972). Protein composition of coronavirus OC43. *Virology* **48,** 516–527.

Hirano, N., Fujiwara, K., Hino, S., and Matumoto, M. (1974). Replication and plaque formation of mouse hepatitis virus (MHV-2) in mouse cell line DBT culture. *Arch. Gesamte Virusforsch.* **44,** 298–302.

Hirano, N., Fujiwara, K., and Matumoto, M. (1976). Mouse hepatitis virus (MHV-2): Plaque assay and propagation in mouse cell line DBT cells. *J. J. Microbiol.* **20,** 219–225.

Hirano, N., Murakami, T., Fujiwara, K., and Matsumoto, M. (1978). Utility of mouse cell line DBT for propagation and assay of mouse hepatitis virus. *J. J. Exp. Med.* **48,** 71–75.

Hirano, N., Goto, N., Makino, S., and Fujiwara, K. (1981). Persistent infection with mouse hepatitis virus JHM strain in DBT cell culture. *In* "Biochemistry and Biology of Coronaviruses" (V. ter Meulen, S. Siddell, and H. Wege, eds.), pp. 301–308. Plenum, New York.

Holland, J., Spindler, K., Horadyski, F., Grabau, E., Nichol, S., and Vandepol, S. (1982). Rapid evolution of RNA genomes. *Science* **215,** 1577–1585.

Holmes, K. V., and Behnke, J. N. (1981). Evolution of a coronavirus during persistent infection *in vitro*. *In* "Biochemistry and Biology of Coronaviruses" (V. ter Meulen, S. Siddell, and H. Wege, eds.), pp. 287–299. Plenum, New York.

Holmes, K. V., Doller, E. W., and Sturman, L. S. (1981a). Tunicamycin resistant glycosylation of a coronavirus glycoprotein: Demonstration of a novel type of viral glycoprotein. *Virology* **115,** 334–344.

Holmes, K. V., Doller, E. W., and Behnke, J. N. (1981b). Analysis of the functions of coronavirus glycoproteins by differential inhibition of synthesis with tunicamycin.*In* "Biochemistry and Biology of Coronaviruses" (V. ter Meulen, S. Siddell, and H. Wege, eds.), pp. 133–142. Plenum, New York.

Horzinek, M. C., Lutz, H., and Pedersen, N. C. (1982). Antigenic relationships among homologous structural polypeptides of procine, feline, and canine coronaviruses. *Infect. Immun.* **37,** 1148–1155.

Hsu, C. H., and Kingsbury, D. W. (1982). Contribution of oligosaccharide sulfation to the charge heterogeneity of viral glycoprotein. *J. Biol. Chem.* **257,** 9035–9038.

Huang, R. T. C., Rott, R., and Klenk, H. -D. (1981). Influenza viruses cause hemolysis and fusion of cells. *Virology* **110,** 243–247.

Huttner, W. B. (1982). Sulfation of tyrosine residues—a widespread modification of proteins *Nature* (*London*) **299,** 273–276.

Jacobs, L., Spaan, W. J. M., Horzinek, M. C., and van der Zeijst, B. A. M. (1981). The synthesis of the subgenomic mRNAs of mouse hepatitis virus is initiated independently: evidence from UV transcription mapping. *J. Virol.* **39,** 401–406.

Kantoch, M., Warwick, A., and Bang, F. B. (1963). The cellular nature of genetic susceptibility to a virus. *J. Exp. Med.* **117,** 781–798.

Kapikian, A. Z., James, H. D., Jr., Kelly, S. J., Dees, H. J., Turner, H. C., McIntosh, K., Kim, H. W., Parrott, R. H., Vincent, M. M., and Chanock, R. M. (1969). Isolation from man of "Avian bronchitis virus-like" viruses (coronaviruses) similar to 229E virus, with some epidemiological observations. *J. Infect. Dis.* **119,** 282–290.

Kaye, H. S., and Dowdle, W. R. (1969). Some characteristics of hemagglutination of certain strains of "IBV-like" virus. *J. Infect. Dis.* **120,** 576–581.

Keller, K. L., Keller, J. M., and Moy, J. M. (1980). Heparan sulfate from Swiss mouse 3T3 and SV3T3 cells: O-sulfate difference. *Biochemistry* **19,** 2529–2536.

Kemp, M. C., Compans, R. W., Caterson, B., and Baker, J. R. (1982). Characterization of glycosaminoglycans associated with Rauscher murine leukemia virus. *Membr. Biochem.* **4,** 219–234.

Kennedy, D. A., and Johnson-Lussenburg, C. M. (1975–1976). Isolation and morphology of the internal component of human coronavirus, strain 229E. *Intervirology* **6,** 197–206.

King, B., and Brian, D. A. (1982). Bovine coronavirus structural proteins. *J. Virol.* **42,** 700–707.

Klenk, H. D., and Rott, R. (1981). Cotranslational and posttranslational processing of viral glycoproteins. *Curr. Top. Microbiol. Immunol.* **90,** 19–48.

Knobler, R. L., Haspel, M. V., Dubois-Dalcq, M., Lampert, P. W., and Oldstone, M. B. A. (1981a). Host and virus factors associated with CNS cellular tropism leading to encephalomyelitis or demyelination induced by the JHM strain of mouse hepatitis virus. *In* "Biochemistry and Biology of Coronaviruses (V. ter Meulen, S. Siddell, and H. Wege, eds.), pp. 341–348. Plenum, New York.

Knobler, R. L., Haspel, M. V., and Oldstone, M. B. A. (1981b). Mouse hepatitis virus type 4 (JHM strain) induced fatal nervous system disease. Part I. Genetic control and the murine neuron as the susceptible site of disease. *J. Exp. Med.* **133,** 832–843.

Knobler, R. L., Dubois-Dalcq, M., Haspel, M. V., Claysmith, A. P., Lampert, P. W., and Oldstone, M. B. A. (1981c). Selective localization of wild type and mutant mouse

hepatitis virus (JHM-strain) antigens in CNS tissue by fluorescence light and electron microscopy. *J. Neuroimmunol.* **1,** 81–92.

Knobler, R. L., Lampert, P. W., and Oldstone, M. B. A. (1982). Virus persistence and recurring demyelination produced by a temperature-sensitive mutant of MHV-4. *Nature (London)* **298,** 279–280.

Koolen, M. J. M., Horzinek, M. C., and van der Zeijst, B. A. M. (1981). Isolation and biochemical characterization of 21 temperature-sensitive mutants of MHV-A59. *Abstr., Intl. Congr. Virol., 5th, 1981* p. 421.

Koolen, M. J. M., Osterhaus, D. M. E., van Steenis, G., Horzinek, M. C., and van der Zeijst, B. A. M. (1983). Temperature sensitive mutants of mouse hepatitis virus strain A59: Isolation, characterization and neuropathogenic properties. *Virology* **125,** 393–402.

Kraaijeveld, C. A., Madge, M. H., and Macnaughton, M. R. (1980). Enzyme-linked immuno-sorbent assay for coronaviruses HCV229E and MHV-3. *J. Gen. Virol.* **49,** 83–89.

Kraemer, P. M., and Smith, D. A. (1974). High molecular weight heparan sulfate from the cell surface. *Biochem. Biophys, Res. Commun.* **56,** 423–430.

Krystyniak, K., and Dupuy, J. M. (1981). Early interaction between mouse hepatitis virus 3 and cells. *J. Gen. Virol.* **57,** 53–61.

Lai, M. M. C., and Stohlman, S. A. (1978). The RNA of mouse hepatitis virus. *J. Virol.* **26,** 236–242.

Lai, M. M. C., and Stohlman, S. A. (1981). Comparative analysis of RNA genomes of mouse hepatitis viruses. *J. Virol.* **38,** 661–670.

Lai, M. M. C., Brayton, P. R., Armen, R. C., Patton, C. D., Pugh, C., and Stohlman, S. A. (1981). Mouse hepatitis virus A59 messenger RNA structure and genetic localization of the sequence divergence from the hepatropic strain MHV3. *J. Virol.* **39,** 823–834.

Lai, M. M. C., Patton, C. D., and Stohlman, S. A. (1982a). Further characterization of mouse hepatitis virus: Presence of common 5′-end nucleotides. *J. Virol.* **41,** 557–565.

Lai, M. M. C., Patton, C. D., and Stohlman, S. A. (1982b). Replication of mouse hepatitis virus: Negative-stranded RNA and replicative form RNA are of genome length. *J. Virol.* **44,** 487–492.

Lanser, J. A., and Howard, C. R. (1980). The polypeptides of infectious bronchitis virus (IBV-41 strain). *J. Gen. Virol.* **46,** 349–361.

LaPierre, L., Marsolais, G., Pilon, P., and Descoteaux, J.-P. (1980). Preliminary report on the observation of a coronavirus in the intestine of the laboratory rabbit. *Can. J. Microbiol.* **26,** 1204–1208.

Laporte, J., and Bobulesco, P. (1981). Growth of human and canine enteric coronaviruses in a highly susceptible cell line: HRT18. *Perspect. Virol.* **11,** 189–193.

Lavelle, G. C., and Bang, F. B. (1971). Influence of type and concentration of sera *in vitro* on susceptibility of genetically resistant cells to mouse hepatitis virus. *J. Gen. Virol.* **12,** 233–238.

Leibowitz, J. L., and Weiss, S. R. (1981). Murine coronavirus RNA. *In* "Biochemistry and Biology of Coronaviruses" (V. ter Meulen, S. Siddell, and H. Wege, eds.), pp. 227–244. Plenum, New York.

Leibowitz, J. L., Wilhelmsen, K. C., and Bond, C. W. (1981). The virus-specific intracellular RNA species of two murine coronaviruses: MHV-A59 and MHV-JHM. *Virology* **114,** 29–51.

Leibowitz, J. L., DeVries, J. R., and Haspel, M. V. (1982a). Genetic analysis of murine hepatitis virus strain JHM. *J. Virol.* **42,** 1080–1087.

Leibowitz, J. L., Weiss, S. R., Paavola, E., and Bond, C. W. (1982b). Cell-free translation of murine coronavirus RNA. *J. Virol.* **43,** 905–913.

LePrevost, C., Virelizier, J. L., and Dupuy, J. M. (1975). Immunopathology of mouse hepatitis virus type 3 infection. III. Clinical and virologic observation of a persistent viral infection. *J. Immunol.* **115,** 640–645.

Lerner, M. R., Boyle, J. B., Mount, S. M., Wolin, S. L., and Steitz, J. A. (1980). Are snRNPs involved in splicing? *Nature* **283,** 220–224.

Lindenmann, J. (1977). Host antigens in eveloped RNA viruses. *In* "Virus Infection and the Cell Surface" (G. Poste and G. I. Nicolson, eds.), pp. 291–329. Elsevier/North-Holland Biomedical Press, Amsterdam.

Lomniczi, B. (1977). Biological properties of avian coronavirus RNA. *J. Gen. Virol.* **36,** 531–533.

Lomniczi, B., and Kennedy, I. (1977). Genome of infectious bronchitis virus. *J. Virol.* **24,** 99–107.

Lomniczi, B., and Morser, J. (1981). Polypeptides of infectious bronchitis virus. I. Polypeptides of the virion. *J. Gen. Virol.* **55,** 155–164.

McIntosh, K. (1974). Coronaviruses. A comparative review. *Curr. Top. Microbiol. Immunol.* **63,** 85–129.

McIntosh, K., Dees, H. J., Becker, W. B., Kapikian, A. Z., and Chanock, R. M. (1967a). Recovery in tracheal organ cultures of novel viruses from patients with respiratory disease. *Proc. Natl. Acad. Sci. U.S.A.* **57,** 933–940.

McIntosh, K., Becker, W. B., and Chanock, R. M. (1967b). Growth in suckling-mouse brain of "IBV-like" viruses from patients with upper respiratory tract disease. *Proc. Natl. Acad. Sci. U.S.A.* **58,** 2268–2273.

McIntosh, K., Kapikian, A. Z., Hardison, K. A., Hartley, J. W., and Chanock, R. M. (1969). Antigenic relationships among the coronaviruses of man and between human and animal coronaviruses. *J. Immunol.* **102,** 1109–1118.

Macnaughton, M. R. (1978). The genomes of three coronaviruses. *FEBS Lett.* **94,** 191–194.

Macnaughton, M. R. (1980). The polypeptides of human and mouse coronaviruses. *Arch. Virol.* **63,** 75–80.

Macnaughton, M. R. (1981). Structural and antigenic relationships between human murine and avian coronaviruses. *In* "The Biology and Biochemistry of Coronaviruses" (V. ter Meulen, S. Siddell, and H. Wege, eds.), pp. 19–28. Plenum, New York.

Macnaughton, M. R., and Davies, H. A. (1980). Two particle types of avian infectious bronchitis virus. *J. Gen. Virol.* **47,** 365–372.

Macnaughton, M. R., and Davies, H. A. (1981). Human enteric coronaviruses: Brief review. *Arch. Virol.* **70,** 301–313.

Macnaughton, M. R., and Madge, H. (1977a). The polypeptide composition of avian infectious bronchitis virus particles. *Arch. Virol.* **55,** 47–54.

Macnaughton, M. R., and Madge, H. M. (1977b). The characterization of the virion RNA of avian infectious bronchitis virus. *FEBS Lett.* **77,** 311–313.

Macnaughton, M. R., and Madge, M. H. (1978). The genome of human coronavirus strain 229E. *J. Gen. Virol.* **39,** 497–504.

Macnaughton, M. R., and Patterson, S. (1980). Mouse hepatitis virus strain 3 infection of C57, A/Sn and A/J strain mice and their macrophages. *Arch. Virol.* **66,** 71–75.

Macnaughton, M. R., Davies, H. A., and Nermut, M. V. (1978). Ribonucleoprotein-like structures from coronavirus particles. *J. Gen. Virol.* **39,** 545–549.

Macnaughton, M. R., Thomas, B. J., Davies, H. A., and Patterson, S. (1980). Infectivity of human coronavirus strain 229E. *J. Clin. Microbiol.* **12,** 462–468.

Macnaughton, M. R., Hasony, H. J., Madge, M. H., and Reed, S. E. (1981). Antibody to virus components in volunteers experimentally infected with HCV 229E group viruses. *Infect. Immun.* **31,** 845–849.

Mahy, B. W. J., Siddell, S., Wege, H., and ter Meulen, V. (1983). RNA-dependent RNA polymerase activity in murine coronavirus-infected cells. *J. Gen. Virol.* **64,** 103–111.

Mallucci, L. (1965). Observations on the growth of mouse hepatitis virus (MHV-3) in mouse macrophages. *Virology* **25,** 30–37.

Mallucci, L. (1966). Effect of chloroquine on lysosomes and on growth of mouse hepatitis virus (MHV-3). *Virology* **28,** 355–362.

Manaker, R. A., Piczak, C. V., Miller, A. A., and Stanton, M. F. (1961). A hepatitis virus complicating studies with mouse leukemia. *JNCI, J. Natl. Cancer Inst.* **27,** 29–51.

Marsh, M., and Helenius, A. (1980). Adsorptive endocytosis of Semliki Forest virus. *J. Mol. Biol.* **142,** 439–454.

Massalski, A., Coulter-Mackie, M., and Dales, S. (1981). Assembly of mouse hepatitis virus strain JHM. *In* "Biochemistry and Biology of Coronaviruses" (V. ter Meulen, S. Siddell, and H. Wege, eds.), pp. 111–118. Plenum, New York.

Massalski, A., Coulter-Mackie, M., Knobler, R. L., Buchmeier, M. J., and Dales, S. (1982). *In vivo* and *in vitro* models of demyelinating diseases. V. Comparison of the assembly of mouse hepatitis virus, strain JHM, in two murine cell lines. *Intervirology* **18,** 135–146.

Matlin, K. S., Reggio, H., Helenius, A., and Simons, K. (1981). Infectious entry pathway of influenza virus in a canine kidney cell line. *J. Cell Biol.* **91,** 601–603.

Matlin, K. S., Reggio, H., Helenius, A., and Simons, K. (1982). Pathway of vesicular stomatitis virus entry leading to infection. *J. Mol. Biol.* **156,** 609–631.

Mengeling, W. L., Booth, A. D., and Ritchie, A. E. (1972). Characteristics of a coronavirus (strain 67N) of pigs. *Am. J. Vet. Res.* **33,** 297–308.

Mosley, J. W. (1961). Multiplication and cytopathogenicity of mouse hepatitis virus in mouse cell cultures. *Proc. Soc. Exp. Biol. Med.* **108,** 524–529.

Nakamura, K., and Compans, R. W. (1977). The cellular site of sulfation of influenza viral glycoproteins. *Virology* **79,** 381–392.

Niemann, H., and Klenk, H.-D. (1981a). Coronavirus glycoprotein E1, a new type of viral glycoprotein. *J. Mol. Biol.* **153,** 993–1010.

Niemann, H., and Klenk, H.-D. (1981b). Glycoprotein E1 of coronavirus A59. A new type of viral glycoprotein. *In* "Biochemistry and Biology of Coronaviruses" (V. ter Meulen, S. Siddell, and H. Wege, eds.), pp. 119–132. Plenum, New York.

Niemann, H., Boschek, B., Evans, D., Rosing, M., Tamura, T., and Klenk, H. -D. (1982). Post-translational glycosylation of corona virus glycoprotein E1: Inhibition by monensin. *Embo. J.* **1,** 1499–1504.

Oldberg, A., Hook, M., Obrink, B., Pertoft, H., and Rubin, K. (1977). Structure and metabolism of rat liver heparan sulfate. *Biochem. J.* **164,** 75–81.

Oldberg, A., Kjellen, L., and Hook, M. (1979). Cell-surface heparan sulfate: Isolation and characterization of a proteoglycan from rat liver membranes. *J. Biol. Chem.* **254,** 8505–8510.

Oshiro, L. S. (1973). Coronaviruses. *In* "Ultrastructure of Animal Viruses and Bacteriophages: An Atlas" (A. J. Dalton and F. Haguenau, eds.), Chapter 18, pp. 331–343. Academic Press, New York.

Oshiro, L. S., Schieble, J. H., and Lennette, E. H. (1971). Electron microscopic studies of a coronavirus. *J. Gen. Virol.* **12,** 161–168.

Otsuki, K., and Tsubokura, M. (1981). Plaque formation by IBV in 1° CEF cells in the presence of trypsin. *Arch. Virol.* **70,** 315–320.

Otsuki, K., Noro, K., Yamamoto, H., and Tsubokura, M. (1979). Studies on avian infectious bronchitis virus (IBV). II. Propagation of IBV in several cultured cells. *Arch. Virol.* **60,** 115–122.

Parker, J. S., Cross, S. S., and Rowe, W. P. 1970. Rat coronavirus (RCV), a prevalent,

naturally-occurring pneumotropic virus of rats. *Arch. Gesamte Virusforsch.* **31,** 293–302.

Patterson, S., and Bingham, R. W. (1976). Electron microscope observations on the entry of avian infectious bronchitis virus into susceptible cells. *Arch. Virol.* **53,** 267–273.

Patterson, S., and Macnaughton, M. R. (1981). The distribution of human coronavirus strain 229E on the surface of human diploid cells. *J. Gen. Virol.* **53,** 267–273.

Pedersen, N. C., Ward, I., and Mengeling, W. L. (1978). Antigenic relationships of the feline infectious peritonitis virus to coronaviruses of other species. *Arch. Virol.* **58,** 45–53.

Pensaert, M. B., and Callebaut, P. (1978). The coronaviruses. Clinical and structural aspects with some practical implications. *Ann. Med. Vet.* **122,** 301–322.

Pensaert, M. B., Debouck, P., and Reynolds, D. J. (1981). An immunoelectron microscopic and immunofluorescent study on the antigenic relationship between the coronavirus-like agent, CV777, and several coronaviruses. *Arch. Virol.* **68,** 45–52.

Petri, W. A., and Wagner, R. R. (1980). Glycoprotein micelles isolated from VSV spontaneously partition into sonicated phosphatidylcholine vesicles. *Virology* **107,** 543–547.

Pike, B. V., and Garwes, D. J. (1977). Lipids of transmissible gastroenteritis virus and their relation to those of two different host cells. *J. Gen. Virol.* **34,** 531–535.

Pinter, A., and Compans, R. W. (1975). Sulfated components of enveloped viruses. *J. Virol.* **16,** 859–866.

Pocock, D. H. (1978). Effect of sulphydryl reagents on the biological activities, polypeptide composition, and morphology of haemagglutinating encephalomyelitis virus. *J. Gen. Virol.* **40,** 93–101.

Pocock, D. H., and Garwes, D. J. (1975). The influence of pH on the growth and stability of transmissible gastroenteritis virus. *Arch. Virol.* **49,** 239–247.

Pocock, D. H., and Garwes, D. J. (1977). The polypeptides of haemagglutinating encephalomyelitis virus and isolated subviral particles. *J. Gen. Virol.* **37,** 487–499.

Prehm, P., Scheid, A., and Choppin, P. W. (1979). The carbohydrate structure of the glycoproteins of the paramyxovirus SV5 grown in bovine kidney cells. *J. Biol. Chem.* **254,** 9669–9677.

Prinz, R., Klein, U., Sudhakaran, P. R., Sinn, W., Ullrich, K., and von Figura, K. (1980). Metabolism of sulfated glycosaminoglycan in rat hepatocytes: Synthesis of heparan sulfate and distribution into cellular and extracellular pools. *Biochim. Biophys, Acta* **630,** 402–413.

Reynolds, D. J., Garwes, D. J., and Lucey, S. (1980). Differentiation of canine coronavirus and porcine transmissible gastroenteritis virus by neutralization with canine, porcine, and feline sera. *Vet. Microbiol.* **5,** 283–290.

Richter, J. M. (1976). The attachment of mouse hepatitis virus to the plasma membrane of L2 cells. Master of Arts Thesis, University of Texas Health Science Center at Dallas, Dallas, Texas.

Robb, J. A., and Bond, C. W. (1979a). Coronaviridae. *Compr. Virol.* **14,** 193–247.

Robb, J. A., and Bond, C. W. (1979b). Pathogenic murine coronaviruses. I. Characterization of biological behaviour *in vitro* and virus-specific intracellular RNA of strongly neurotropic JHMV and weakly neurotropic A59V viruses. *Virology* **94,** 352–370.

Robb, J. A., Bond, C. W., and Leibowitz, J. L. (1979). Pathogenic murine coronaviruses. III. Biological and biochemical characterization of temperature-sensitive mutants of JHMV. *Virology* **91,** 385–399.

Roden, L. (1980). Structure and metabolism of connective tissue proteoglycans. *In* "The Biochemistry of Glycoproteins and Proteoglycans" (W. J. Lennarz, ed.), pp. 267–371. Plenum, New York.

Rodriguez-Boulan, E., and Sabatini, D. D. (1978). Asymmetric budding of viruses in epithelial monolayers: A model system for study of epithelial polarity. *Proc. Natl. Acad Sci. U.S.A.* **75,** 5071–5075.

Rollins, B. J., and Culp, L. A. (1979). Glycosaminoglycans in the substrate adhesion sites of normal and virus-transformed murine cells. *Biochemistry* **18,** 141–148.

Rottier, P. J. M., Spaan, W. J. M., Horzinek, M., and van der Zeijst, B. A. M. (1981a). Translation of three mouse hepatitis virus (MHV-A59) subgenomic RNAs in *Xenopus laevis* oocytes. *J. Virol.* **38,** 20–26.

Rottier, P. J. M., Horzinek, M. C., and van der Zeijst, B. A. M. (1981b). Viral protein synthesis in mouse hepatitis virus train A59-infected cells: Effect of tunicamycin. *J. Virol.* **40,** 350–357.

Sabesin, S. M. (1971). The role of lysosomes in the pathogenesis of experimental viral hepatitis. *Am. J. Gastroenterol.* **55,** 539–563.

Schlesinger, M. J., and Kaariainen, L. (1980). Translation and processing of alphavirus proteins. *In* "The Togaviruses: Biology, Structure, Replication" (R. W. Schlesinger, ed.), pp. 371–392. Academic Press, New York.

Schmidt, M. F. G. (1982a). Acylation of viral spike glycoproteins, a feature of enveloped RNA viruses. *Virology* **116,** 327–338.

Schmidt, M. F. G. (1982b). Acylation of proteins—a new type of modification of membrane proteins. *Trends Biochem. Sci. (Pers. Ed.)* **7,** 322–324.

Schmidt, M. F. G., and Schlesinger, M. J. (1979). Fatty acid binding to vesicular stomatitis virus glycoprotein: A new type of post-translational modification of the viral glycoprotein. *Cell* **17,** 813–819.

Schmidt, M. F. G., and Schlesinger, M. J. (1980). Relation of fatty acid attachment to the translation and maturation of vesicular stomatitis and Sindbis virus membrane glycoproteins. *J. Biol. Chem.* **255,** 3334–3339.

Schmidt, M. F. G., Bracha, M., and Schlesinger, M. J. (1979). Evidence for covalent attachment of fatty acids to Sindbis virus glycoproteins. *Proc. Natl. Acad. Sci. U.S.A.* **76,** 1687–1691.

Schmidt, O. W., and Kenny, G. E. (1981). Immunogenicity and antigenicity of human coronaviruses 229E and OC43. *Infect. Immun.* **32,** 1000–1006.

Schmidt, O. W., and Kenny, G. E. (1982). Polypeptides and functions of antigens from human coronaviruses 229E and OC43. *Infect. Immun.* **35,** 515–522.

Schmidt, O. W., Cooney, M. K., and Kenny, G. E. (1979). Plaque assay and improved yield of human coronaviruses in a human rhabdomyosarcoma cell line. *J. Clin. Microbiol.* **9,** 722–728.

Schochetman, G., Stevens, R. H., and Simpson, R. W. (1977). Presence of infectious polyadenylated RNA in the coronavirus avian infectious bronchitis virus. *Virology* **77,** 772–782.

Sharpee, R. L., Mebus, C. A., and Bass, E. P. (1976). Characterization of a calf diarrheal coronavirus. *Am. J. Vet. Res.* **37,** 1031–1041.

Shif, I., and Bang, F. B. (1970). *In vitro* interaction of mouse hepatitis virus and macrophages from genetically resistant mice. I. Adsorption of virus and growth curves. *J. Exp. Med.* **131,** 843–850.

Siddell, S. G., Wege, H., Barthel, A., and ter Meulen, V. (1980). Coronavirus JHM. Cell-free synthesis of structural protein p60. *J. Virol.* **33,** 10–17.

Siddell, S. G., Barthel, A., and ter Meulen, V. (1981a). Coronavirus JHM. A virion-associated protein kinase. *J. Gen. Virol.* **52,** 235–243.

Siddell, S. G., Wege, H., Barthel, A., and ter Meulen, V. (1981b). Coronavirus JHM. Intracellular protein synthesis. *J. Gen. Virol.* **53,** 145–155.

Siddell, S., Wege, H., Barthel, A., and ter Meulen, V. (1981c). Intracellular protein

synthesis and the *in vitro* translation of coronavirus JHM mRNA. *In* "Biochemistry and Biology of Coronaviruses" (V. ter Meulen, S. Siddell, and H. Wege, eds.), pp. 193–208. Plenum, New York.

Siddell, S., Wege, H., and ter Meulen, V. (1982). The structure and replication of coronaviruses. *Curr. Top. Microbiol. Immunol.* **99,** 131–163.

Small, J. D., Aurelian, L., Squire, R. A., Strandberg, J. D., Melby, E. C., Jr., Turner, T. B., and Newman, B. (1979). Rabbit cardiomyopathy associated with a virus antigenically related to human coronavirus strain 229E. *Am. J. Pathol.* **95,** 709–729.

Spaan, W. J. M., Rottier, P. J. M., Horzinek, M. C., and van der Zeijst, B. A. M. (1981). Isolation and identification of virus-specific mRNAs in cells infected with mouse hepatitis virus (MHV-A59). *Virology* **108,** 424–434.

Spaan, W. J. M., Rottier, P. J. M., Horzinek, M. C., and van der Zeijst, B. A. M. (1982). Sequence relationships between the genome and the intracellular RNA species 1, 3, 6, and 7 of mouse hepatitis virus strain A59. *J. Virol.* **42,** 432–439.

Stern, D. F., and Kennedy, S. I. T. (1980a). Coronavirus multiplication strategy. I. Identification and characterization of virus-specified RNA. *J. Virol.* **34,** 665–674.

Stern, D. F., and Kennedy, S. I. T. (1980b). Coronavirus multiplication strategy. II. Mapping the avian infectious bronchitis virus intracellular RNA species to the genome. *J. Virol.* **36,** 440–449.

Stern, D. F., and Sefton, B. M. (1982a). Synthesis of coronavirus mRNAs: Kinetics of inactivation of IBV RNA synthesis by UV light. *J. Virol.* **42,** 755–759.

Stern, D. F., and Sefton, B. M. (1982b). Coronavirus proteins: Biogenesis of avian infectious bronchitis virus virion proteins. *J. Virol.* **44,** 794–803.

Stern, D. F., and Sefton, B. M. (1982c). Coronavirus proteins: Structure and function of the oligosaccharides of the avian infectious bronchitis virus glycoproteins. *J. Virol.* **44,** 804–812.

Stern, D. F., Burgess, L., and Sefton, B. M. (1982). Structural analysis of virion proteins of the avian coronavirus infectious bronchitis virus. *J. Virol.* **42,** 208–219.

Stohlman, S. A., and Frelinger, J. A. (1981). Macrophages and resistance to JHM virus. *In* "Biochemistry and Biology of Coronaviruses" (V. ter Meulen, S. Siddell, and H. Wege, eds.), pp. 387–398. Plenum, New York.

Stohlman, S. A., and Lai, M. M. C. (1979). Phosphoproteins of murine hepatitis viruses. *J. Virol.* **32,** 672–675.

Stohlman, S. A., Sakaguchi, A. Y., and Weiner, L. P. (1979). Characterization of the cold-sensitive murine hepatitis virus mutants rescued from latently-infected cells by cell fusion. *Virology* **98,** 448–455.

Stohlman, S. A., Woodward, J. G., and Frelinger, J. A. (1982a). Macrophage antiviral: extrinsic versus intrinsic activity. *Infect. Immun.* **36,** 672–677.

Stohlman, S. A., Brayton, P. R., Fleming, J. O., Weiner, L. P., and Lai, M. M. C. (1982b). Murine coronaviruses: Isolation and characterization of two plaque morphology variants of the JHM neurotropic strain. *J. Gen. Virol.* **63,** 265–275.

Storz, J., Kaluza, G., Niemann, H., and Rott, R. (1981a). On enteropathogenic bovine coronavirus. *In* "Biochemistry and Biology of Coronaviruses" (V. ter Meulen, S. Siddell, and H. Wege, eds.), pp. 171–180. Plenum, New York.

Storz, J., Rott, R., and Kaluza, G. (1981b). Enhancement of plaque formation and cell fusion of an enteropathogenic coronavirus by trypsin treatment. *Infect. Immun.* **31,** 1214–1222.

Sturman, L. S. (1977). Characterization of a coronavirus. I. Structural proteins: Effects of preparative conditions on the migration of protein in polyacrylamide gels. *Virology* **77,** 637–649.

Sturman, L. S. (1980). Coronavirus-associated glycosaminoglycan. *Soc. Microbiol., Abstr. Annu. Meet.* Abstract No. T-192.

Sturman, L. S. (1981). The structure and behaviour of coronavirus A59 glycoproteins. *In* "Biochemistry and Biology of Coronaviruses" (V. ter Meulen, S. Siddell, and H. Wege, eds.), pp. 1–18. Plenum, New York.

Sturman, L. S., and Holmes, K. V. (1977). Characterization of a coronavirus. II. Glycoproteins of the viral envelope: Tryptic peptide analysis. *Virology* **77,** 650–660.

Sturman, L. S., and Takemoto, K. K. (1972). Enhanced growth of a murine coronavirus in transformed mouse cells. *Infect. Immun.* **6,** 501–507.

Sturman, L. S., Holmes, K. V., and Behnke, J. (1980). Isolation of coronavirus envelope glycoproteins and interaction with the viral nucleocapsid. *J. Virol.* **33,** 449–462.

Sugiyama, K., and Amano, Y. (1980). Haemagglutination and structural polypeptides of a new coronavirus associated with diarrhoea in infant mice. *Arch. Virol.* **66,** 95–105.

Sugiyama, K., and Amano, Y. (1981). Morphology and biological properties of a new coronavirus associated with diarrhea in infant mice. *Arch. Virol.* **66,** 241–251.

Svoboda, D., Neilson, A., Werder, A., and Higginson, J. (1962). An electron microscopic study of viral hepatitis in mice. *Am. J. Pathol.* **41,** 205–224.

Taguchi, F., Yamaguchi, R., Makino, S., and Fujiwara, K. (1981). Correlation between growth potential of mouse hepatitis viruses in macrophages and their virulence for mice. *Infect. Immun.* **34,** 1059–1061.

Takeuchi, A., Binn, L. N., Jervis, H. R., Keenan, K. P., Hilderbrandt, P. K., Valas, R. B., and Bland, F. F. (1976). Electron microscope study of experimental enteric infection in neonatal dogs with a canine coronavirus. *Lab. Invest,* **34,** 539–549.

Tanaka, H., Suzuki, S., and Ichida, F. (1962). Electron microscopic study on the cultured liver cells infected with mouse hepatitis virus—a preliminary report. *Annu. Rep. Inst. Virus Res., Kyoto Univ.* **5,** 95–102.

Tannock, G. A. (1973). The nucleic acid of infectious bronchitis virus. *Arch. Gesamte Virusforsch.* **43,** 259–271.

Tannock, G. A., and Hierholzer, J. A. (1977). The RNA of human coronavirus OC43. *Virology* **78,** 500–510.

Taylor, C. E., Weiser, W. Y., and Bang, F. B. (1981). *In vitro* macrophage manifestation of cortisone-induced decrease in resistance to mouse hepatitis virus. *J. Exp. Med.* **153,** 732–737.

ter Meulen, V., Siddell, S., and Wege, H. eds. (1981). "Biochemistry and Biology of Coronaviruses." Plenum, New York.

Toth, T. E. (1982). Trypsin-enhanced replication of neonatal calf diarrhea coronavirus. *Am. J. Vet. Res.* **43,** 967–972.

Tyrrell, D. A. J., and Almedia, J. D. (1967). Direct electron-microscopy of organ cultures for the detection and characterization of viruses. *Arch. Gesamte Virusforsch.* **22,** 417–425.

Tyrrell, D. A. J., and Bynoe, M. L. (1965). Cultivation of a novel type of common-cold virus in organ culture. *Br. Med. J.* **1,** 1467–1470.

Tyrrell, D. A. J., Almedia, J. D., Berry, D. M., Cunningham, C. H., Hamre, D., Hofstad, M. S., Mallucci, L., and McIntosh, K. (1968). Coronaviruses. *Nature (London)* **220,** 650.

Tyrrell, D. A. J., Almedia, J. D., Cunningham, C. H., Dowdle, W. R., Hofstad, M. S., McIntosh, K., Tajima, M., Zakstelskaya, L. Y. A., Easterday, B. C., Kapikian, A., and Bingham, R. W. (1975). Coronaviridae. *Intervirology* **5,** 76–82.

Tyrrell, D. A. J., Alexander, D. J., Almeida, J. D., Cunningham, C. H., Easterday, B. C.,

Garwes, D. J., Hierholzer, J. C., Kapikian, A., Macnaughton, M. R., and McIntosh, K. (1978). Coronaviridae, 2nd report. *Intervirology* **10,** 321–328.

Uhlenbeck, G. E. (1971). Statistical mechanics and quantum mechanics. *Nature (London)* **232,** 449–450.

Vannuchi, S., and Chiarugi, V. (1977). Surface exposure of glycosaminoglycans in resting, growing, and virus-transformed 3T3 cells. *J. Cell Physiol.* **90,** 503–510.

Virelizier, J. L. (1981). Role of macrophages and interferon in natural resistance to mouse hepatitis virus infection. *Curr. Top. Microbiol. Immunol.* **92,** 105–127.

Virelizier, J. L., and Allison, A. C. (1976). Correlation of persistent mouse hepatitis virus (MHV-3) infection with its effect on mouse macrophage cultures. *Arch. Virol.* **50,** 279–285.

Wadey, C. N., and Westaway, E. G. (1981). Structural proteins and glycoproteins of infectious bronchitis virus particles labelled during growth in chick embryo fibroblasts. *Intervirology* **15,** 19–27.

Walker, D. P., and Cleator, G. M. (1980. Haemagglutination by mouse hepatitis virus type 3. *Ann. Virol. (Inst. Pasteur)* **131E,** 517–520.

Watanabe, K. (1969). Electron microscopic studies of experimental viral hepatitis in mice. II. *J. Electron Microsc.* **18,** 173–189.

Watkins, H., Reeve, P., and Alexander, D. J. (1975). The ribonucleic acid of infectious bronchitis virus. *Arch. Virol.* **47,** 279–286.

Wege, H., Muller, A., and ter Meulen, V. (1978). Genomic RNA of the murine coronavirus JHM. *J. Gen. Virol.* **41,** 217–227.

Wege, H., Wege, H., Nagashima, K., and ter Meulen, V. (1979). Structural polypeptides of the murine coronavirus JHM. *J. Gen. Virol.* **42,** 37–47.

Wege, H., Stephenson, J. R., Koga, M., Wege, H., and ter Meulen, V. (1981a). Genetic variation of neurotropic and non-neurotropic murine coronaviruses. *J. Gen. Virol.* **54,** 67–74.

Wege, H., Siddell, S., Sturm, M., and ter Meulen, V. (1981b). Coronavirus JHM: Characterization of intracellular viral RNA. *J. Gen. Virol.* **54,** 213–217.

Wege, H., Koga, M., Wege, H., and ter Meulen, V. (1981c). JHM infection in rats as a model for acute and subacute demyelinating disease. *In* "Biochemistry and Biology of Coronaviruses" (V. ter Meulen, S. Siddell, and H. Wege, eds.), pp. 327–349. Plenum, New York.

Wege, H., Siddell, S., and ter Meulen, V. (1982). The biology and pathogenesis of coronaviruses. *Curr. Top. Microbiol. Immunol.* **99,** 165–200.

Wege, H., Koga, M., Wanatabe, R., Nagashima, K., and ter Meulen, V. (1983). Neurovirulence of murine coronavirus JHM temperature-sensitive mutants in rats. *Infect. and Immun.* **39,** 1316–1324.

Weiser, W. Y., and Bang, F. (1976). Macrophages genetically resistant to mouse hepatitis virus converted *in vitro* to susceptible macrophages. *J. Exp. Med.* **143,** 690–695.

Weiser, W. Y., and Bang, F. B. (1977). Blocking of *in vitro* and *in vivo* susceptibility to mouse hepatitis virus. *J. Exp. Med.* **146,** 1467–1472.

Weiser, W. Y., Vellisto, I., and Bang, F. B. (1976). Congenic strains of mice susceptible and resistant to mouse hepatitis virus. *Proc. Soc. Exp. Biol. Med.* **152,** 499–502.

Weiss, S. R., and Leibowitz, J. L. (1981). Comparison of the RNAs of murine and human coronaviruses. *In* "Biochemistry and Biology of Coronaviruses" (V. ter Meulen, S. Siddell, and H. Wege, eds.), pp. 245–260. Plenum, New York.

White, J., Matlin, K., and Helenius, A. (1981). Cell fusion by Semliki Forest, influenza, and vesicular stomatitis viruses. *J. Cell Biol.* **89,** 674–679.

Wilhelmsen, K. C., Leibowitz, J. L., Bond, C. W., and Robb, J. A. (1981). The replication of murine coronaviruses in enucleated cells. *Virology* **110,** 225–230.

Willingham, M. C., and Pastan, I. (1980). The receptosome: An intermediate organelle of receptor-mediated endocytosis in cultured fibroblasts. *Cell* **21,** 67–77.

Winterbourne, D. J., and Mora, P. T. (1981). Cells selected for high tumorigenicity or transformed by Simian virus 40 synthesize heparan sulfate with reduced degree of sulfation. *J. Biol. Chem.* **256,** 4310–4320.

Yamada, A., Taguchi, F., and Fujiwara, K. (1979). T-lymphocyte dependent difference in susceptibility between DDD and C3H mice to mouse hepatitis virus, MHV-3. *Jpn. J. Exp. Med.* **49,** 413–421.

Yogo, Y., Hirano, N., Hino, S., Shibuta, H., and Matumoto, M. (1977). Polyadenylate in the virion RNA of mouse hepatitis virus. *J. Biochem. (Tokyo)* **82,** 1103–1108.

Yoshikura, H., and Tejima, S. (1981). Role of proteins in MHV-induced cell fusion. *Virology* **113,** 503–511.